UNIVERSIDADE DE LISBOA
FACULDADE DE CIÊNCIAS
DEPARTAMENTO DE FÍSICA

Investigating Neural Signatures of Trail Making Test Performance in Healthy Subjects using High-Density EEG

Inês Martins Lopes

Mestrado em Engenharia Biomédica e Biofísica

Dissertação orientada por:
Professor Nuno Miguel de Pinto Lobo e Matela
Professor e Dr. Ardalan Aarabi

2023

Resumo

A cognição é essencial para as funções intelectuais, abrangendo a percepção, atenção, resolução de problemas, etc. As funções executivas (FEs) emergem como componentes cruciais de alto nível da cognição, incluindo a flexibilidade cognitiva, memória de trabalho, tomada de decisões, entre outras. O acidente vascular cerebral (AVC) é uma das principais causas de deficiência cognitiva em adultos. Estudos identificaram que cerca de 44% dos sobreviventes de AVC mostram comprometimento na função cognitiva geral, entre 30% a 35%. Deste modo, o reconhecimento e o diagnóstico atempados de perturbações cognitivas pós AVC são essenciais para um tratamento eficaz e atenuação do declínio cognitivo. O Trail Making Test (TMT) é uma ferramenta de avaliação neuropsicológica amplamente utilizada para avaliar o défice cognitivo após um diagnóstico de AVC. O TMT é composto por duas partes: TMT-A e TMT-B. No TMT-A, os participantes são instruídos a conectar números em sequência numérica (ou seja, 1-2-3...), dispostos aleatoriamente. Por outro lado, no TMT-B os participantes devem conectar números e letras em sequência alternada (ou seja, 1-A-2-B-3-C...), também dispostos aleatoriamente. Assim, o TMT-A avalia principalmente a velocidade de processamento, enquanto o TMT-B fornece uma medida da flexibilidade mental e da capacidade de modificação cognitiva. Uma variação do TMT tradicional é o Color Trails Test (CTT), que utiliza círculos numerados e coloridos em vez de letras. Foi projetado para ser uma alternativa mais acessível, pois supera barreiras linguísticas, abordando dificuldades relacionadas com a utilização do alfabeto latino. A revisão de literatura destaca estudos que investigaram deficiências cognitivas por meio da aplicação do TMT. Dentre desses, em Talwar et al., 2020, um grupo de idosos realizaram o TMT num ambiente de ressonância magnética funcional (fMRI), utilizando um tablet compatível com fMRI. Semelhantemente, em Karimpoor et al., 2017, 22 jovens adultos realizaram o TMT utilizando o mesmo sistema. Por outro lado, no estudo de Lin et al., 2021, utilizou-se eletroencefalografia (EEG) em jovens adultos para avaliar o seu desempenho durante a realização do TMT.

Portanto, o estudo realizado no âmbito desta tese de mestrado teve como objetivo investigar os mecanismos executivos da atividade neuronal e definir as estruturas cerebrais envolvidas na execução de três versões do TMT computorizado: TMT clássico, TMT clássico a cores (ccTMT), e TMT a cores (cTMT), recentemente desenvolvido no laboratório. Dados de eletroencefalografia de alta densidade (HD-EEG) de 30 participantes saudáveis foram analisados para examinar as variações nas quatro bandas de frequência, delta, teta, alfa e beta, nos espaços dos sensores e de fonte. Além disso, a conetividade funcional e a dinâmica da rede foram avaliadas usando tomografia electromagnética de baixa resolução normalizada (sLORETA). Portanto, este estudo diferenciou-se dos restantes ao empregar HD-EEG para investigar as estruturas e os padrões de dessincronização cerebral durante o TMT, oferecendo novas perspectivas sobre suas demandas cognitivas, durante a realização de diferentes TMT computorizados: clássico e a cores.

No que diz respeito ao protocolo experimental deste estudo, apenas foi aceite a participação de indivíduos com idades entre 18 e 30 anos, fluentes em francês e saudáveis (sem deficiências cognitivas; não medicados para psicose, depressão, ansiedade, etc.). Por sua vez, cada participante passou por um pro-

tocolo que incluiu um período inicial de repouso de 5 minutos, seguido por 6 blocos consecutivos. Cada bloco continha uma versão diferente do TMT, a saber: TMT-A, TMT-B, cTMT-A, cTMT-B, ccTMT-A e ccTMT-B. Os estímulos visuais foram apresentados aos participantes num ecrã LCD de 21 polegadas posicionado a 50 centímetros do participante, que estava sentado. Os participantes responderam aos estímulos utilizando um rato, efetuando um único clique esquerdo para cada resposta. O protocolo do teste foi desenvolvido utilizando o MATLAB. Simultaneamente, os dados de EEG foram registados utilizando um sistema BioSemi com uma taxa de amostragem de 2048Hz, utilizando um capacete com 128 elétrodos ativos, posicionados de acordo com o sistema 10-10. Após a obtenção dos dados experimentais, procedeu-se ao processamento dos dados adquiridos. Reduziu-se a taxa de amostragem de 2048Hz para 256Hz e aplicou-se um filtro passa-banda com uma largura de banda de 0,5-30 Hz. Além disso, para remover artefactos, utilizou-se o método Independent Component Analysis (ICA). Em seguida, procedeu-se à análise espectral das bandas de frequência, incluindo delta (0,5-4 Hz), teta (4-8 Hz), alfa (8-13 Hz) e beta (13-30 Hz), para todas as diferentes versões do TMT, bem como para o estado de repouso (RS). Também realizou-se a localização da fonte utilizando o método Standardized Low Resolution Electromagnetic Tomography (sLORETA). Por fim, examinou-se a conectividade funcional utilizando o sLORETA, definindo as regiões de interesse (ROIs) com base no atlas de Brodmann. Todos os resultados estatisticamente significativos foram obtidos para um valor de $p < 0,05$. Realizaram-se comparações entre as partes A e B para as versões TMT, cTMT e ccTMT; entre o RS e todos os testes; e entre TMT-A vs. cTMT-A, TMT-B vs. cTMT-B, TMT-A vs. ccTMT-A, TMT-B vs. ccTMT-B, cTMT-A vs. ccTMT-A e cTMT-B vs. ccTMT-B.

Os resultados deste estudo destacaram o papel fundamental do córtex pré-frontal (PFC) e do córtex cingulado anterior (ACC) na realização das tarefas do TMT, sublinhando o envolvimento destas áreas no processamento cognitivo e nas funções executivas. Durante a análise dos nossos resultados, concentramo-nos principalmente nas bandas de frequência teta e beta, que estão mais diretamente relacionadas com os processos cognitivos e motores relevantes para a tarefa do TMT. Além disso, quando se comparou as diferentes versões do TMT, notou-se um padrão de maior ativação teta no ACC para o TMT-A em comparação com o cTMT-A, e para o ccTMT-A em comparação com o cTMT-A. Da mesma forma, o TMT-B e o ccTMT-B mostraram maior ativação teta no ACC em comparação com o cTMT-B. Estes resultados sugerem que tanto o TMT como o ccTMT requerem uma atenção cognitiva acrescida em comparação com o cTMT. Assim, o cTMT mostra-se promissor como uma ferramenta valiosa para avaliar as capacidades executivas, particularmente em pacientes pós-AVC com capacidade de atenção comprometida e reduzida. Observou-se também um aumento da atividade da banda teta no PFC durante a parte B, o que reflecte um maior esforço cognitivo e flexibilidade mental, em comparação com a parte A. Por fim, observou-se uma redução da conetividade nas bandas teta e beta entre o TMT-B e o TMT-A em várias regiões corticais. Uma maior dessincronização na atividade cerebral do EEG tem sido associada a processos cognitivos e processamento sensorial.

Algumas limitações deste estudo incluíram a baixa resolução espacial do EEG, apesar da sua alta resolução temporal. Assim, para superar esta limitação, usou-se uma técnica de localização de fonte. No entanto, localizar estruturas profundas do cérebro ainda é desafiador. Estudos futuros podem explorar abordagens avançadas, como a combinação de EEG com fMRI, para obter uma compreensão mais abrangente das correlações neurais no desempenho do TMT. Outra limitação foi o tamanho modesto da amostra, com apenas 30 participantes saudáveis, podendo ter dificultado a detecção de efeitos estatisticamente significativos e levantado questões sobre a generalização dos resultados. Embora as versões informatizadas do TMT ofereçam vantagens, como a automação da coleta de dados, é importante considerar as limitações de um protocolo de teste longo, como a fadiga dos participantes e seu impacto no

desempenho.

A investigação futura deve incluir diversas populações clínicas, como indivíduos com AVC e doenças neurodegenerativas, para avaliar a utilidade clínica do TMT e do HD-EEG como ferramentas de rastreio cognitivo. Isto tem o potencial de melhorar os cuidados e os resultados dos doentes na reabilitação do AVC e na avaliação de doenças neurodegenerativas. Esta abordagem proactiva visa melhorar a qualidade de vida global dos indivíduos afectados por deficiências cognitivas relacionadas com o AVC.

Palavras chave: Acidente Vascular Cerebral, Trail Making Test, EEG de Alta Densidade, Localização de Fontes, Conetividade Funcional

Abstract

Timely recognition and diagnosis of post-stroke cognitive disorders is essential for effective treatment and mitigating cognitive decline. This approach aims to improve the overall quality of life for individuals affected by stroke-related cognitive impairments. The Trail Making Test (TMT) is a valuable tool for assessing cognitive function following a stroke diagnosis. The TMT consists of two parts: TMT-A and TMT-B. TMT-A primarily assesses processing speed, while TMT-B provides a measure of mental flexibility and cognitive shifting ability. This study investigated executive mechanisms of neuronal activity and define the brain structures involved in the execution of three versions of the computerized TMT: classic TMT, color classic TMT (ccTMT), and color TMT (cTMT), newly developed on the laboratory. High-density electroencephalography (HD-EEG) data from 30 healthy participants were analyzed to examine variations in four frequency bands, delta, theta, alpha, and beta, in sensor and source spaces. Additionally, functional connectivity and network dynamics were assessed using standardized low resolution electromagnetic tomography (sLORETA). Our findings indicate that TMT tasks strongly activate regions of the prefrontal cortex (PFC) and anterior cingulate cortex (ACC), highlighting their involvement in cognitive processing and executive functions. We observed increased theta band activity in the PFC during part B, reflecting greater cognitive effort for set-switching and mental flexibility. Additionally, we observed reduced connectivity in the four frequency bands, between TMT-B and TMT-A in various cortical regions. All of our findings suggest that both the TMT and ccTMT require stronger cognitive attention compared to the cTMT. The cTMT shows promise as a valuable tool for assessing executive abilities, particularly in post-stroke patients with compromised attentional capacity. Future research should include diverse clinical populations, such as individuals with stroke and neurodegenerative diseases, to assess the clinical utility of TMT and HD-EEG as cognitive screening tools, potentially enhancing patient care and stroke rehabilitation outcomes.

Keywords: Stroke, Trail Making Test, High Density EEG, Source Localization, Functional Connectivity

Acknowledgements

First and foremost, I would like to express my sincere gratitude to my external supervisor, Dr. Ardalan Aarabi, for his invaluable guidance and unwavering support throughout this project. His expertise, knowledge, and assistance have been instrumental in shaping this work. I am also thankful to him for helping me find accommodation in a university residence. I am truly fortunate to have had the opportunity to work with such an exceptional mentor. He's the best, really.

I would like to extend my appreciation to Professor Olivier Godefroy for granting me the opportunity to pursue my internship in the Laboratoire de Neurosciences Fonctionnelles et Pathologies (LNFP). His support and encouragement have been very precious.

I am also grateful to my internal supervisor, Professor Nuno Matela, for his continuous support and valuable advice throughout my internship.

I would like to acknowledge the entire team at the LNFP for their welcoming and collaborative environment, specially to my work colleague Louison Bompais. Their collective knowledge and expertise have greatly contributed to my learning and growth during my internship.

I would like to thank the Universidade de Lisboa for granting me the ERASMUS scholarship, which has been instrumental in supporting my academic pursuits and providing me with valuable international experience.

I would also like to extend my sincere gratitude to my dear friends from FCUL. Their support and camaraderie have been invaluable throughout my academic journey. They know who they are, and I am deeply grateful for their friendship.

Last but not least, muito obrigado às minhas besties Irene e Sofia <3.

Index

List of Figures

List of Tables

Chapter 1

Introduction

1.1 Cognitive impairment and Stroke

Cognition involves various intellectual functions and processes, including perception, attention, working memory, problem-solving, etc. Executive functions (EFs) emerge as the pivotal higher-level cognitive abilities responsible for controlling and coordinating various aspects of your thinking and actions. EFs include cognitive processes such as cognitive flexibility (the ability to adapt and switch between different strategies or tasks), working memory (the capacity to temporarily hold and manipulate relevant information in mind for complex tasks), decision-making, and more (Sira et al., 2014). Cognitive deficits can arise either from birth or be acquired later in life due to various environmental factors, such as brain injury, mental illness, or neurological disorders (Dhakal et al., 2023). Stroke is considered a major cause of long-term physical disabilities in adults and it is the second most common cause of cognitive impairment (Leys et al., 2005). Post-stroke cognitive impairment (PSCI) has been shown to be common among stroke survivors. Barbay et al., 2018 identified a prevalence of PSCI of 53.4% measured within 1.5 years post-stroke. Furthermore, according to the findings reported in Lo et al., 2019, a study involving a sample of 3,146 individuals who were hospitalized for stroke, it was observed that approximately 44% of the participants showed impairment in overall cognitive function, while around 30% to 35% exhibited impairment in specific cognitive domains. These impairments were observed during the period of 2 to 6 months following the stroke event. Hence, cognitive impairment and memory dysfunction following stroke diagnosis are common symptoms that significantly affect the survivors' quality of life (Al-Qazzaz et al., 2014). Approximately 30% of stroke patients develop dementia within 1 year of stroke onset (Cullen et al., 2007). The significance of identifying and monitoring cognitive impairment following a stroke has been consistently emphasized in the literature (Yap et al., 2021; Al-Qazzaz et al., 2014). Recognizing and diagnosing post-stroke cognitive disorders in a timely manner is crucial as it allows for the appropriate adjustment of treatment strategies and helps mitigate the progression of cognitive deficits. This proactive approach not only aims to enhance the overall quality of life for individuals affected by stroke but also ensures that necessary interventions and support are provided to optimize their long-term cognitive well-being.

1.2 Trail Making Test

Neuropsychological assessments play a vital role in the evaluation of cognitive impairment subsequent to a stroke diagnosis. Among the various assessment tools, the Trail Making Test (TMT) stands out as one of the most commonly used tests of EF in clinical neuropsychological (Delis et al., 2001) and

set-switching assessmentments. Set-switching is defined as the ability to flexibly switch attention between competing task-set representations (Varjacic et al., 2018). Therefore, TMT encompasses multiple cognitive processes, including visuomotor tracking, scanning, divided attention, and cognitive flexibility (Kortte et al., 2002).The standard version of the TMT involves two components: TMT-A and TMT-B. In the TMT-A task, participants are instructed to connect circled number numbers in a numerical sequence (i.e. 1–2–3 etc.) randomly arranged (see left side of Figure 1.1). On the other hand, in the TMT-B task, participants are required to connect circled numbers and letters in an alternating numeric and alphabetic sequence (i.e., 1-A-2-B etc.), also randomly arranged (see right side of Figure 1.1). The participants are required to perform the TMT as fast as possible without lifting the pen from the paper (Corrigan et al., 1987). Moreover, the TMT-A is typically administered prior to the TMT-B task. TMT-A is a good measure for processing speed, and TMT-B for mental flexibility, since the test requires multiple abilities to complete it (Reimers, 2019).

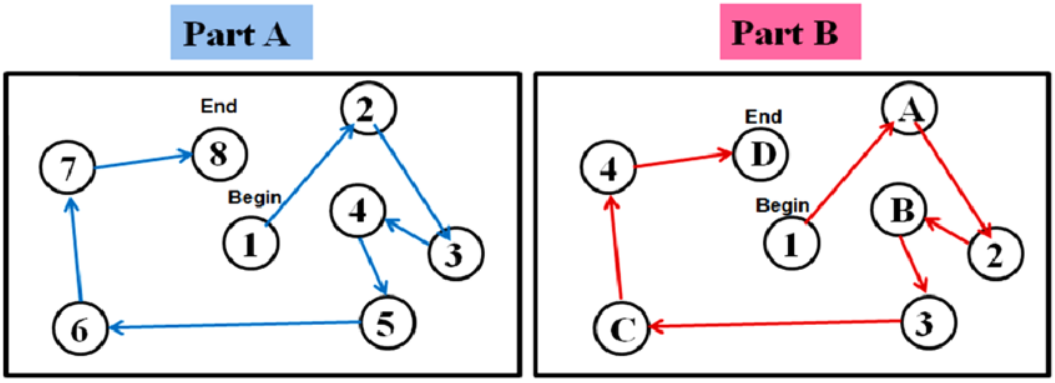

Figure 1.1: Sample of TMT-A (left side) and TMT-B (right side) test sheet (Kim et al., 2016).

Furthermore, the performance in each part of the TMT is scored by the use of metrics that evaluate completion time and the number of errors committed. One common approach is to calculate the difference between completion times for TMT-A and TMT-B (i.e., "TMT-B - TMT-A"), by removing the speed element (Corrigan et al., 1987). Additionally, researchers have also employed the ratio of completion times (i.e., "TMT-B / TMT-A") or a proportional score (i.e., "TMT-B - TMT-A / TMT-A") to further analyze and compare performance on both tasks (Corrigan et al., 1987; Stuss et al., 2001). Distinct types of errors can also be defined in the TMT-B task. Shifting errors refer to the failure to alternate between letters and numbers (e.g., connecting A-B... or 1-2...), while sequencing errors indicate the failure to connect letters or numbers in the correct order after a set shift (e.g., connecting A-2-C... or 1-A-3...) (Klusman et al., 1989).

1.3 Color Trails Test

Another variation of the traditional TMT, the Color Trails Test (CTT), employs numbered colored circles instead of alphabetic letters. The CTT was specifically designed to facilitate broader cross-cultural applications, overcome language barriers, and address difficulties associated with alphabet-based tasks (D'Elia et al., 1996). The CTT was not intended to produce equivalent or similar completion time scores when compared to the standard TMT, but rather to provide a more accessible alternative for assessment purposes. The CTT developed by D'Elia et al., 1996, consists of two separate tests: CTT1 and CTT2. In CTT1, participants are instructed to connect numbers in an ascending sequence while alternating between different colors (see left side of Figure 1.2). On the other hand, CTT2 requires participants to connect

numbers in an ascending sequence while alternating between colors, but with the additional challenge of having two numbers of the same color on the board (see right side of Figure 1.2).

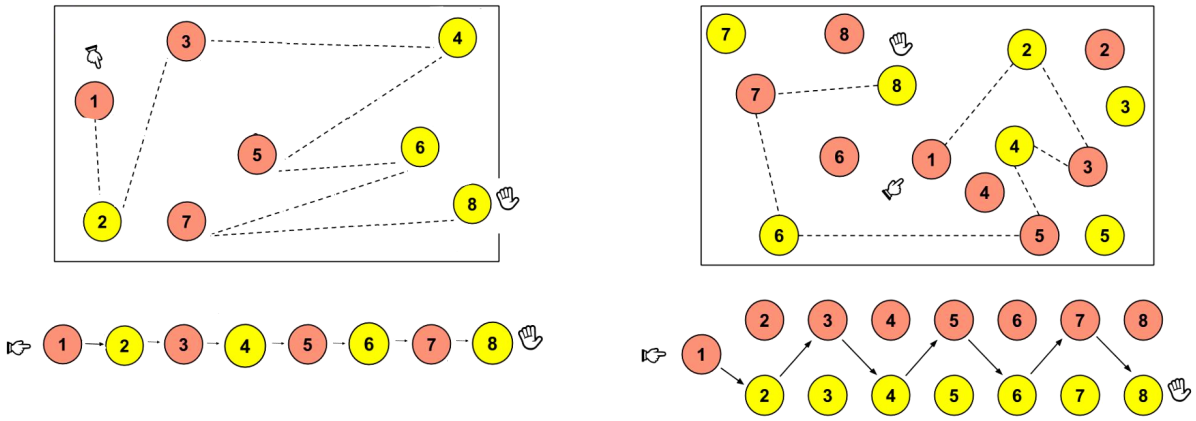

Figure 1.2: Color Trails Test (CTT). CTT1 on the left and CTT2 on the right (D'Elia et al., 1996).

Additionally, a study conducted by Messinis et al., 2011 investigated the application of the CTT in a Greek adult population comprising two clinical groups: patients with Parkinson's disease (PD), acute stroke patients, as well as healthy participants, aged 19-75. The researchers found that the completion time for both CTT tasks was significantly slower in older individuals with lower levels of education. Additionally, the CTT demonstrated the ability to differentiate between the performance of PD and acute stroke patients and their respective healthy controls. These findings highlight the potential of the CTT as a valuable tool for assessing cognitive impairment and distinguishing between different clinical populations.

1.4 Electroencephalography

The use of electroencephalography (EEG) in cognitive research provides valuable insights into the neuroanatomical and neurophysiological mechanisms underlying tasks such as the TMT. EEG is a non-invasive measurement of the brain's electric fields, offering temporal information on cognitive processes and their neural correlates. By integrating EEG with cognitive assessments, researchers can investigate the neural markers associated with cognitive flexibility, attention, and working memory assessed by the TMT. In Chapter 1.5, we will review relevant studies that have employed EEG (and fMRI) to investigate the neurocognitive aspects of TMT performance.

EEG recording involves the placement of electrodes on the scalp, with conductive gel facilitating the measurement of electrical potentials. This technique captures the difference in electrical potentials between two different sites on the head overlying cerebral cortex — the outer layer of the brain closest to the electrodes (Tatum et al., 2008). It is important to note that EEG primarily detects postsynaptic potentials (PSPs), which are slower currents following neurotransmitter release at the axon terminals, rather than action potentials (APs) (Biasiucci et al., 2019). Additionally, the electric potentials generated by individual neurons are too weak to be detected outside the scalp. Therefore, EEG activity reflects the summation of synchronous activity from thousands or millions of neurons with similar spatial orientation (Nunez et al., 1981).

Quantitative electroencephalography (qEEG) is a valuable method for analyzing the digitized EEG data obtained from multiple channels. Through the utilization of modern analytic software, the data

is processed and statistically analyzed, often resulting in the creation of color-coded "brain maps" that depict brain functioning. This approach allows for the visualization of dynamic changes in brain activity during cognitive tasks, enabling the identification of the specific brain regions involved. Our study incorporates various advanced analysis techniques, some of which will be discussed in Chapter 2.

1.4.1 Low-Density Electroencephalography

In standard EEG applications, electrode locations and names are specified by the International 10–20 system (Towle et al., 1993), which uses four reference point on the head surface for electrode positioning - the nasion, the inion, and the left and right preauricular points. These sites are then subdivided by intervals of 10% to 20% of the length inion-nasion and left-right preauricular points, in order to determine the precise electrode location (see Figure 1.3). Each electrode site is identified by a letter corresponding to different lobes or brain areas: pre-frontal (Fp), frontal (F), temporal (T), parietal (P), occipital (O), and central (C). The first letter can be followed by a letter or number. Zero (Z) refers to an electrode placed on the midline sagittal plane. Even-numbered electrodes refer to electrode placement on the right-hemisphere, whereas odd numbers refer to those on the left hemisphere.

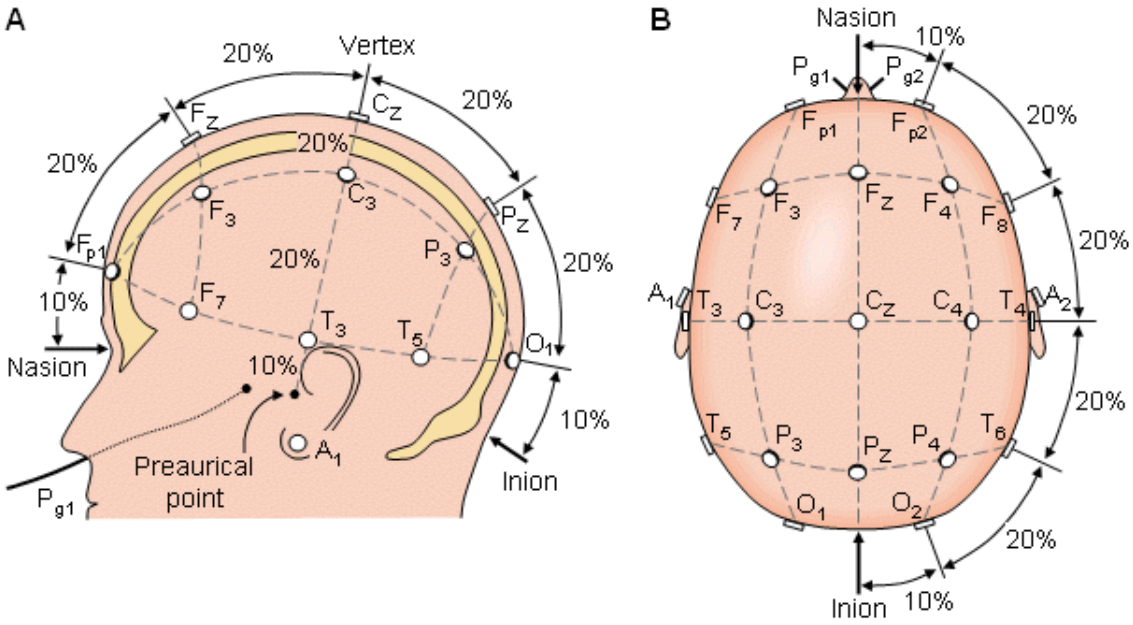

Figure 1.3: EEG 10-20 Electrode Placement. (A) Sagittal plane. (B) Transverse plane. (Shriram et al., 2012).

1.4.2 High-Density Electroencephalography

In contrast, high-density EEG (HD-EEG) recordings provide a more detailed spatial representation by using a greater number of scalp electrodes compared to the standard 10-20 system. An extension to the original 10-20 system was introduced, increasing the number of electrodes from 21 to 74 (Chatrian et al., 1985). This expanded electrode placement system, referred to as the "10% system" or "10-10 system" (Sharbrough et al., 1991), offers enhanced spatial coverage and resolution for capturing neural activity (see Figure 1.4).

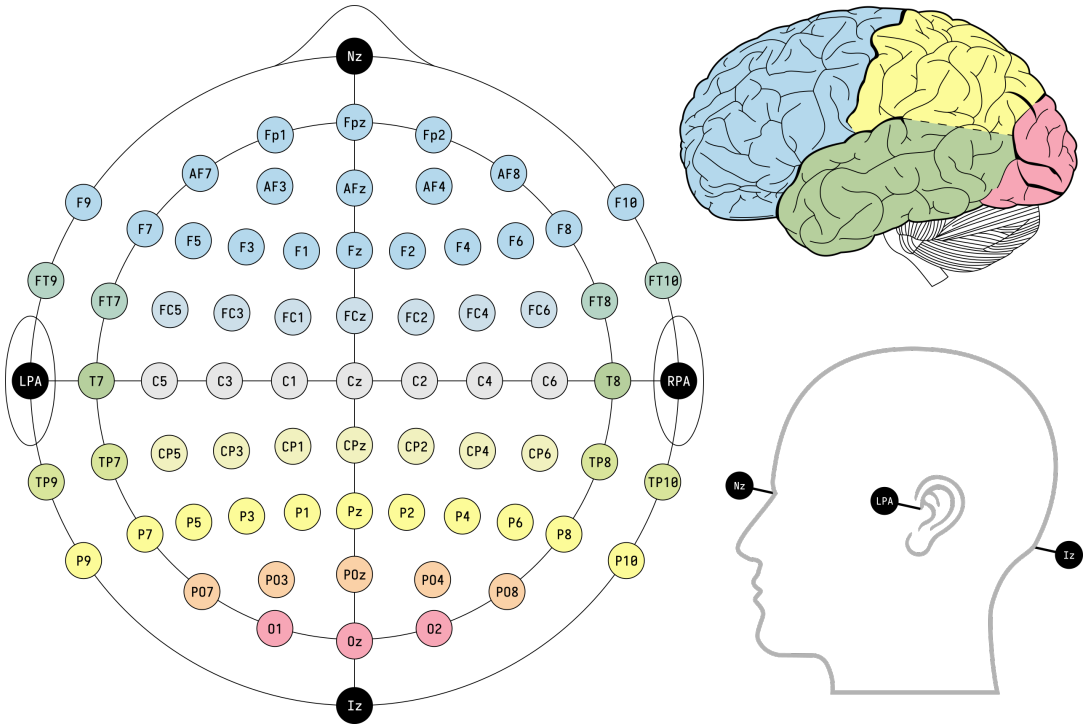

Figure 1.4: EEG electrode positions in the 10-10 system using modified combinatorial nomenclature as presented by Klem et al., 1999. The electrode sites are colour-coded according to the lobes of the brain which their labels (F, C, P, O, and T) represent. The head indicates the location of the fiducials: the nasion, the (left) pre-auricular point, and the inion.

1.5 Literature Review

Several studies have focused on the study of cognitive impairment using TMT. In the study conducted by Talwar et al., 2020, a healthy older-aged population underwent the TMT in an MRI setting, using an MRI-compatible tablet. This innovative system allowed participants to see their hand and receive real-time visual feedback of hand and stylus position through an augmented reality system (see Figure 1.5). The TMT consisted of two parts: TMT-A (40 s) and TMT-B (60 s), with a visual fixation condition (10 s) interleaved between them. The findings revealed a significant decrease in brain activity, particularly in the bilateral occipital, temporal, and parietal lobes, associated with older age, as well as worse performance on the task, similar to the finding in MacPherson et al., 2017. Additionally, a positive activity was predominantly observed in the left hemisphere of the frontal and parietal lobes, which aligns with previous neuroimaging studies comparing TMT-B to TMT-A (Moll et al., 2002; Karimpoor et al., 2017). Similar to findings in this study, previous investigations examining the TMT in younger populations (Karimpoor et al., 2017) have also reported increased activity in the frontal, parietal, and temporal lobes during TMT-B compared to TMT-A. These consistent findings across different age groups suggest that the cognitive demands of TMT-B, which involve greater attentional and executive functions, elicit enhanced neural activation in these specific brain regions. Furthermore, there was reduced task-related activity in the medial temporal lobe, which is a common biomarker for dementia.

In another similar study conducted by Karimpoor et al., 2017, a group of 22 young healthy adults was recruited to perform the TMT using the same augmented reality system that provided visual feedback of hand position (VFHP) embedded in the fMRI setup. Half of the participants performed the TMT with VFHP, while the other half performed it without VFHP. Contrasting TMT-B vs. TMT-A for the two tablet modes revealed no statistically significant differences in brain activity. However, when comparing TMT-A vs. baseline (see upper row of Figure 1.6), activated brain regions included the bilateral superior

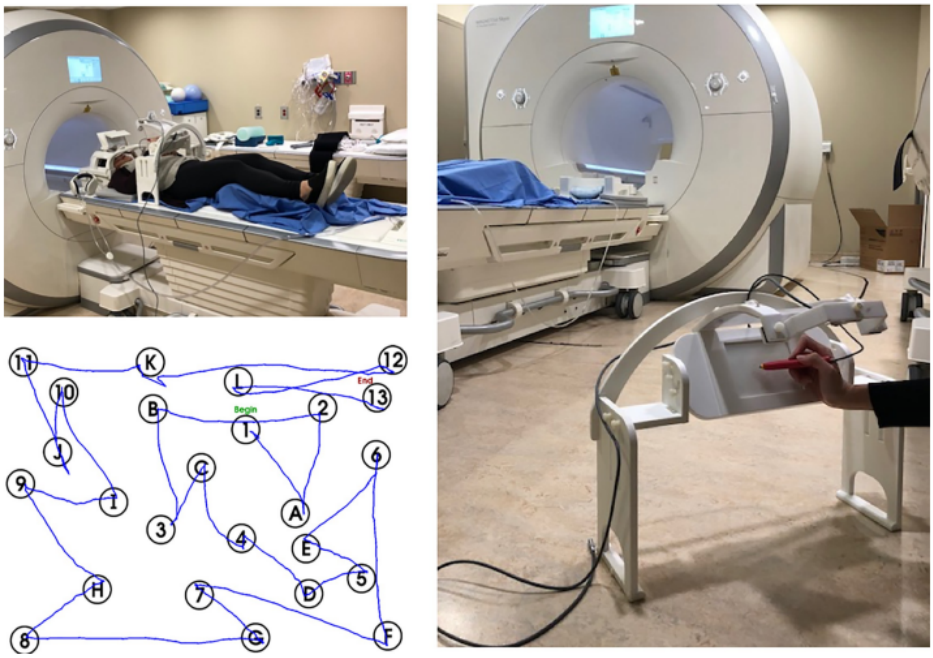

Figure 1.5: Images of the tablet system set-up. (A) The participant lies supine on the MRI table before entering the magnet, with the tablet mounted at the waist using an adjustable stand. The head coil for receiving fMRI signals includes a mirror to view the task in an augmented reality environment on a display screen using an fMRI compatible projector (not shown). (B) The tablet mount includes an fMRI-compatible video camera for a top-down view of tablet interactions. (C) Image results of the participant completing the TMT-B task on the tablet (Talwar et al., 2020).

parietal lobule (SPL), consistent with dynamic visuospatial imagery which subjects may engage in the process of planning to create each linkage and mental processing that supports visual search behavior; supplementary motor area (SMA) and premotor region of the middle frontal gyrus (MiFG), for planning stylus movements that are required to complete linkages between successive numbers; and left lateralized pre-central and postcentral gyri, associated with the tactile and proprioceptive sensory inputs used ultimately to direct hand and arm movement. On the other hand, comparing TMT-B vs. baseline (see lower row of Figure 1.6), showed higher activation in the inferior frontal gyrus (IFG), inferior parietal lobule (IPL), and middle temporal gyrus (MiTG). The IFG is involved in language processing, especially in the left hemisphere, which supports the increased language processing demands of TMT-B. The right IFG is also engaged during set-switching. The IPL is responsible for number processing, and the MiTG is involved in working memory processing during number-letter sequencing tasks and semantic memory processing. Although TMT-B and TMT-A both require number processing, the TMT-B scenario is more demanding because of the set-switching between number processing and letter processing.

Furthermore, in a study conducted by Lin et al., 2021 a touch-sensitive tablet was used to perform the TMT on sixteen healthy young adults. Unlike previous studies mentioned, simultaneous signal acquisition was performed using EEG instead of fMRI (see Figure 1.7). The performance analysis included both digitized tablet metrics (such as SPL - seconds per link, linking and non-linking periods) and conventional metrics (completion times, number of errors). The linking periods relate to the stylus movements to connect two characters; and non-linking periods reflect visual search and cognitive processes. The results revealed that SPL values for TMT-B were significantly larger than those for TMT-A, consistent with previous behavioral findings (Karimpoor et al., 2017; Talwar et al., 2020). Also, both linking and non-linking periods were longer in TMT-B compared to TMT-A. EEG measurements showed greater desynchronization during linking periods compared to non-linking periods, and TMT-B exhibited greater

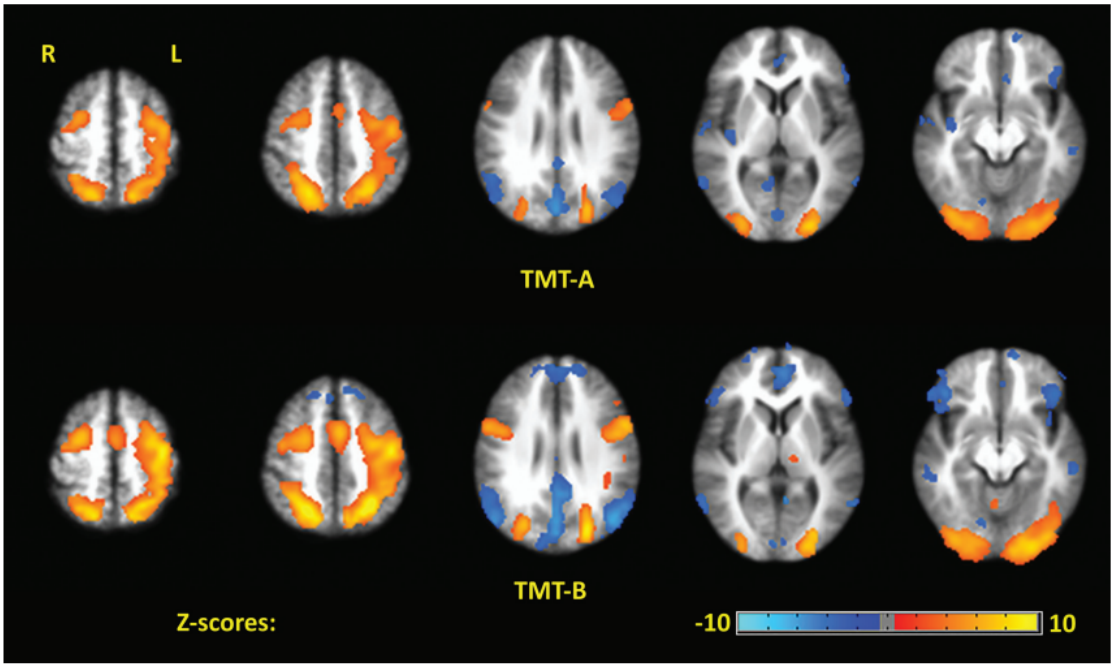

Figure 1.6: Brain activity for commonly activated brain regions in TMT-A vs. baseline and TMT-B vs. baseline for the two tablet interaction modes with fMRI. (Karimpoor et al., 2017)

desynchronization compared to TMT-A during linking periods. Desynchronization in EEG signals has been associated with higher cognitive processes, sensory processing, and movement (Pfurtscheller et al., 1999). TMT-A exhibited increased left lateralized delta band power and posterior midline theta band power compared to TMT-B. These findings suggest that TMT-A required less attentional and working memory demands compared to TMT-B. During non-linking periods, there was an increase in beta power in frontal regions with a slight right lateralization, indicating the involvement of working memory and interference inhibition.

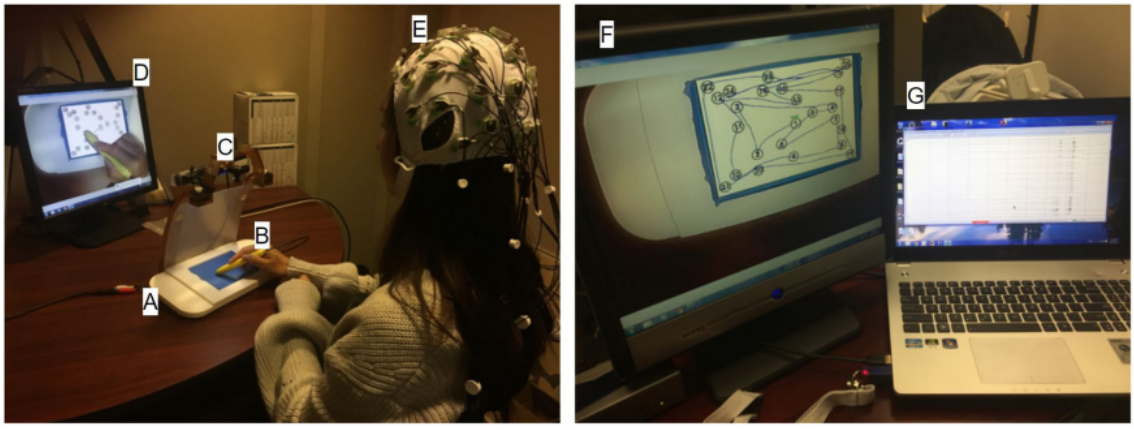

Figure 1.7: The experimental setup inside (left) and outside (right) the acoustically shielded room. (A) Touch-sensitive tablet, (B) Stylus, (C) Video camera, (D) Visual feedback of stimulus response and hand position, (E) EEG cap and electrodes, (F) Stimulus/response computer, (G) EEG recording computer (Lin et al., 2021).

These studies highlight the utility of different neuroimaging techniques in investigating cognitive impairment using the TMT. fMRI provides excellent spatial resolution but lower temporal resolution, while EEG offers high temporal resolution but lower spatial resolution. Furthermore, fMRI machines are more expensive to acquire and maintain, and their operation requires extensive training compared to

EEG, and longer times to acquire data. Motion artifacts caused by patient movement are also a limitation in fMRI studies, since they can affect the quality of data collected the performance of TMT.

1.6 Main Objective of our Study

In this study, we are going to implement three versions of the TMT: the classic one (referred by "TMT"); its color variation (referred by color classic TMT, or ccTMT); and a new developed version in the laboratory (referred by color TMT, or cTMT). Therefore, our objective is to investigate the electrophysiological mechanisms underlying executive processes in healthy subjects. We will achieve this by conducting a series of computerized TMTs combined with HD-EEG. By analyzing cortical and source activity, and exploring the functional connectivity of executive processes during TMT performance, we aim to define the specific brain structures involved and understand their interconnections. Additionally, we aim to examine potential differences in cognitive activity between TMT, cTMT and ccTMT.

Chapter 2

Materials and Methods

2.1 Participants

The study participants consisted of volunteers primarily recruited from the graduate student population at Université de Picardie Jules Verne. Prior to their participation, individuals were required to complete a consent form and undergo a thorough assessment to ensure their eligibility based on specific inclusion and exclusion criteria. Some of the exclusion criteria included: visual, hearing, or motor impairment that would interfere with test execution; insufficient knowledge of counting, the alphabet, and reading or writing in French; neurological conditions likely to interfere with cognitive assessment; and the use of antidepressant, antipsychotic, anxiolytic, or antiepileptic medications (for more information, see Table 6.1). Ultimately, a total of 30 healthy participants (15 females and 15 males) were included, with ages ranging from 19 to 25 and a mean age of 20.03 ±1.67 years.

2.2 Experimental Protocol

Participants who met the inclusion criteria and expressed their willingness to participate in the study proceeded to undergo the following tests in accordance with our experimental protocol.

2.2.1 Cognition Evaluation

To access the general cognition of every participant, two testes were employed: the french version (Kalafat et al., 2003) of the MiniMental State Examination (MMSE) (Folstein et al., 1975) and the Wais-III (Wechsler, 1997) Digit Symbol Substitution Test (DS).

Firstly, the paper version of the MMSE was presented to every participant with supervision. The MMSE uses 30 items to observe subjects' temporo-spatial orientation, immediate and delayed memory (learning, immediate recall, then delayed recall of three words), mental arithmetic, language and visuo-constructive abilities (Shigemori et al., 2010). A score ≥ 27 out of 30 corresponds to a healthy individual (Herrera Pino et al., 2014). Secondly, the The WaisIII DS involved associating the corresponding symbol with numbers as quickly as possible over a 2-minute period. It measured information processing speed.

2.2.2 TMT and CTT Design

The complete protocol consisted of several components, starting with a 5-minute rest period where participants were instructed to close their eyes. This was followed by the completion of 6 blocks, each

one containing a different version of the TMT (TMT-A, TMT-B, cTMT-A, cTMT-B, ccTMT-A, ccTMT-B) consecutively, without any breaks between them. For more information see Figures 2.1, 2.2, 2.3, 2.4, 2.5, 2.6. The visual stimuli were presented to the participants on a 21-inch LCD screen positioned 50 cm away from the seated participants. Each block was built in the same way. During the fixation period (10sec), a centrally located cross was presented on a white frame. The block starts by displaying the instructions (30sec). This is followed by a control test (60sec) to familiarize participants with the task and ensure they understood the test procedure. The control condition consisted of a test's version with reduced numbered circles. After, a visual warning stimulus (2sec) marks the start of the TMT task. The 6 TMT blocks follow each other without pause. Participants responded to the stimuli using a mouse, with a single left click for each response. To ensure that the stimuli filled the entire screen, a black border was added to all frames. At the completion of each test (180sec), participants were instructed to click on a black dot ("●") to indicate that they had finished the test. The test codes were developed using MATLAB 2018b.

After the 5 minutes resting state period, the initial phase of the protocol, as illustrated in Figure 2.1, consisted of administering the TMT-A test, following a similar approach as described in the literature (Corrigan et al., 1987). However, a slight modification was introduced after presenting the first TMT-A task. This modification involved displaying a new frame that contained the previous test inverted 180º along the vertical axis. Additional details can be found in Figures 6.1 and 6.2. The TMT-A test required participants to connect encircled numbers from 1 to 25: "1 - 2 - 3 - ... - 25 - ("●") with the numbers randomly positioned on the screen. Participants were instructed to connect the circles as quickly and as closely to their center as possible. Also, the control condition for TMT-A involved connecting encircled numbers from 1 to 8.

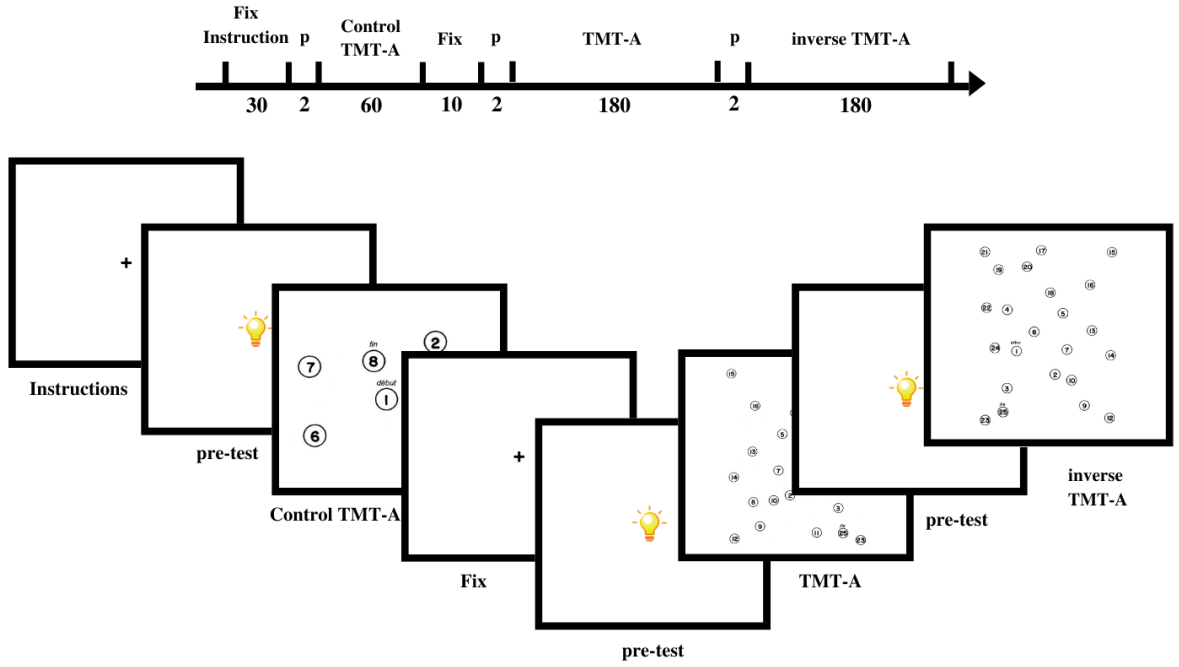

Figure 2.1: TMT-A block design. First, participants are presented with instructions, displayed for a duration of 30 seconds. The second stage involves a control test, lasting 60 seconds. Subsequently, the third stage comprises two trials: TMT-A trial 1, lasting 180 seconds, followed by TMT-A trial 2, which is inverted 180º. Each stage and trial is separated by a fixation cross displayed for 10 seconds. A brief warning signal of 2 seconds precedes both the start of the control test and the start of trials 1 and 2. TMT = Trail Making Test.

For the second block of the study (see Figure 2.2), the TMT-B task was administered. This task required participants to connect numbers (1-13) and letters (A-L) in a random spatial distribution: "1 - A - 2 - B - ... - 13 - ("●")". A control condition was also included, which involved connecting numbers (1-4) alternating with letters (A-D). Additionally, a frame displaying the inverted 180º version of TMT-B about the vertical axis was presented to the participants (see Figures 6.3, 6.4).

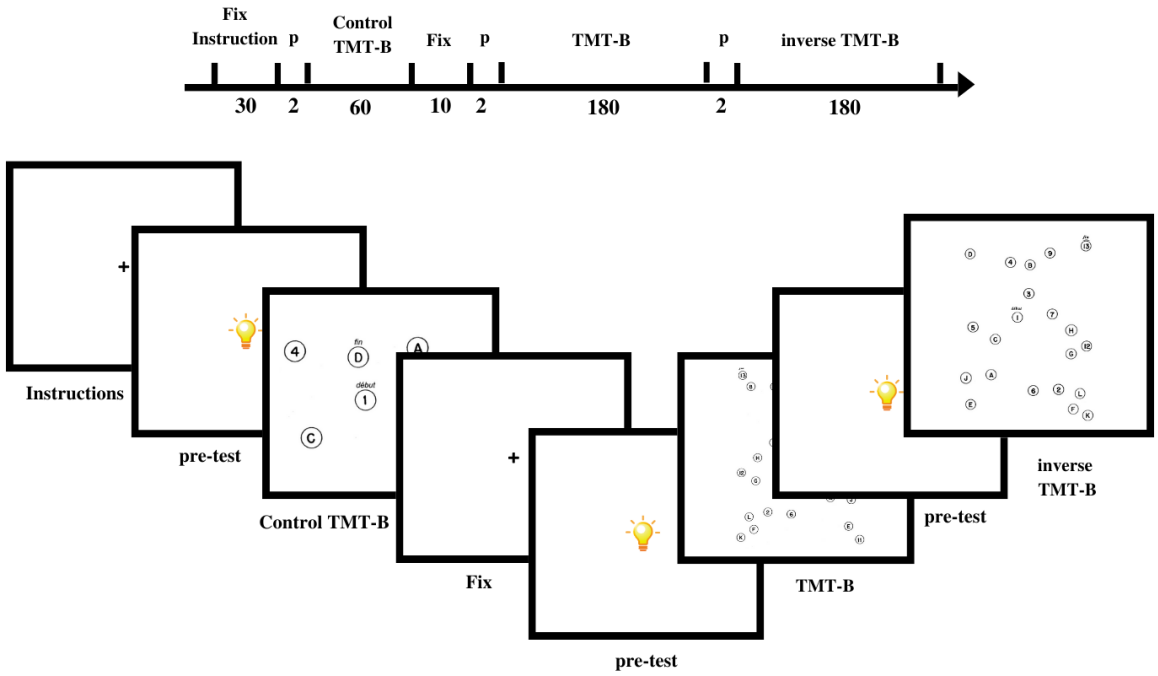

Figure 2.2: TMT-B block design. First, participants are presented with instructions, displayed for a duration of 30 seconds. The second stage involves a control test, lasting 60 seconds. Subsequently, the third stage comprises two trials: TMT-B trial 1, lasting 180 seconds, followed by TMT-B trial 2, which is 180º. Each stage and trial is separated by a fixation cross displayed for 10 seconds. A brief warning signal of 2 seconds precedes both the start of the control test and the start of trials 1 and 2. TMT = Trail Making Test.

In the third block (see Figure 2.3), the cTMT-A was performed. This TMT's variation required participants to sequentially connect green encircled numbers from 1 to 36, followed by blue encircled numbers also ranging from 1 to 36: "1 - 2 - ... - 36 -1 - 2 - ... - 36 - ("●"). For additional information see Figure 6.5. In total, the participant had to connect 72 encircled colored numbers. This task aimed to assess cognitive processing speed and attentional control. A control condition was included, involving the connection of green encircled numbers from 1 to 8, followed by blue encircled numbers also ranging from 1 to 8.

Additionally, in the fourth block of the study (see Figure 2.4), the cTMT-B was implemented. Participants were required to connect alternating green encircled numbers with blue encircled numbers in sequential order: "1 - 2 - 3 - 4 - ... - 36 - ("●"). For additional details, please refer to Figure 6.6. This task aimed to assess cognitive flexibility and set-shifting abilities. A control condition was included, involving the connection of alternating green encircled numbers with blue encircled numbers from 1 to 8. Similar to the previous part, the modified color version of the task featured smaller and more controlled distances between the numbered circles compared to the classic TMT and its colored version.

Next, in the fifth block of the experiment (see Figure 2.5), the ccTMT-A was implemented. This version required participants to connect encircled numbers colored in blue, ranging from 1 to 25: "1 - 2 - ... - 25 - ("●"). Subsequently, in the following frame, participants were instructed to connect encircled numbers colored in green, also ranging from 1 to 25: "1 - 2 - ... - 25 - ("●"). Importantly, the colored

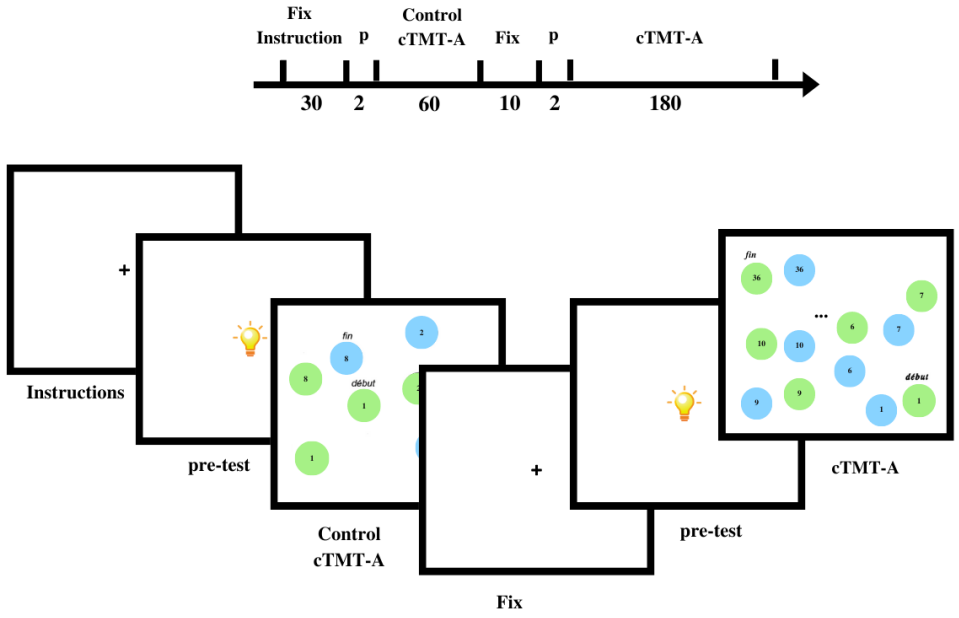

Figure 2.3: cTMT-A block design. First, participants are presented with instructions, displayed for a duration of 30 seconds. The second stage involves a control test, lasting 60 seconds. Subsequently, the third stage comprises one trial: cTMT-A trial 1, lasting 180 seconds. Each stage and trial is separated by a fixation cross displayed for 10 seconds. A brief warning signal of 2 seconds precedes both the start of the control test and the start of trial 1. cTMT = color Trail Making Test.

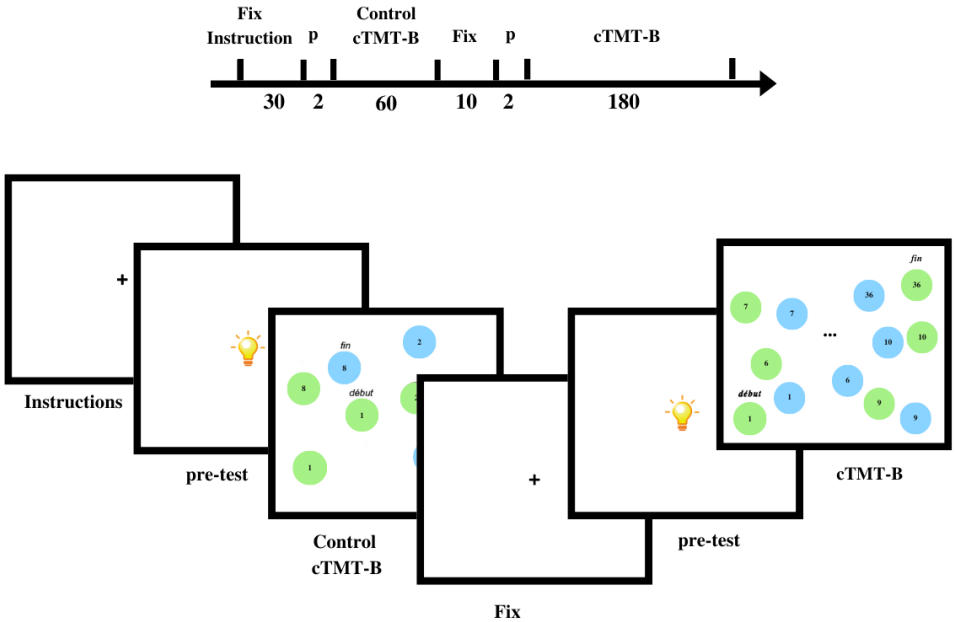

Figure 2.4: cTMT-B block design. First, participants are presented with instructions, displayed for a duration of 30 seconds. The second stage involves a control test, lasting 60 seconds. Subsequently, the third stage comprises one trial: cTMT-B trial 1, lasting 180 seconds. Each stage and trial is separated by a fixation cross displayed for 10 seconds. A brief warning signal of 2 seconds precedes both the start of the control test and the start of trial 1. cTMT = color Trail Making Test.

numbers in both frames occupied the same positions. A control condition was included, involving the connection of encircled numbers colored in blue from 1 to 8. Detailed illustrations of the task can be found in Figures 6.7 and 6.8.

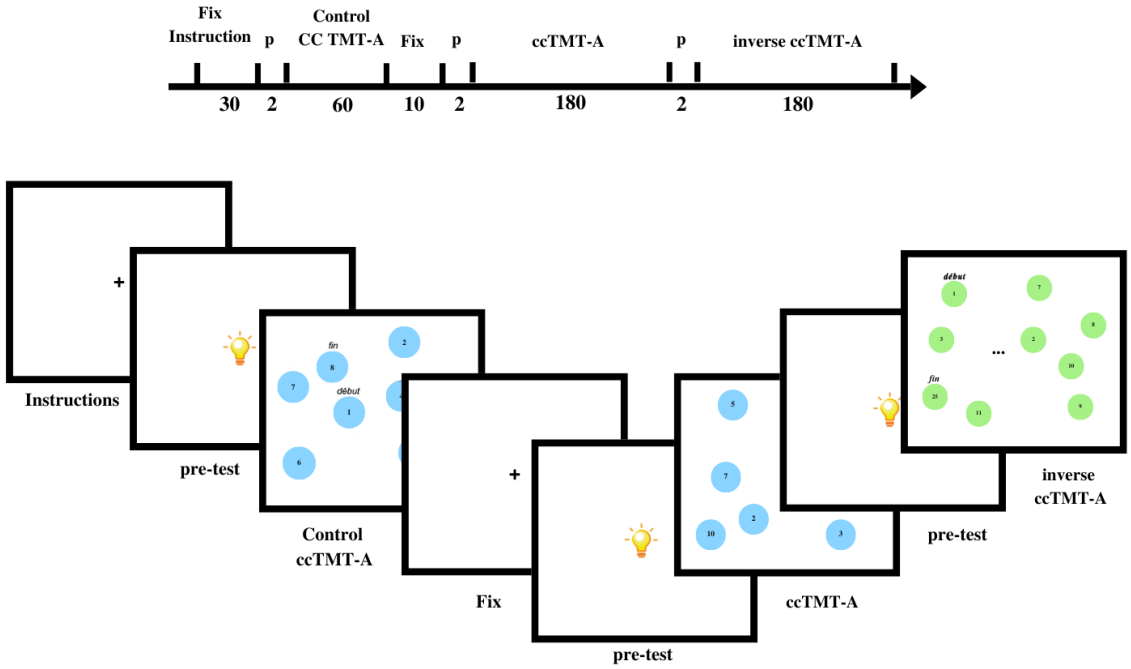

Figure 2.5: ccTMT-A block design. First, participants are presented with instructions, displayed for a duration of 30 seconds. The second stage involves a control test, lasting 60 seconds. Subsequently, the third stage comprises two trials: ccTMT-A trial 1, lasting 180 seconds, followed by ccTMT-A trial 2, which is inverted 180º with a different color. Each stage and trial is separated by a fixation cross displayed for 10 seconds. A brief warning signal of 2 seconds precedes both the start of the control test and the start of trials 1 and 2. ccTMT = color classic Trail Making Test.

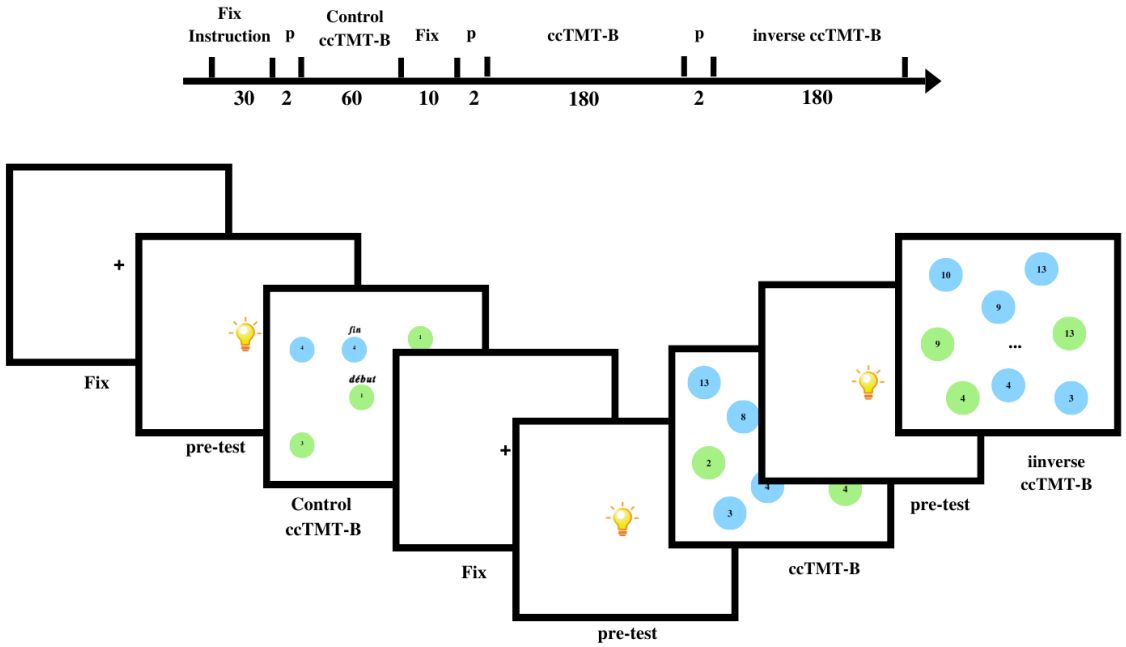

Figure 2.6: ccTMT-B block design. First, participants are presented with instructions, displayed for a duration of 30 seconds. The second stage involves a control test, lasting 60 seconds. Subsequently, the third stage comprises two trials: ccTMT-B trial 1, lasting 180 seconds, followed by ccTMT-B trial 2, which is inverted 180º. Each stage and trial is separated by a fixation cross displayed for 10 seconds. A brief warning signal of 2 seconds precedes both the start of the control test and the start of trials 1 and 2. ccTMT = color classic Trail Making Test.

Finally, the sixth block of the study (see Figure 2.6), the ccTMT-B was employed. It involved connecting alternating green encircled numbers with blue encircled numbers in sequential order: "1 - 2 - 3 - ... - 13 - ("●")" (for additional information, refer to Figure 6.9). Similar to previous sections, an inverted 180º version of this task was also included (for additional information, refer to Figure 6.10). The control condition for this part required connecting alternating green encircled numbers with blue encircled numbers from 1 to 8. It is important to note that in the TMT-A and ccTMT-A versions, as well as in the TMT-B and ccTMT-B versions, the encircled numbers occupy the same spatial positions. This design feature ensures consistency across the tasks and allows for a more accurate comparison of participants' performance and cognitive abilities between the different conditions.

2.3 Electroencephalography Recording

The EEG data was recorded using a BioSemi system at a sampling rate of 2048Hz. The recording setup consisted of a BioSemi headcap with 128 channels; a BioSemi 256-channel ActiveTwo AD-box; 128 BioSemi "pin-type" active electrodes with sintered Ag-AgCl electrode tips, known for their low noise and stable performance, divided into four sets (A, B, C, and D). For more information about the rest of the materials see Figure 2.7. The electrodes were position according to the 10-10 system (for more information about the electrode's placement see Figure 6.11). The recorded data was processed using BioSemi software. During the recording, a laptop computer equipped with an Intel i3-10100 CPU 3.60GHz and 8 GB RAM was used. In addition to the hardware setup, a code was implemented in MATLAB 2018b to register different types of triggers corresponding to the stimuli presented during each task phase. These triggers included the beginning and end of the experiment, the beginning and end of a task, as well as individual mouse clicks. To ensure optimal signal quality, the impedance between each electrode and the scalp was monitored during the gel injection process, in order to be below $10k\Omega$ (Nuwer, 1997).

2.4 Electroencephalography Data Processing

2.4.1 Pre-Processing

The acquired data was processed using the FieldTrip toolbox, a MATLAB software toolbox design for EEG analysis (R. e. a. Oostenveld, 2011). Initially, to optimize memory usage and speed up signal processing, we reduced the sampling rate from 2048Hz to 256Hz. This downsampling was performed in accordance with the Nyquist theorem, which states that the sampling frequency must be at least twice the highest frequency of interest in the signal. Afterwards, the signal was subjected to band-pass filtering using a finite impulse response (FIR) filter with a bandwidth of 0.5-30 Hz.

The EEG data for each subject was subsequently segmented into epochs for the different tasks: TMT-A, TMT-B, cTMT-A, cTMT-B, ccTMT-A, and ccTMT-B. The segmentation was performed using 10-second epochs with a 50% overlap.

2.4.1.1 Artifact Rejection

In order to remove artifacts from the acquired EEG data, we initially employed the method of Independent Component Analysis (ICA) (Delorme, 2019). ICA is a signal processing technique used to separate independent sources that are linearly mixed in multiple sensors. It is commonly used to solve problems such as the "cocktail party problem," where the goal is to isolate the speech of one person in

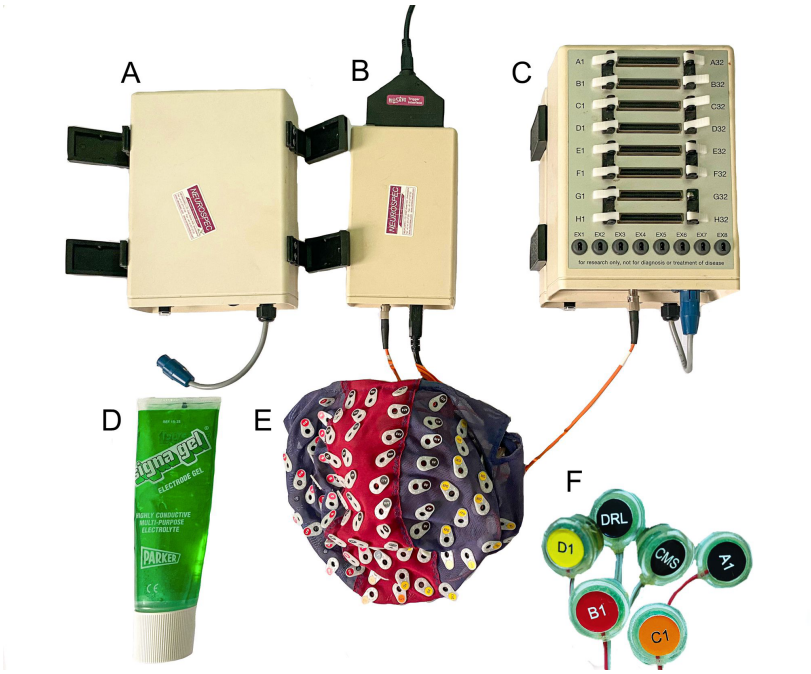

Figure 2.7: **(A)** BioSemi Battery Box. **(B)** USB2.0 receiver. **(C)** BioSemi 256 channel ActiveTwo AD-box. **(D)** Electrode Gel. **(E)** BioSemi headcap with 128 channels (for additional information about the BioSemi cap with 128 channels layout see Figure 6.11). **(F)** BioSemi Pin-Type Active-electrodes (includes CMS/DRL, 32 channel A-set, 32 channel B-set, 32 channel C-set and 32 channel D-set).

a noisy room (Hyvärinen, 2013). Similarly, in EEG analysis, ICA can be applied to separate the contributions of different brain sources that are projected onto scalp sensors. Mathematically, ICA recovers versions of the original independent sources U (components $\times$ time) by multiplying the data X (channels $\times$ time) by an unmixing matrix W (components $\times$ channels), as shown in Equation 2.1.

$$U = WX \tag{2.1}$$

In our study, we utilized ICA implemented within the FieldTrip toolbox to decompose our data, for each subject. The number of ICA components was incrementally increased from 10 to 60, and after careful consideration, we determined that 60 components provided the appropriate level of decomposition for our number of channels. The identification of artifactual independent components (ICs) was performed visually. We visually inspected the ICs and selected those representing artifacts such as muscle activity, eye blinks, eye movements, ECG activity, noise, etc. Specifically, we found noisy artifacts and ECG-related artifacts, as illustrated in Figures 2.8 and 2.9, respectively.

After applying ICA we conducted a visual inspection of the EEG data for each subject. This inspection involved generating plots for each channel in each trial, based on a selected metric. The metrics that could be considered were "var" (variance within each channel, which was the default choice), "min" (minimum value in each channel), "max" (maximum value in each channel), "maxabs" (maximum absolute value in each channel), "range" (range from minimum to maximum value in each channel), "kurtosis" (a measure of the peakedness of the amplitude distribution), and "zvalue" (mean and standard deviation computed over all time and trials per channel). Then, we examined the metrics of "variance," "kurtosis," and "zvalue" for each trial and each channel. We visually assessed the data and identified trials and/or channels that appeared as outliers. These outliers were characterized by abnormal values or deviating patterns compared to the overall data distribution. The goal of removing the chosen outliers was to improve the reliability of our findings by reducing the impact of artifacts. Figures 2.10 and 2.12 illustrate

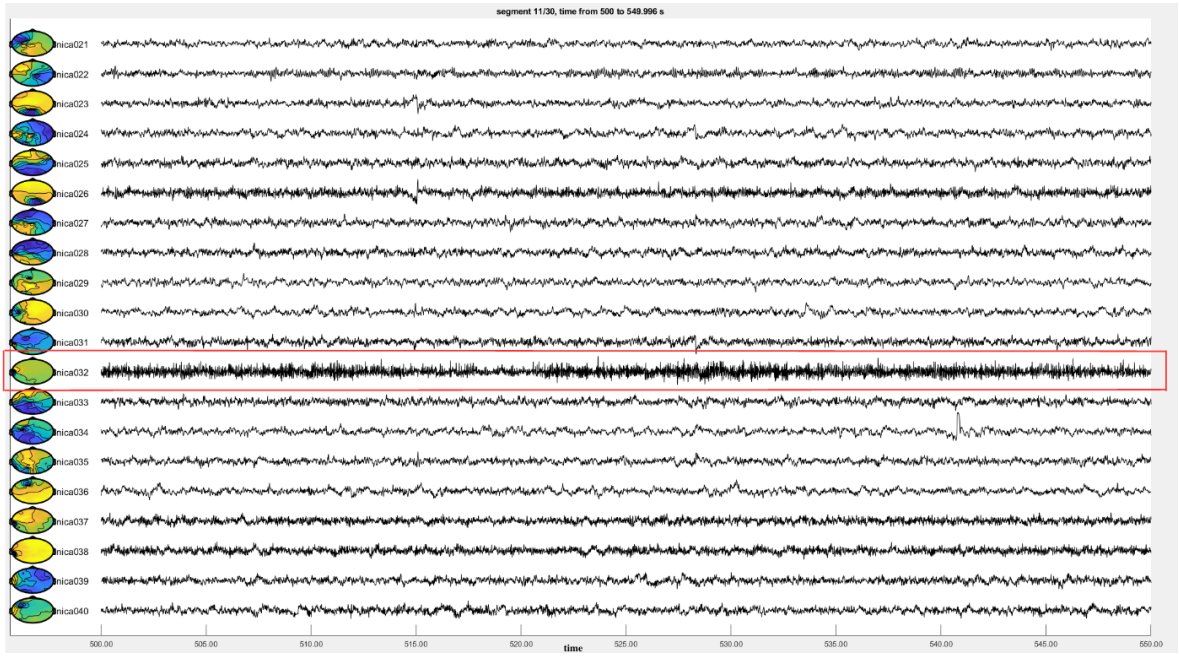

Figure 2.8: IC exhibiting noisy artifact.

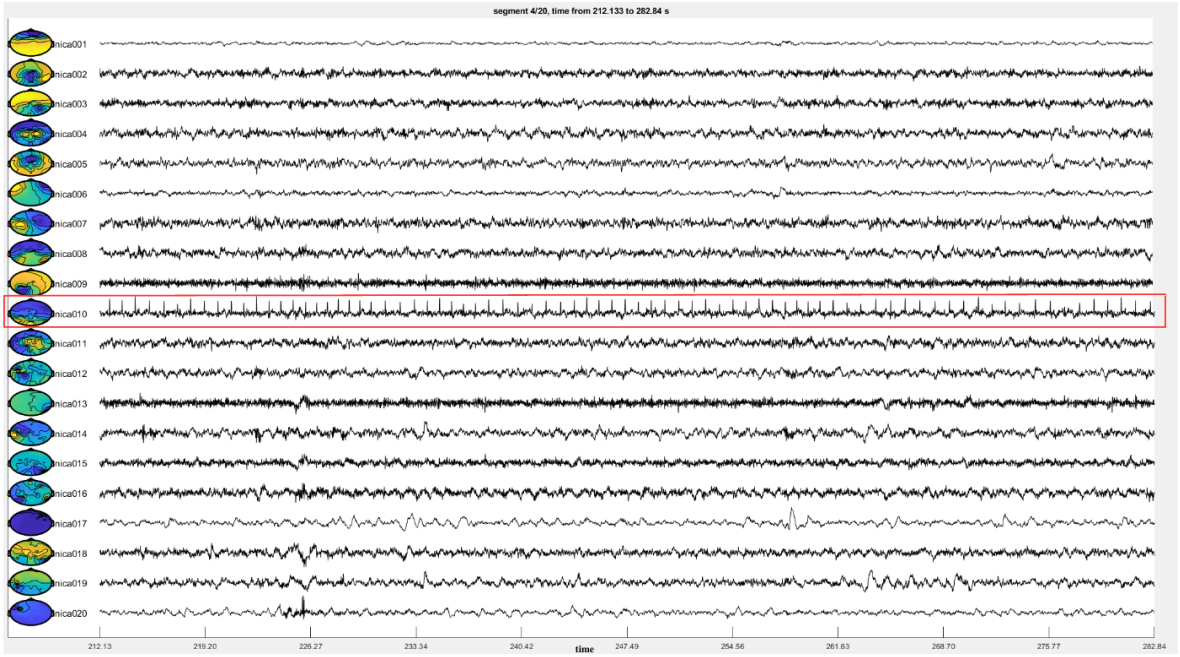

Figure 2.9: IC exhibiting ECG artifact.

the impact of the artifact rejection process. The plots show the data before and after the removal of trials and/or channels that exhibited outlier characteristics. This visual inspection allowed us to identify and exclude problematic data segments, and ensuring the integrity and quality of the remaining EEG data.

For subjects who had at least one channel removed, the missing channels were repaired through interpolation. In this process, the removed channel was replaced with the average of its neighboring channels. The determination of neighboring channels was done using the "triangulation" method in the FieldTrip function *ft_prepare_neighbours*. This algorithm constructs triangles between nearby nodes, effectively filling the entire area covered by the nodes (for more information see Figure 6.12), regardless of the distance between sensors (R. Oostenveld et al., 2022), and is based solely on their spatial coordinates.

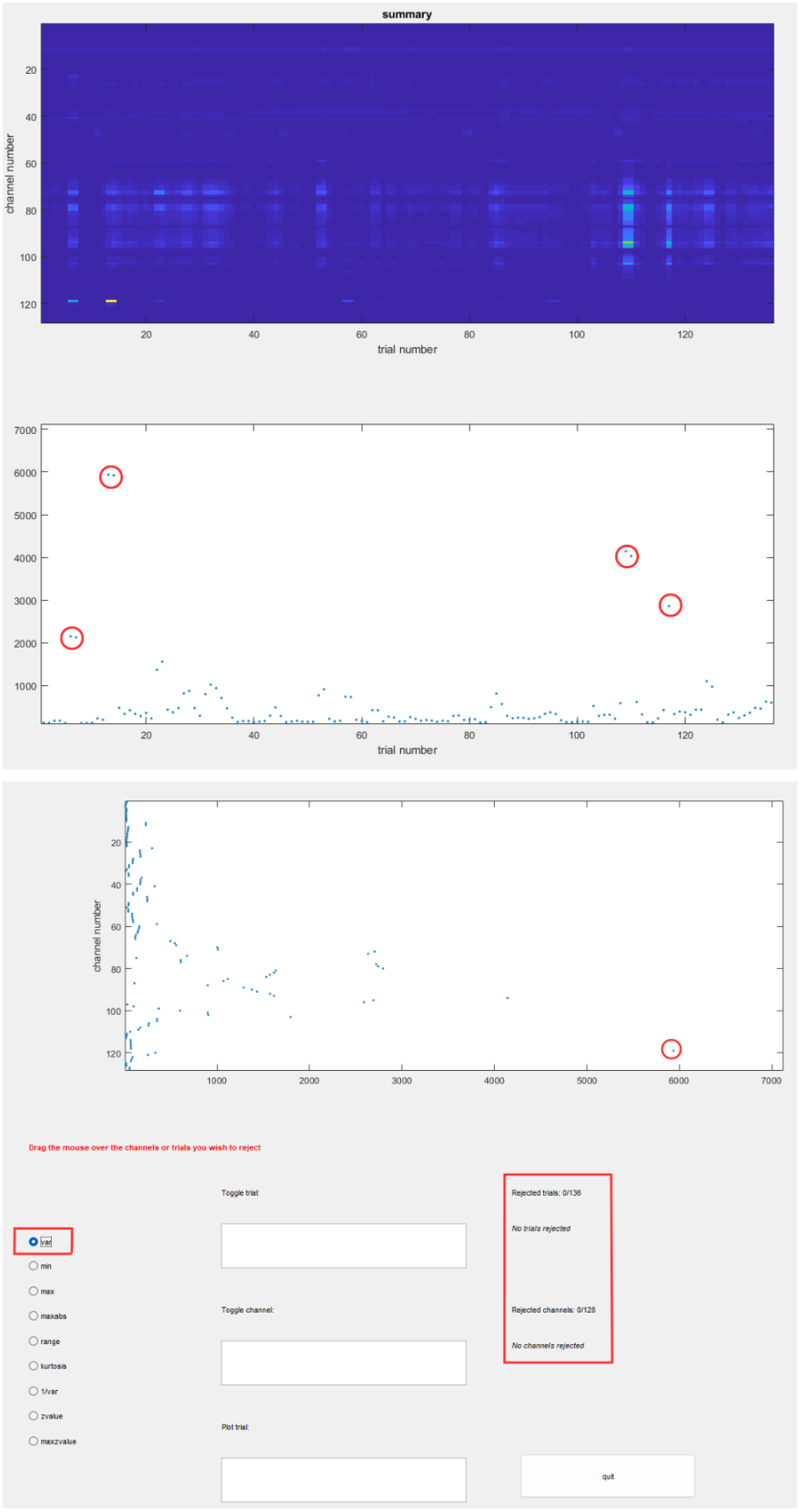

Figure 2.10: Variance plot for each trial and channel of subject no.2 before removing outliers. The "variance" metric was used, and the trials and channels that are soon to be removed are highlighted in red.

2. MATERIALS AND METHODS

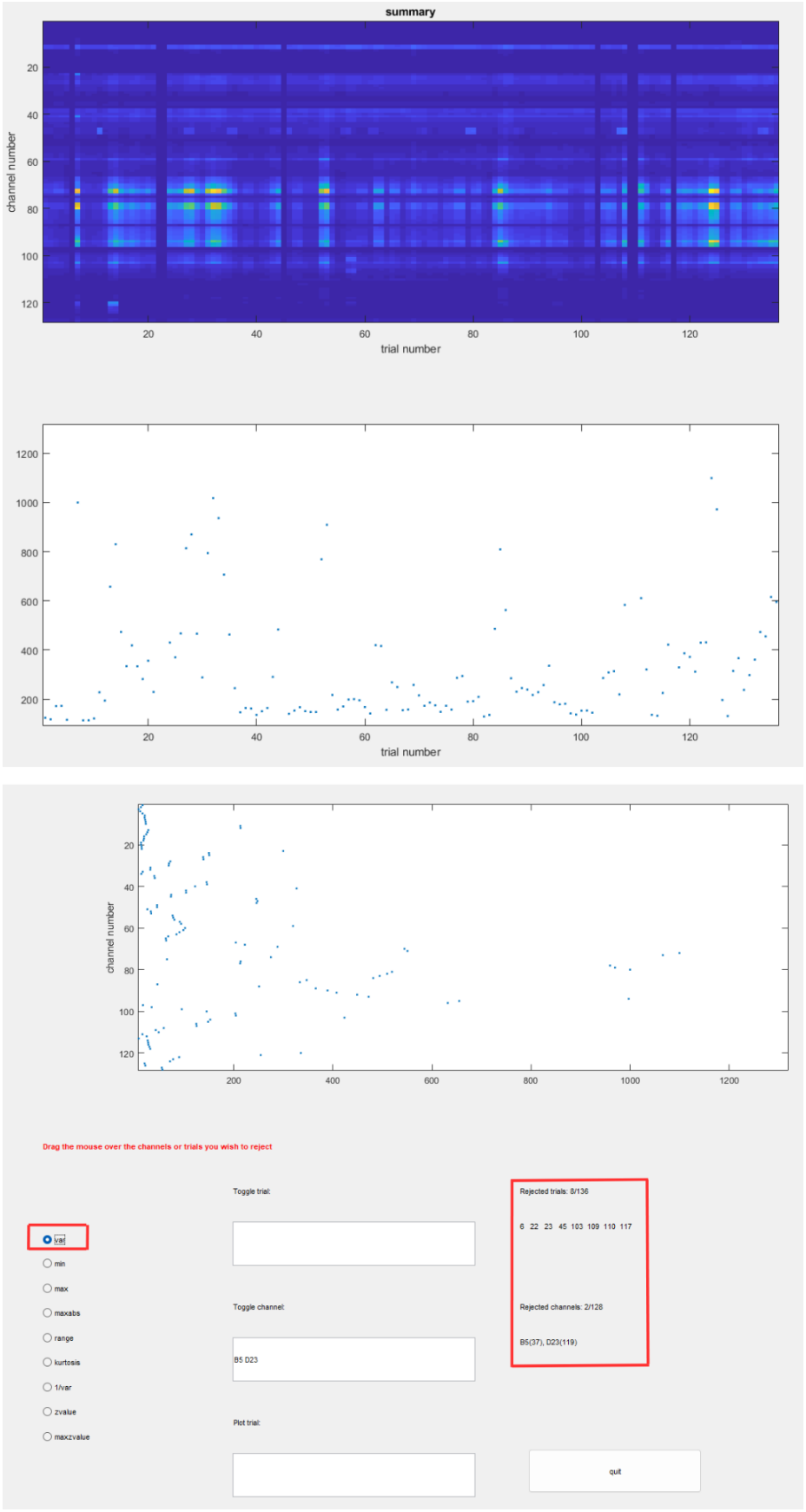

Figure 2.11: Variance plot for each trial and channel of subject no.2 after removing outliers. The trials and channels that were removed are indicated inside the red squared box.

2.5 Spectral Analysis

Spectral analysis, a commonly used technique for quantifying EEG signals, was employed to decompose our EEG data into its constituent frequency components. By applying Fourier transform, the segmented epochs in the time domain were transformed into the frequency domain, resulting in a power spectrum encompassing various frequency bands, including delta (0.5-4 Hz), theta (4-8 Hz), alpha (8-13 Hz), and beta (13-30 Hz). The power spectral density, also known as the power spectrum, provides valuable insights into the distribution of signal power across frequencies. In our study, for each of the four frequency bands (delta, theta, alpha, and beta), we calculated the average spectral power density for every electrode across the different 6 TMT conditions (i.e., TMT-A, TMT-B, cTMT-A, cTMT-B, ccTMT-A, and ccTMT-B) as well as the resting state (RS). This involved measuring the average spectrum density for each electrode and frequency band across all subjects (n=30). A 2D topographical map of spectral power density for each frequency band is thus obtained for each TMT condition.

2.6 EEG Source Localization

The EEG forward problem involves simulating the potentials measured at electrode locations based on the current sources inside the brain. In contrast, the EEG inverse problem, also known as EEG source imaging problem, aims to determine the location of current sources based on the recorded electrode potentials (Grech et al., 2008). This is necessary because scalp measurements do not directly reflect the true neuronal activity due to volume conduction effects and signal attenuation. However, the inverse problem is considered ill-posed as it does not have a unique solution, meaning that multiple combinations of simultaneously active sources can generate the same electric field on the scalp surface. To overcome this challenge and obtain an approximate solution, a widely used technique called Low Resolution Electrical Activity Tomography (LORETA) is commonly employed (Pascual-Marqui et al., 1994). By applying source analysis, it becomes possible to estimate the underlying neuronal generators responsible for the measured electrical potentials.

2.6.1 Standardized Low Resolution Electromagnetic Tomography

In our study, we employed Standardized Low Resolution Electromagnetic Tomography (sLORETA), which is a variant of LORETA that incorporates additional normalization procedures to enhance the accuracy and comparability of source localization results across individuals and studies (Pascual-Marqui, 2002). This allowed us to reconstruct the three-dimensional distribution of brain electrical activity. In sLORETA, the brain volume is divided into a grid of voxels at a spatial resolution of 5 mm, totaling 2394 voxels (Dattola et al., 2020). Also, sLORETA employs a three-shell spherical head model aligned with the Talairach human brain atlas (Talairach, 1988). Each source is represented by a fixed position on the grid (voxel) and characterized by a current density vector with unknown components. The electrical activity's intensity and direction at each point determine the electromagnetic field measured on the scalp. The solution space is restricted to the grey matter and hippocampus.

The implementation of sLORETA for source localization involved several steps. Firstly, valid head coordinates and previously obtained EEG data were required. The head cartesian coordinates (x, y, z) provided by the website BioSemi, were used to map the spatial locations of brain regions. Next, a transformation matrix was generated to convert the head coordinates into a grid of voxels representing the brain. This mapping took into account the specific locations of different brain regions. Subsequently,

the patient-specific segmented EEG data for each condition TMT condition were processed to create files containing continuous recordings of scalp signals. These recordings were analyzed in terms of the number of time frames per epoch (2560), the sampling rate (256Hz), and the different frequency bands of interest, delta (δ), theta (θ), alpha (α), and beta (β). Finally, the processed data were used for source localization.

2.7 Functional Connectivity Analysis

We performed an analysis of brain functional connectivity (FC) using sLORETA to investigate the organization and interconnections of different brain regions during cognitive processes, specifically for all 6 TMT conditions. FC refers to the statistical relationship between the recorded measures of activity in spatially distant brain regions (Friston, 1994), allowing us to identify the networks involved in task execution. In our study, we employed sLORETA for the analysis of FC. The first step involved defining the regions of interest (ROIs) based on the Brodmann atlas. The ROIs were represented by MNI coordinates, lobe, structure, Brodmann area, and ROI number of each voxel. We considered 42 Brodmann areas, 84 ROIs (left and right Brodmann areas), and 6239 voxels for connectivity analysis between the centroids of the ROIs. Each voxel was considered essential for assessing functional connectivity. Specifically, we employed lagged linear connectivity analysis to examine functional connectivity during the TMT tasks. Then, for each subject, sLORETA computed FC matrices in four frequency bands, δ, θ, α and β.

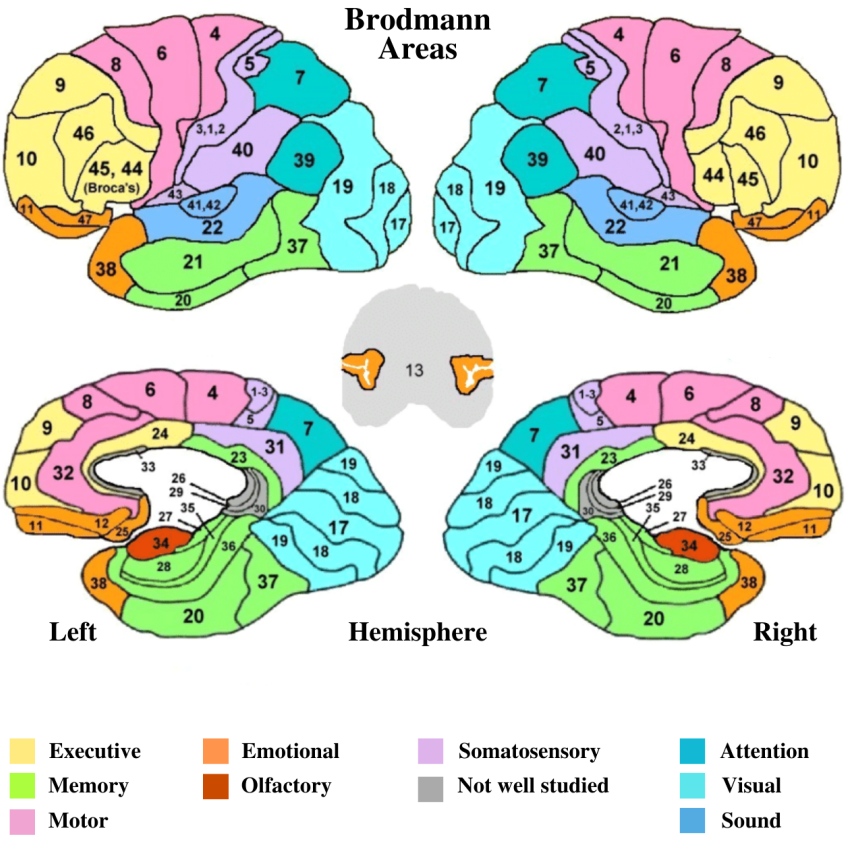

Figure 2.12: Brodmann Areas in the Human Brain, and their function (Gollahalli, 2013).

2.8 Statistical Analysis

We conducted statistical comparisons within the δ, θ, α, and β frequency bands for both spectral and source analysis, as well as FC. These comparisons involved pairwise comparisons between various conditions listed in Table 2.1. The goal was to asses differences on the neural activity associated with the cognitive performance on the different TMT tests. In the sensor space, we performed statistical comparisons of the obtained power spectrum using a bilateral non-parametric t-test with FieldTrip on Matlab. The Monte Carlo method was utilized to generate a null distribution of test statistics with 1000 randomizations and a cluster threshold of 0.0001. Only clusters of adjacent electrodes with statistically significant values below this threshold were considered. By analyzing the null distribution, p-values were calculated to determine the statistical significance of the observed differences in the EEG data between test conditions. Electrode values that were statistically significant (p-value $< \alpha = 0.05$) were visually represented on a color map using a distinct marker.

To assess the statistical significance of our results in both source and connectivity analysis, we performed a bilateral non-parametric t-test between two paired conditions (according to Table 2.1), with subject-wise normalization on LORETA. Additionally, we employed Spatial Nonparametric Mapping (SnPM) by performing 5000 iterations of randomization. This allowed LORETA to generate a null distribution of source/connectivity statistics, enabling comparison with the observed data and obtaining p-values to identify significant regions/connections (p-value $< \alpha = 0.05$).

Table 2.1: Statistical comparison between the tests presented on this table, using a non-parametric t-test method, within δ, θ, α and β frequency bands, for a significance of 5%. TMT = Trail Making Test. cTMT = color Trail Making Test. ccTMT = classic color Trail Making Test. RS = resting state. α = Level of significance.

Statistical Comparison $\alpha = 5\%$		
	Group A	Group B
TMT-A vs. TMT-B	TMT-B	TMT-A
	cTMT-B	cTMT-A
	ccTMT-B	ccTMT-A
RS vs. TMT-A /B	TMT-A	RS
	TMT-B	
	cTMT-A	
	cTMT-B	
	ccTMT-A	
	ccTMT-B	
TMT-A vs. TMT-A'	cTMT-B	TMT-B
	cTMT-A	TMT-A
TMT-B vs. TMT-B'	ccTMT-B	TMT-B
	ccTMT-A	TMT-A
	ccTMT-B	cTMT-A
	ccTMT-A	cTMT-B

Chapter 3

Results

3.1 Spectral Analysis

The spectral analysis aimed to investigate the activity patterns in different frequency bands (δ, θ, α, and β) during the TMT tasks. Figure 3.1 displays the 2D topographical map of spectral power density for RS, TMT-A, cTMT-A, and ccTMT-A.

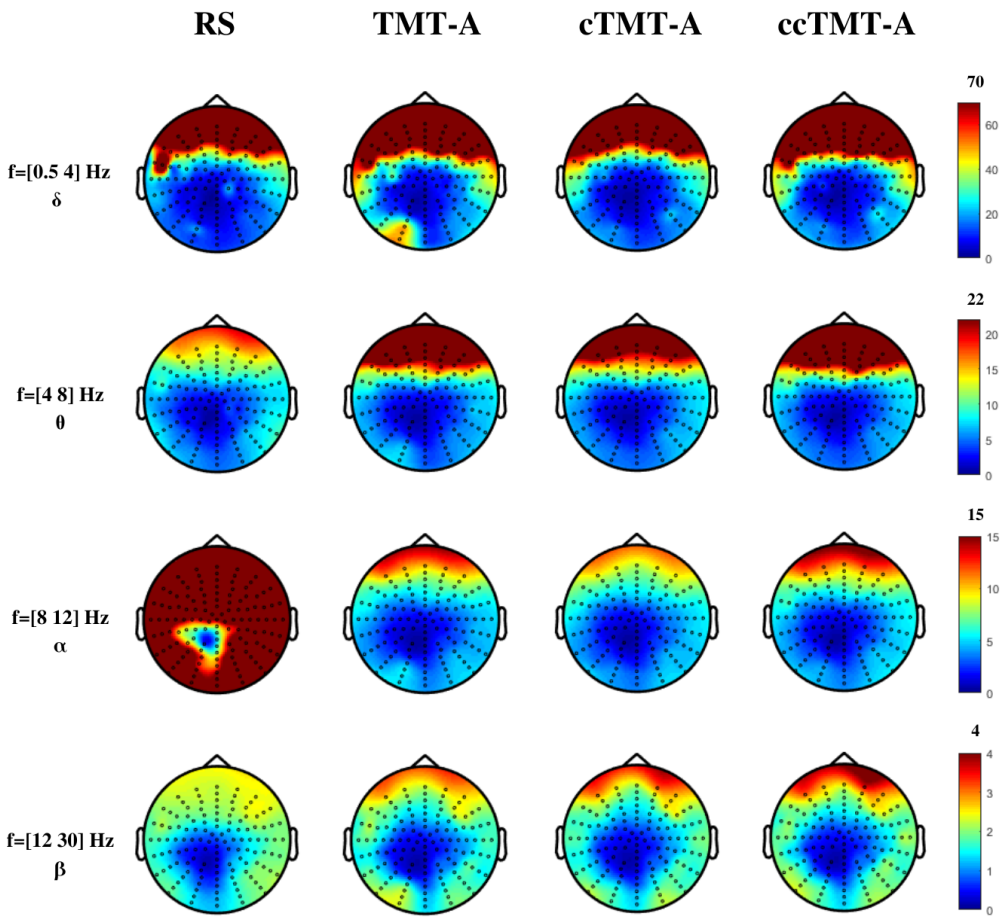

Figure 3.1: 2D topographical map of spectral power density across all subjects (n=30), for each frequency band (δ: 0.5-4 Hz, θ: 4-8 Hz, α: 8-12 Hz, and β: 12-30 Hz) in RS, TMT-A, cTMT-A, and ccTMT-A conditions. The color scale represents the relative intensity of the values in the graph: red for higher amplitude and blue for the lowest. RS = Resting State. TMT = Trail Making Test. cTMT = color Trail Making Test. ccTMT = color classic Trail Making Test.

The color-coded map represents the relative contribution of spectral power intensity in different brain regions based on electrode recordings. Distinct patterns of activity can be observed in various brain regions. The δ and θ bands exhibit increased activity in the frontal regions, indicating greater involvement of the prefrontal cortex (PFC) during TMT-A compared to the α and β bands. Additionally, in the δ band during TMT-A and in the β band during all TMT-A versions, there is observable activity in the left/right occipital lobe, suggesting specific engagement of the occipital cortex during task execution. When comparing the three TMT-A versions, it is evident that cTMT-A elicits the least activation of the PFC in the θ and α bands. Furthermore, during RS in the α band, all brain regions show significant involvement. Additionally, Figure 3.2 presents the 2D topographical map of spectral power density for RS, TMT-B, cTMT-B, and ccTMT-B. Similarly to Figure 3.1, same patterns were observed for all test versions in δ, θ, α, and β bands.

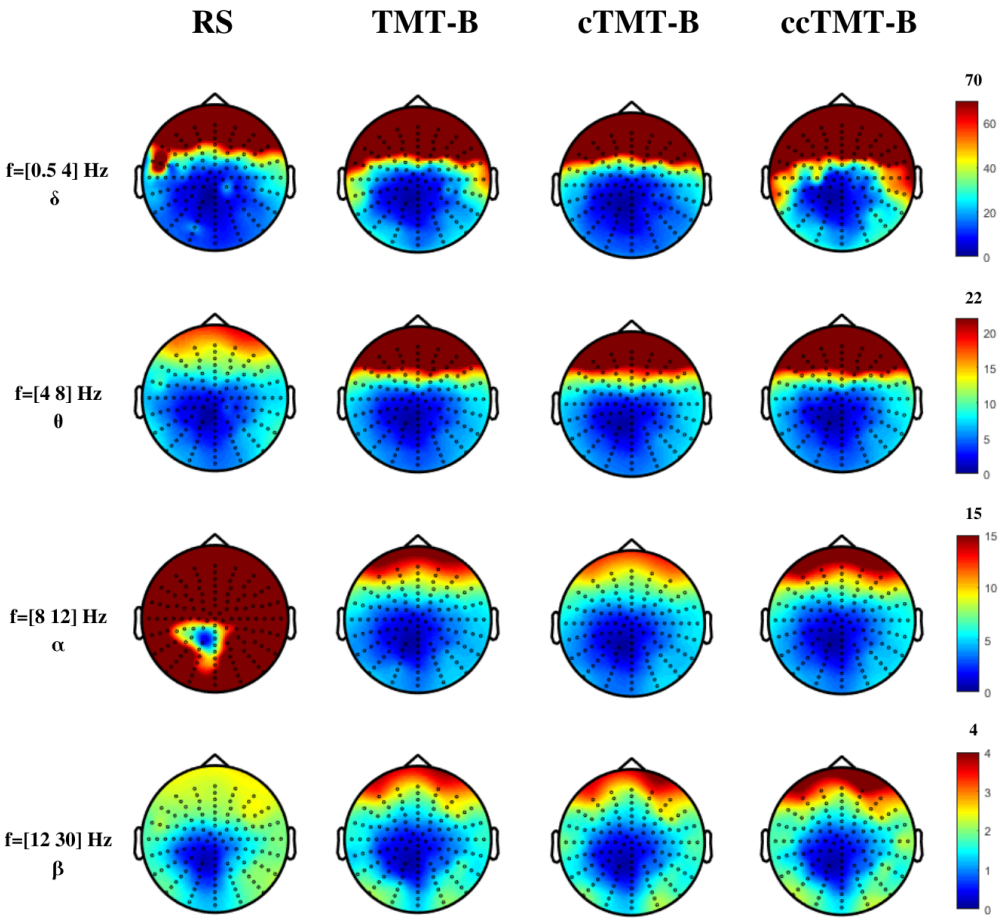

Figure 3.2: 2D topographical map of spectral power density across all subjects (n=30), for each frequency band (δ: 0.5-4 Hz, θ: 4-8 Hz, α: 8-12 Hz, and β: 12-30 Hz) in RS, TMT-B, cTMT-B, and ccTMT-B conditions. The color scale represents the relative intensity of the values in the graph: red for higher amplitude and blue for the lowest. RS = Resting State. TMT = Trail Making Test. cTMT = color Trail Making Test. ccTMT = color classic Trail Making Test.

Moreover, we performed paired non-parametric two-tailed t-tests to examine the statistical differences in density values between the conditions specified in Table 2.1. The significance level for all tests was set at 5%. While visual inspection suggests that dark red/blue areas in the brain may indicate differences or higher activity at the corresponding electrode locations, it is important to note that statistically significant differences (p-value $< \alpha = 0.05$) are marked by an asterisk ($*$). Figure 3.3 displays the results

of the paired t-tests between TMT-A and TMT-B, cTMT-A and cTMT-B, and ccTMT-A and ccTMT-B conditions.

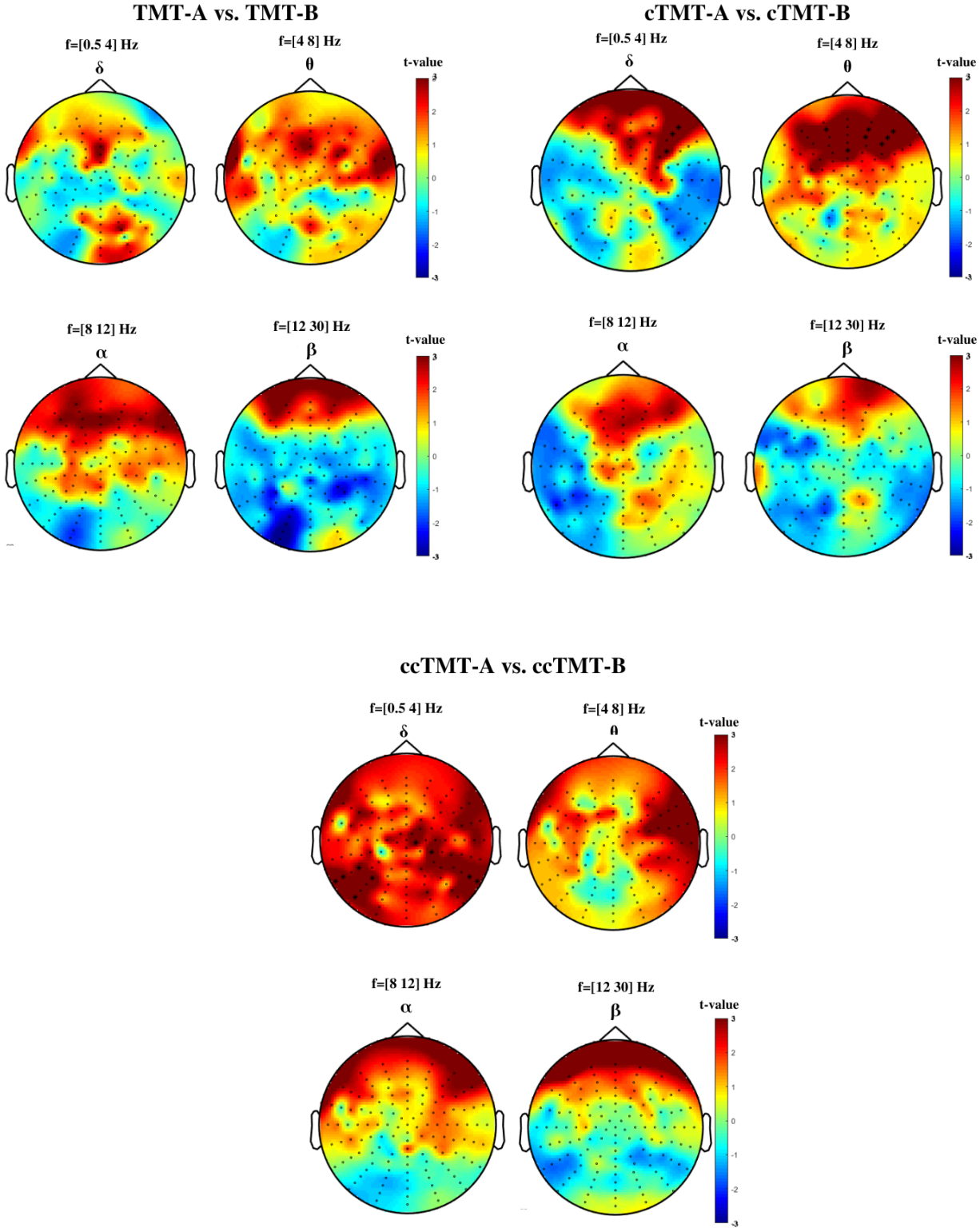

Figure 3.3: 2D topographical maps depicting the statistical differences in density values between part A and B for TMT, cTMT, and ccTMT versions. The significance of the differences was determined using non-parametric two-tailed t-test. Statistically significant electrode values (p-value $< \alpha = 0.05$) are indicated by the marker "$*$". Warmer colors indicate higher activity for part B, while colder colors indicate higher activity for part A. TMT = Trail Making Test. cTMT = color Trail Making Test. ccTMT = color classic Trail Making Test.

Additionally, Figures 3.4 and 3.5 show the results of the paired t-tests between RS and TMT-A, TMT-B, cTMT-A, cTMT-B, ccTMT-A and ccTMT-B conditions.

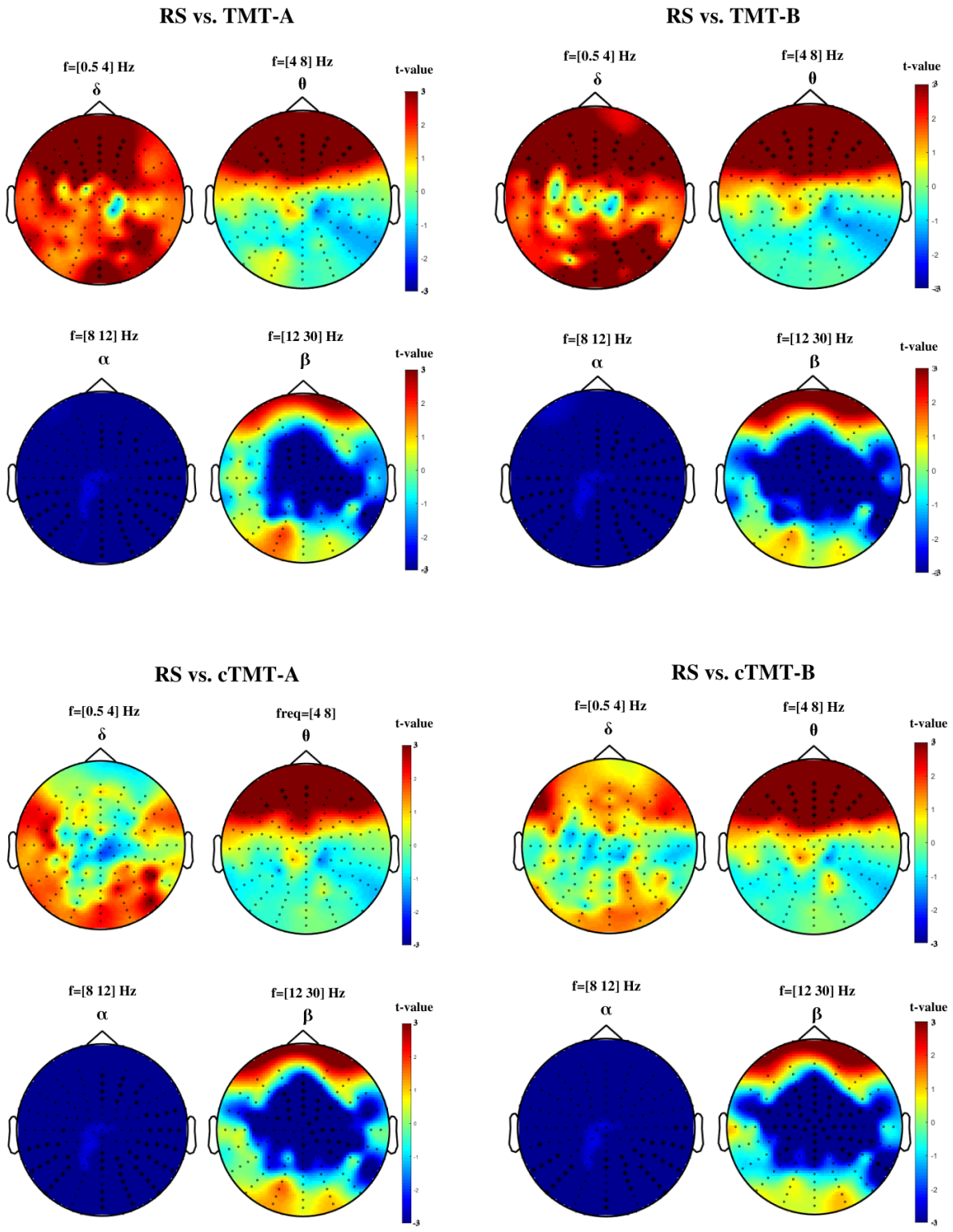

Figure 3.4: 2D topographical maps depicting the statistical differences in density values between RS and TMT-A, TMT-B, cTMT-A, and cTMT-B. The significance of the differences was determined using non-parametric two-tailed t-test. Statistically significant electrode values (p-value $< \alpha = 0.05$) are indicated by the marker "$*$". Warmer colors indicate higher activity for condition TMT-A, TMT-B, cTMT-A and cTMT-B, while colder colors indicate higher activity for RS. RS = Resting State. TMT = Trail Making Test. cTMT = color Trail Making Test.

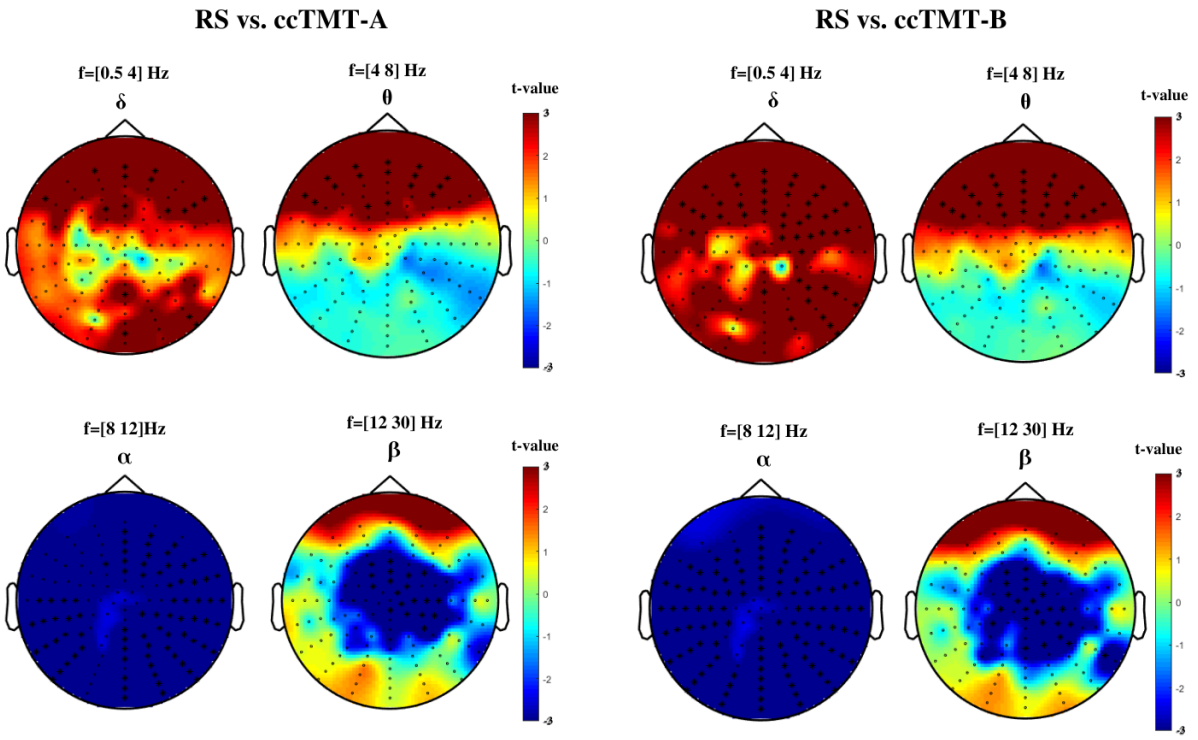

Figure 3.5: 2D topographical maps depicting the statistical differences in density values between RS vs. ccTMT-A and RS vs. ccTMT-B. The significance of the differences was determined using non-parametric two-tailed t-test. Statistically significant electrode values (p-value $< \alpha = 0.05$) are indicated by the marker "$*$". Warmer colors indicate higher activity for condition ccTMT-A and ccTMT-B, while colder colors indicate higher activity for RS. RS = Resting State. ccTMT = color classic Trail Making Test.

Although there appears to be greater activation of the PFC during TMT-A compared to TMT-B, as shown in the first row of Figure 3.3 for the α and β bands, these differences are not statistically significant. The same applies to the left occipital cortex, which shows increased activation during TMT-A but does not reach statistical significance. However, in the comparison between cTMT-A and cTMT-B, there is a statistically significant difference (p-value $< \alpha = 0.05$) in the activation of the right PFC in the δ band and the PFC in the θ band, indicating greater engagement of the PFC during TMT-B. Finally, for the comparison between ccTMT-A and ccTMT-B, as shown in the second row of Figure 3.3 there is a significant (p-value $< \alpha = 0.05$) and higher activation of the right and left parietal cortex in the δ band during ccTMT-B.

In the δ band, there is a significant increase (p-value $< \alpha = 0.05$) in activity observed in the frontal and occipital cortex for TMT-A, TMT-B, ccTMT-A, and ccTMT-B versions compared to RS, as seen in both Figures 3.4 and 3.5. This activation is more extensive for ccTMT compared to TMT. Also, in the α band, there are significant differences observed in all brain regions between the RS and all TMT versions. This aligns with previous research in cognitive neuroscience, which has shown that α activity in visual brain regions increases when individuals close their eyes, indicating a state of relaxation (Berger, 1929). Furthermore, a significant increase (p-value $< \alpha = 0.05$) in activity was observed in frontal cortex for all TMT versions compared to the RS in the θ band, suggesting involvement in cognitive processes related to attention, working memory, and more during TMT tasks. Additionally, a significant increase (p-value $< \alpha = 0.05$) in activity was observed in the medial parietal cortex for the RS compared to all TMT versions in both the θ and β bands.

Significant differences (p-value $< \alpha = 0.05$) in cortical activation were observed between TMT-A and

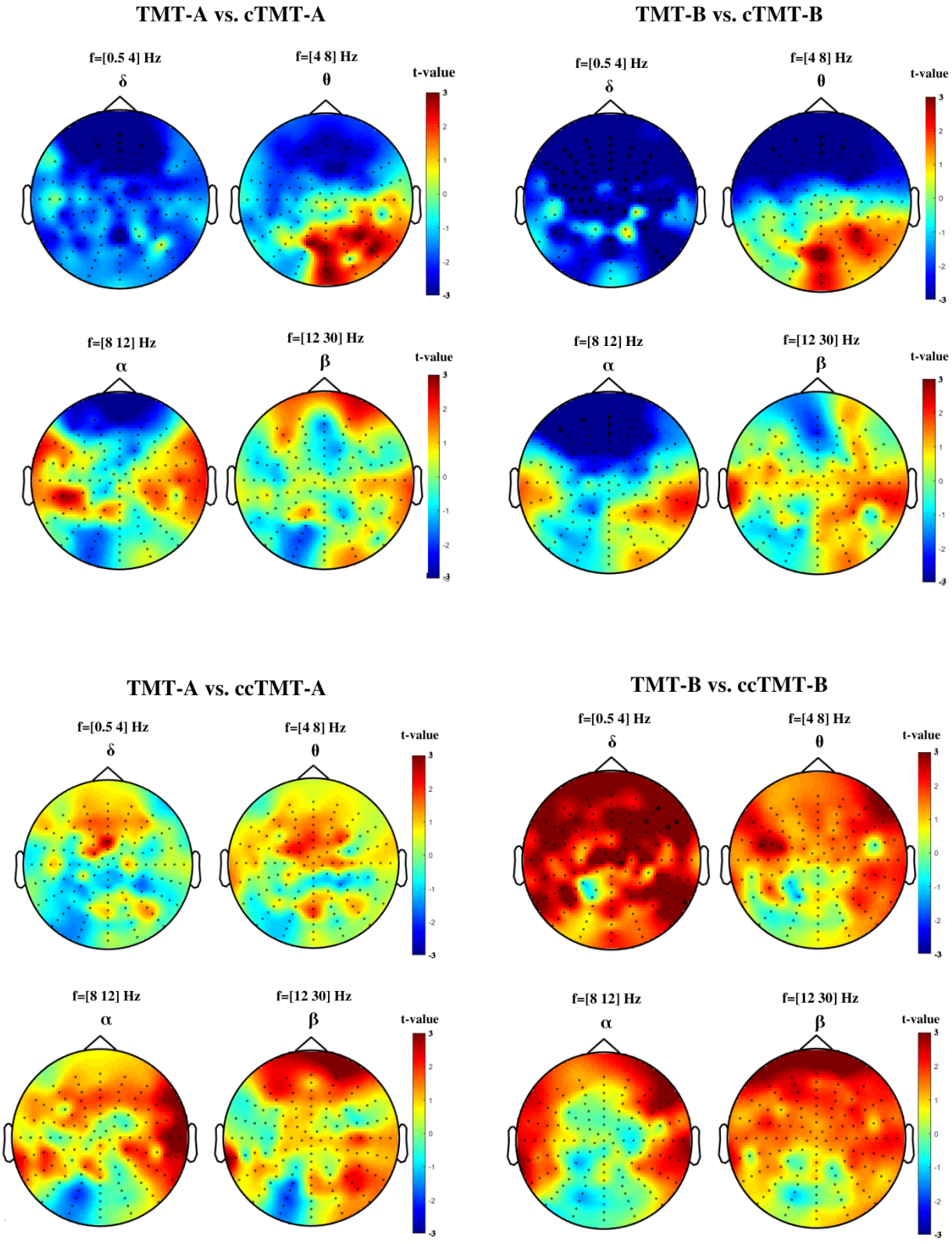

Figure 3.6: 2D topographical maps depicting the statistical differences in density values between TMT-A vs. cTMT-A, TMT-B vs. cTMT-B, TMT-A vs. ccTMT-A, and TMT-B vs. ccTMT-B. The significance of the differences was determined using non-parametric two-tailed t-test. Statistically significant electrode values (p-value $< \alpha = 0.05$) are indicated by the marker "$*$". Warmer colors indicate higher activity for condition cTMT-A, cTMT-B, ccTMT-A, and ccTMT-B, while colder colors indicate higher activity for TMT-A or TMT-B.

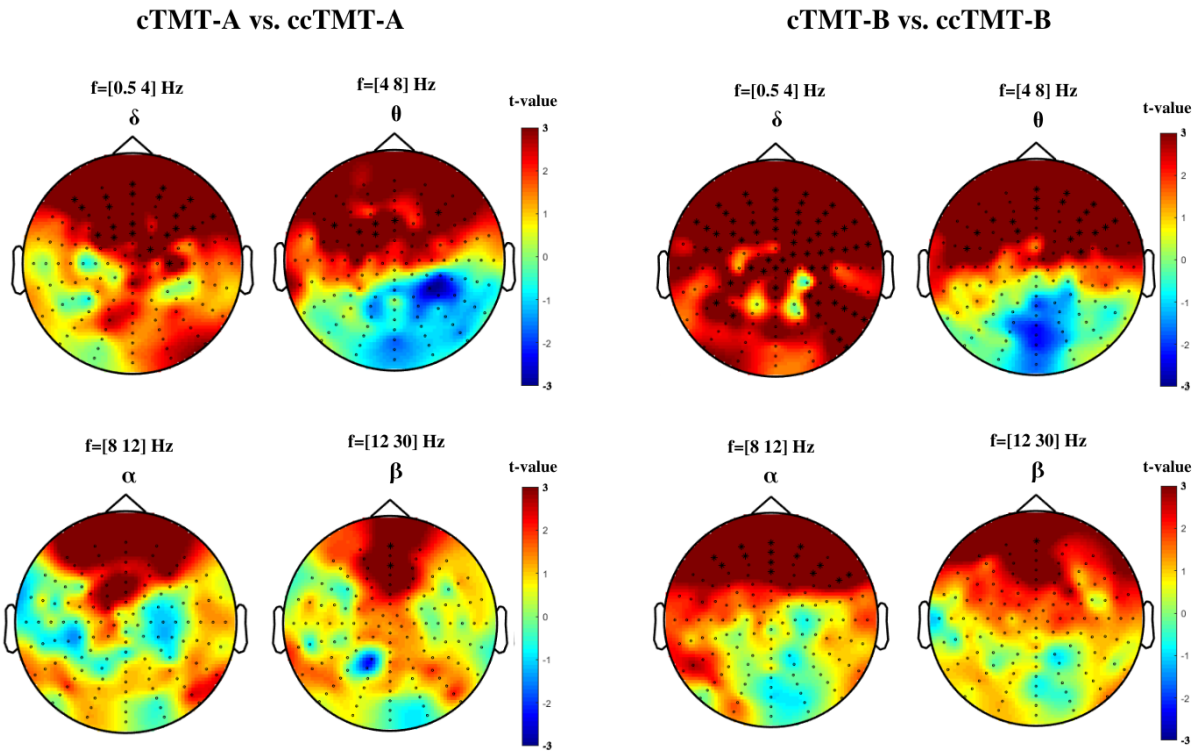

Figure 3.7: 2D topographical maps depicting the statistical differences in density values between cTMT-A vs. ccTMT-A and cTMT-B vs. ccTMT-B. The significance of the differences was determined using non-parametric two-tailed t-test. Statistically significant electrode values (p-value < α = 0.05) are indicated by the marker "$*$". Warmer colors indicate higher activity for condition ccTMT-A or ccTMT-B, while colder colors indicate higher activity for cTMT-A or cTMT-B.

cTMT-A, as well as between TMT-B and cTMT-B. Specifically, TMT-A showed a significant increase in activity in the PFC, particularly in the δ band, indicating higher engagement compared to cTMT-A. This pattern was similarly observed for TMT-B, with significant increases in the θ and α bands compared to cTMT-B. These findings suggest that the TMT task elicit greater PFC activation than the cTMT. No significant differences were found when comparing TMT-A and ccTMT-A, indicating similar levels of cortical activation between these versions. However, between TMT-B and ccTMT-B, there was a significantly higher activation observed in the right PFC in the δ band. Furthermore, significant activation in the PFC was consistently observed across all frequency bands when comparing the cTMT and ccTMT A and B parts, except for the α band in part A. These findings highlight the critical involvement of the PFC in cognitive processes related to attention, working memory, and executive functions during the different versions of the TMT tasks.

3.2 Source Localization

The sLORETA source localization analysis yielded statistical brain maps for the δ, θ, α, and β frequency bands, as shown in Figures 3.8, 3.9, and 3.10. These maps were color-coded to represent t-values, with negative t-values (blue) indicating higher activity in group B tasks and positive t-values (red) indicating higher activity in group A tasks (see Table 2.1). Detailed results for each pairwise comparison of the TMT tasks can be found in Tables 3.1, 3.2, 3.3, and 3.4. These tables provide significant t-values, MNI (X,Y,Z) coordinates, and corresponding Brodmann areas, gyrus, and lobes associated with the

observed differences in brain activity.

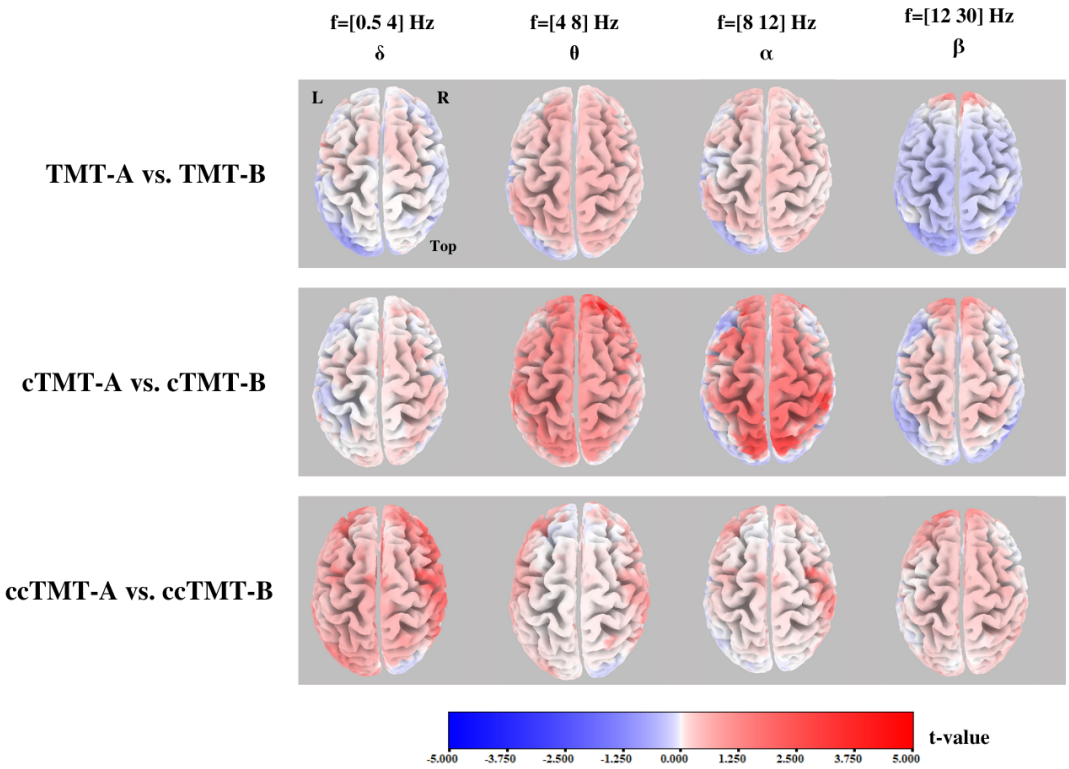

Figure 3.8: sLORETA statistical brain maps of source localization results between part A and B for TMT (t = 3.727, p < 0.05), cTMT (t = 4.057, p < 0.05), and ccTMT (t = 3.717, p < 0.05) versions. The significance of the differences was determined using a non-parametric two-tailed t-test. Warmer colors indicate higher activity for part B, while colder colors indicate higher activity for part A. TMT = Trail Making Test. cTMT = color Trail Making Test. ccTMT = color classic Trail Making Test. L = left. R = right.

Table 3.1: sLORETA statistical significant t-values, MNI (X,Y,Z) coordinates, corresponding Brodmann areas, gyrus and lobes between part A and B for TMT (t = 3.727, p < 0.05), cTMT (t = 4.057, p < 0.05), and ccTMT (t = 3.717, p < 0.05) versions. The significance of the differences was determined using a non-parametric two-tailed t-test. TMT = Trail Making Test. cTMT = color Trail Making Test. ccTMT = color classic Trail Making Test. mm = millimeters.

		t-value	MNI coordinates (X,Y,Z)mm	Brodmann Area	Gyrus	Lobe
TMT-A	**delta**					
vs.	**theta**					
TMT-B	**alpha**					
t(0.05)=3.727	**beta**					
cTMT-A	**delta**					
vs.	**theta**	4.52	(25, 55, 25)	10	Middle Frontal	Frontal
cTMT-B	**alpha**	4.13	(50, -35, 55)	40	Postcentral	Parietal
t(0.05)=4.057	**beta**					
ccTMT-A	**delta**	3.89	(-10, 55, -5)	10	Medial Frontal	Frontal
vs.	**theta**					
ccTMT-B	**alpha**	3.92	(-5, 55, 5)	10	Medial Frontal	Frontal
t(0.05)=3.717	**beta**					

3. RESULTS

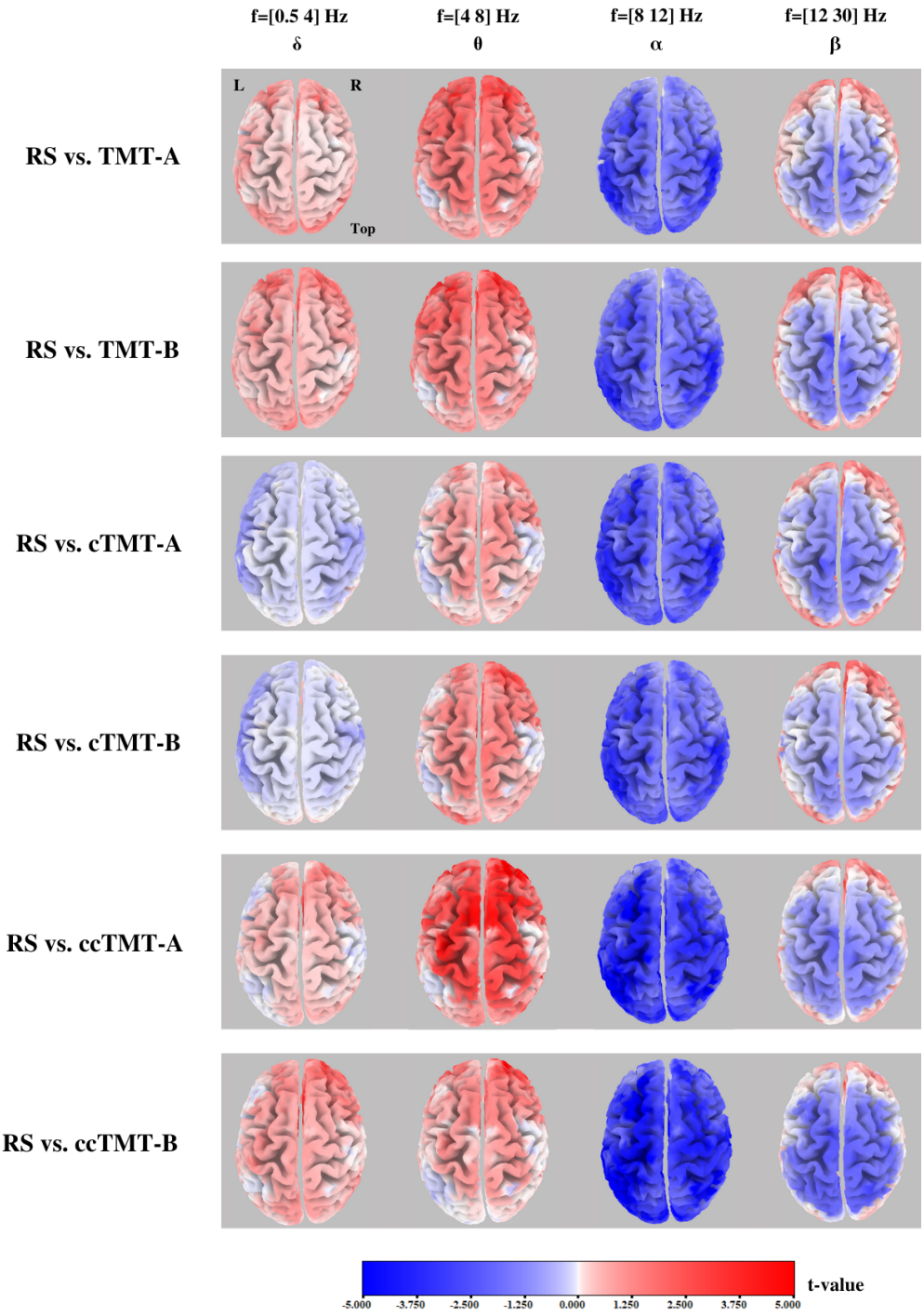

Figure 3.9: sLORETA statistical brain maps of source localization results between RS vs. TMT-A (t = 3.717, p < 0.05), TMT-B (t = 3.816, p < 0.05), cTMT-A (t = 4.086, p < 0.05), cTMT-B (t = 3.996, p < 0.05), ccTMT-A (t = 4.250, p < 0.05), and ccTMT-B (t = 4.277, p < 0.05). The significance of the differences was determined using a non-parametric two-tailed t-test. Warmer colors indicate higher activity for TMT versions, while colder colors indicate higher activity for RS. RS = Resting State. TMT = Trail Making Test. cTMT = color Trail Making Test. ccTMT = color classic Trail Making Test. L = left. R = right.

Among all pairwise comparisons of the TMT tasks for source localization, statistically significant differences were observed except for TMT-A vs. TMT-B ($t = 3.727, p < 0.05$), TMT-A vs. ccTMT-A ($t = 3.811, p < 0.05$), and TMT-B vs. ccTMT-B ($t = 3.884, p < 0.05$). However, when comparing the different parts (A and B) within each TMT version (refer to Figure 3.8 and Table 3.1), significant

Table 3.2: sLORETA statistical significant t-values, MNI (X,Y,Z) coordinates, corresponding Brodmann areas, gyrus and lobes between RS vs. TMT-A (t = 3.717, p < 0.05), TMT-B (t = 3.816, p < 0.05), and cTMT-A (t = 4.086, p < 0.05). The significance of the differences was determined using a non-parametric two-tailed t-test. RS = Resting State. TMT = Trail Making Test. cTMT = color Trail Making Test. mm = millimeters.

		t-value	MNI coordinates (X,Y,Z)mm	Brodmann Area	Gyrus	Lobe
RS	**delta**	3.77	(20, 40, 45)	8	Superior Frontal	Frontal
vs.		4.55	(25, 40, 35)	9	Superior Frontal	Frontal
TMT-A	**theta**	4.12	(-10, 25, 35)	32	Cingulate	Limbic
t(0.05)=3.717		3.94	(-25, 56, 4)	10	Superior Frontal	Frontal
		-4.86	(-5, -50, 50)	7	Precuneus	Parietal
		-4.07	(-51, -39, 50)	40	Inferior Parietal Lobule	Parietal
		-4.42	(49, -20, 50)	3	Postcentral	Parietal
	alpha	-4.41	(50, -25, 50)	2	Postcentral	Parietal
		-4.05	(54, -25, 0)	22	Superior Temporal	Temporal
		-4.28	(-1, -25, 31)	23	Cingulate	Limbic
		-4.16	(36, -15, 21)	13	Insula	Sub-lobar
	beta	3.73	(5, 60, -5)	10	Superior Frontal	Frontal
RS	**delta**	4.05	(-25 , 50, -15)	11	Superior Frontal	Frontal
vs.		5.58	(-20, 50, 0)	10	Superior Frontal	Frontal
TMT-B	**theta**	5.37	(46, 51, 0)	10	Inferior Frontal	Frontal
t(0.05)=3.816		4.41	(-4, 50, 0)	32	Anterior Cingulate	Limbic
		-5.15	(15, -55, 50)	7	Precuneus	Parietal
		-4.16	(-36 , -55, 50)	40	Inferior Parietal Lobule	Parietal
		-3.88	(-43, -24, 50)	2	Postcentral	Parietal
	alpha	-4.03	(-40, -25, 50	3	Postcentral	Parietal
		-4.24	(-51, -59 , 8)	39	Middle Temporal	Temporal
		-4.53	(-14, -29, 38)	31	Cingulate	Limbic
		-3.96	(-47, -42 , 18)	13	Insula	Sub-lobar
	beta	-4.12	(5, -5, 70)	6	Superior Frontal	Frontal
		3.83	(-5, 57, -1)	11	Medial Frontal	Frontal
RS	**delta**					
vs.	**theta**					
cTMT-A		-5.20	(-5, -50, 50)	7	Precuneus	Parietal
t(0.05)=4.086		-4.51	(-45, -46, 53)	40	Inferior Parietal Lobule	Parietal
	alpha	-4.30	(-47, -34 , 53)	2	Postcentral	Parietal
		-4.23	(-55 , -64, 16)	19	Middle Temporal	Occipital
		-4.26	(-1 , -89, 16)	18	Cuneus	Occipital
		-5.10	(-41, -5, 39)	6	Precentral	Frontal
	beta	-4.42	(-15, -35, 60)	4	Precentral	Frontal

differences were observed. Specifically, the middle frontal lobe showed significantly higher activation for cTMT-B than cTMT-A in the θ band ($t = 4.52, p < 0.05$), and the postcentral gyrus in the parietal lobe exhibited significantly higher activation for cTMT-B than cTMT-A in the α band ($t = 4.13, p < 0.05$). Additionally, the medial frontal gyrus in the frontal lobe demonstrated significantly higher activation for ccTMT-B than ccTMT-A in both the δ ($t = 3.89, p < 0.05$) and α ($t = 3.92, p < 0.05$) bands.

Regarding the pairwise comparisons between the RS and each TMT task (refer to Figure 3.9 and Tables 3.2 and 3.3), significant differences were observed in various brain regions across different lobes, specifically in the α band. The frontal lobe showed statistical significance for cTMT-A

Table 3.3: sLORETA statistical significant t-values, MNI (X,Y,Z) coordinates, corresponding Brodmann areas, gyrus and lobes between RS vs. cTMT-B (t = 3.996, p < 0.05), ccTMT-A (t = 4.250, p < 0.05), and ccTMT-B (t = 4.277, p < 0.05). The significance of the differences was determined using a non-parametric two-tailed t-test. RS = Resting State. cTMT = color Trail Making Test. ccTMT = color classic Trail Making Test. mm = millimeters.

		t-value	MNI coord (X,Y,Z)mm	Brodmann Area	Gyrus	Lobe
RS vs. cTMT-B t(0.05)=3.996	**delta**					
	theta	4.43	(20 , 55, 3)	9	Superior Frontal	Frontal
		4.15	(31, 46, 30)	10	Middle Frontal	Frontal
	alpha	-5.16	(-35, -55, 4)	40	Inferior Parietal Lobule	Parietal
		-4.95	(-40, -28, 4)	2	Postcentral	Parietal
		-4.06	(41, -24, 41)	3	Postcentral	Parietal
		-4.29	(-9, -55, 40)	7	Precuneus	Parietal
		-4.13	(-11, -49, 4)	31	Cingulate	Limbic
		-4.34	(-54, -55, 12)	39	Superior Temporal	Temporal
	beta	4.16	(30, 50, -5)	10	Middle Frontal	Frontal
		4.02	(30, 48, -9)	11	Middle Frontal	Frontal
RS vs. ccTMT-A t(0.05)=4.250	**delta**					
	theta	6.06	(-40 , 40, -5)	47	Middle Frontal	Frontal
		5.06	(-44 , 50, -5)	10	Middle Frontal	Frontal
		4.66	(-29, -9, 46)	6	Middle Frontal	Frontal
		4.30	(-29, -24 , 48)	3	Postcentral	Parietal
		4.73	(-37, -5 , 1)	13	Insula	Sub-lobar
		4.37	(2, -7 , 35)	24	Cingulate	Limbic
		4.49	(2, 14 , 53)	8	Superior Frontal	Frontal
	alpha	-6.51	(-35, -25, 40)	3	Postcentral	Frontal
		-5.01	(5, -15 , 40)	24	Cingulate	Limbic
		-5.19	(5, -65 , 42)	7	Precuneus	Parietal
		-6.22	(-36, -30, 42)	2	Sub-Gyral	Parietal
		-4.70	(-26, 25 , 46)	8	Middle Frontal	Frontal
		-5.12	(4, -20, 37)	23	Cingulate	Limbic
		-4.94	(-42, -9, 16)	13	Insula	Sub-lobar
		-5.59	(-54, -27, 16)	40	Postcentral	Parietal
		-5.49	(-53, -29, 16)	42	Superior Temporal	Temporal
		-5.18	(-41, -80, 26)	19	Superior Occipital	Occipital
	beta					
RS vs. ccTMT-B t(0.05)=4.277	**delta**	5.29	(-5, 25, 20)	24	Anterior Cingulate	Limbic
		4.47	(-5, 45, -22)	11	Orbital	Frontal
		4.62	(31, 17, 16)	13	Insula	Sub-lobar
		4.60	(5, 31, 16)	24	Anterior Cingulate	Limbic
		5.01	(-4, 21, 22)	33	Anterior Cingulate	Limbic
	theta	5.53	(-30, 40, -5)	11	Middle Frontal	Frontal
		4.43	(-30, 55, -5)	10	Middle Frontal	Frontal
	alpha	-6.85	(-40, -65, 50)	7	Superior Parietal Lobule	Parietal
		-5.63	(-43, -56 , 50)	40	Inferior Parietal Lobule	Parietal
		-5.49	(-31, -28 , 50)	4	Precentral	Frontal
		-5.44	(-35, -26 , 50)	3	Postcentral	Parietal
		-5.33	(-26, -9 , 50)	6	Middle Frontal	Frontal
		-5.02	(-24, 20 , 50)	8	Middle Frontal	Frontal
		-5.38	(-5, -46 , 50)	5	Paracentral Lobule	Frontal
		-5.59	(-2, -24 , 35)	23	Cingulate	Limbic
		-5.04	(-14, -86, 36)	19	Cuneus	Occipital
	beta					

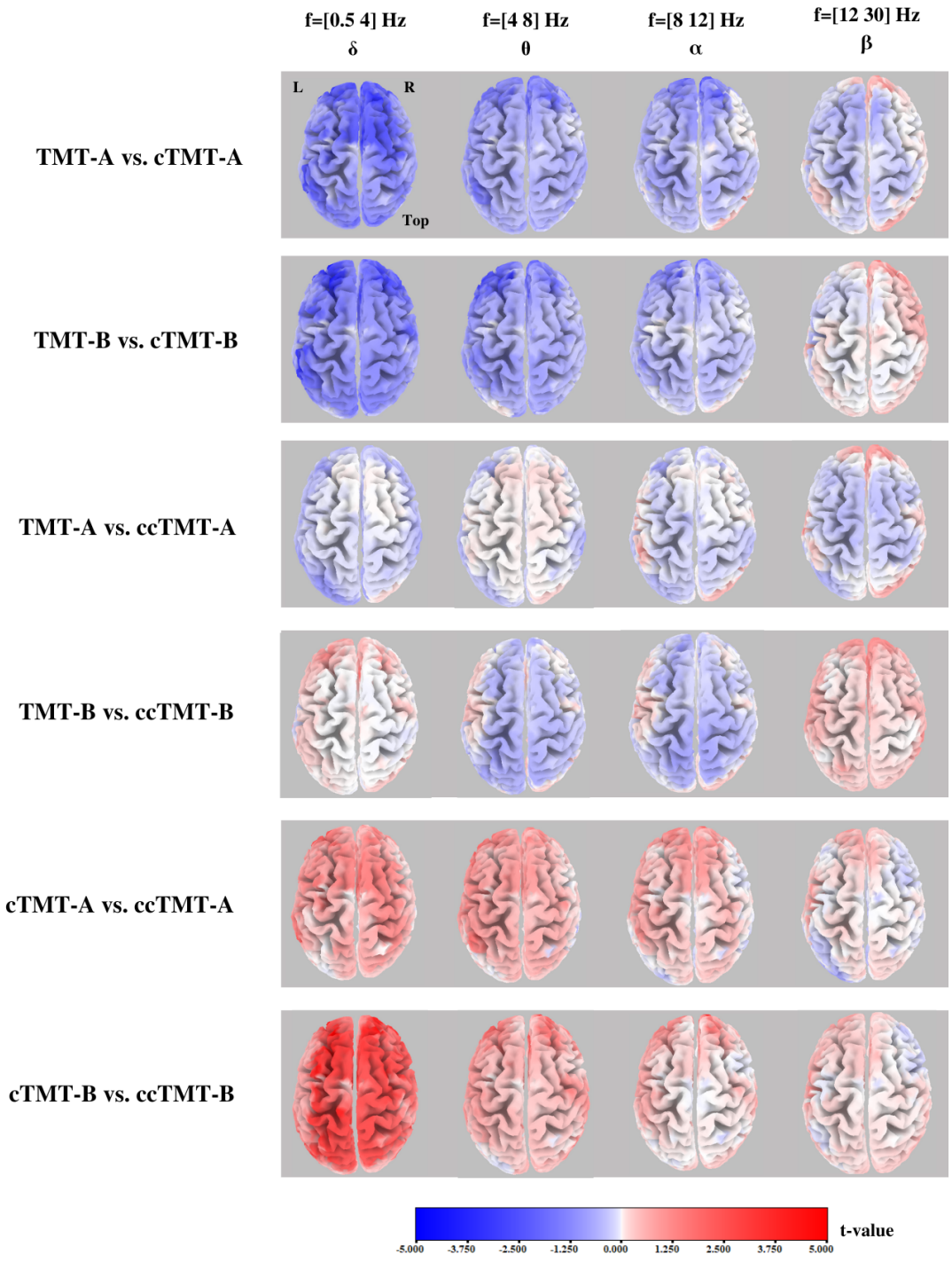

Figure 3.10: sLORETA statistical brain maps of source localization results for TMT-A vs. cTMT-A (t = 3.869, p < 0.05), TMT-B vs. cTMT-B (t = 3.851, p < 0.05), TMT-A vs. ccTMT-A (t = 3.811, p < 0.05), TMT-B vs. ccTMT-B (t = 3.844, p < 0.05), cTMT-A vs. ccTMT-A (t = 4.027, p < 0.05), and cTMT-B vs. ccTMT-B (t = 3.894, p < 0.05). The significance of the differences was determined using a non-parametric two-tailed t-test. Warmer colors indicate higher activity for condition 2, while colder colors indicate higher activity for condition 1. TMT = Trail Making Test. cTMT = color Trail Making Test. ccTMT = color classic Trail Making Test. L = left. R = right.

($t = -5.10, p < 0.05$), ccTMT-A ($t = -6.51, p < 0.05$), and ccTMT-B ($t = -5.49, p < 0.05$). The parietal lobe exhibited significance for TMT-A ($t = -4.86, p < 0.05$), TMT-B ($t = -5.15, p < 0.05$), cTMT-A ($t = -5.20, p < 0.05$), cTMT-B ($t = -5.16, p < 0.05$), ccTMT-A ($t = -6.22, p < 0.05$), and ccTMT-B ($t = -6.85, p < 0.05$). The temporal lobe showed significance for , TMT-B ($t = -4.24, p < 0.05$), cTMT-

Table 3.4: sLORETA statistical significant t-values, MNI (X,Y,Z) coordinates, corresponding Brodmann areas, gyrus and lobes for TMT-A vs. cTMT-A (t = 3.869, p < 0.05), TMT-B vs. cTMT-B (t = 3.851, p < 0.05), TMT-A vs. ccTMT-A (t = 3.811, p < 0.05), TMT-B vs. ccTMT-B (t = 3.844, p < 0.05), cTMT-A vs. ccTMT-A (t = 4.027, p < 0.05), and cTMT-B vs. ccTMT-B (t = 3.894, p < 0.05). The significance of the differences was determined using a non-parametric two-tailed t-test. TMT = Trail Making Test. cTMT = color Trail Making Test. ccTMT = color classic Trail Making Test. mm = millimeters.

		t-value	MNI coordinates (X,Y,Z)mm	Brodmann Area	Gyrus	Lobe
TMT-A vs. cTMT-A t(0.05)=3.869	**delta**	-4.61	(-30 , -5, 4)	6	Middle Frontal	Frontal
		-3.92	(-9, -1, 45)	24	Cingulate	Limbic
		-4.10	(19, 42, 45)	8	Superior Frontal	Frontal
	theta	-3.98	(5, 40, 10)	32	Anterior Cingulate	Limbic
	alpha					
	beta					
TMT-B vs. cTMT-B t(0.05)= 3.851	**delta**	-5.36	(-20 , 45, 4)	9	Superior Frontal	Frontal
		-4.11	(23 , 40 , 4)	9	Middle Frontal	Frontal
		-4.17	(-57, -44, 40)	40	Inferior Parietal Lobule	Parietal
	theta	-4.74	(-25, 50, 5)	10	Superior Frontal	Frontal
		-4.03	(-25, 40, 39)	9	Middle Frontal	Frontal
	alpha	-4.28	(-25, 50, 5)	10	Superior Frontal	Frontal
	beta					
TMT-A vs. ccTMT-A t(0.05)= 3.811	**delta**					
	theta					
	alpha					
	beta					
TMT-B vs. ccTMT-B t(0.05)= 3.884	**delta**					
	theta					
	alpha					
	beta					
cTMT-A vs. ccTMT-A t(0.05)= 4.027	**delta**					
	theta	4.04	(-10, 45, 5)	32	Anterior Cingulate	Limbic
	alpha					
	beta					
cTMT-B vs. ccTMT-B t(0.05)= 3.894	**delta**	5.14	(-25, 60, 15)	10	Middle Frontal	Frontal
		4.58	(-25 , 31 , 44)	8	Middle Frontal	Frontal
		4.40	(-25 , -8 , 4)	6	Middle Frontal	Frontal
		4.27	(-25, -51, 61)	7	Superior Parietal Lobule	Parietal
		4.01	(-25, -50, 70)	5	Postcentral	Parietal
		4.09	(-19 , -28, 45)	31	Cingulate	Limbic
		4.02	(-33,-26, 45)	3	Postcentral	Parietal
		4.22	(41, -19, 4)	4	Precentral	Frontal
		3.91	(4, 5, 33)	24	Cingulate	Limbic
		4.59	(-18 , 4 , 49)	32	Cingulate	Limbic
		4.43	(-13, 24, 37)	9	Medial Frontal	Frontal
	theta	4.32	(20, 65, 10)	10	Superior Frontal	Frontal
		3.94	(9, 46, 10)	32	Anterior Cingulate	Limbic
		4.09	(9, 64, -9)	11	Superior Frontal	Frontal
	alpha	4.87	(15, 50, 10)	10	Medial Frontal	Frontal
	beta					

A ($t = -4.05, p < 0.05$), cTMT-B ($t = -4.34, p < 0.05$), and ccTMT-A ($t = -5.49, p < 0.05$). The occipital lobe demonstrated significance for cTMT-A ($t = -5.23, p < 0.05$), ccTMT-A ($t = -5.18, p < 0.05$), and ccTMT-B ($t = -5.04, p < 0.05$). Lastly, the limbic lobe exhibited significance for TMT-B ($t = -4.53, p < 0.05$), cTMT-A ($t = -4.28, p < 0.05$), cTMT-B ($t = -4.13, p < 0.05$), ccTMT-A ($t = -5.12, p < 0.05$), and ccTMT-B ($t = -5.59, p < 0.05$). Therefore, the parietal lobe consistently exhibits prominent and visually evident significant differences across all tested conditions in the α band for RS. In the δ band, a significant increase in activity was found in the superior frontal lobe for TMT-A ($t = 3.77, p < 0.05$) and TMT-B ($t = 4.05, p < 0.05$), compared to the RS. Moreover, in the ccTMT-B, there was a significant increase in activity observed in the anterior cingulate cortex (ACC) ($t = 5.29, p < 0.05$), compared to the RS. Additionally, in the θ band, the ccTMT-A task exhibits a pronounced and statistically significant difference in the frontal lobe ($t = 6.06, p < 0.05$), indicating higher activation compared to the other tested tasks in this brain region. Furthermore, TMT-A ($t = 4.55, p < 0.05$) shows higher activation in the superior frontal cortex, as well as TMT-B ($t = 5.88, p < 0.05$), cTMT-B ($t = 4.43, p < 0.05$), and the middle frontal cortex for ccTMT-B ($t = 5.53, p < 0.05$) compared to the RS. Moreover, in both TMT-A ($t = 4.12, p < 0.05$) and TMT-B ($t = 4.41, p < 0.05$) tasks, as well as in ccTMT-A ($t = 4.37, p < 0.05$), the cingulate gyrus demonstrated higher activation compared to the RS. Furthermore, Additionally, in the β band, there was higher activation observed in the frontal lobe for TMT-A ($t = 3.73, p < 0.05$), TMT-B ($t = 3.83, p < 0.05$), and cTMT-B ($t = 4.16, p < 0.05$) tasks, compared to the RS.

Finally, in the pairwise comparisons between part A and B for TMT vs. cTMT, TMT vs. ccTMT, and cTMT vs. ccTMT (see Figure 3.10 and Table 3.4), no significant differences were found between part A and B for TMT-A vs. ccTMT-A tasks across all four frequency bands. However, in the δ band, both parts A and B of TMT showed higher activity compared to cTMT, specifically in the MiFG ($t = -4.61, p < 0.05$) and superior frontal gyrus ($t = -5.36, p < 0.05$). Moreover, significant and extensive differences were observed in the δ band for cTMT-B vs. ccTMT-B, involving the middle frontal lobe ($t = 5.14, p < 0.05$), parietal lobe ($t = 4.27, p < 0.05$), and cingulate gyrus ($t = 4.59, p < 0.05$). Additionally, significant higher activity was observed in TMT-A compared to cTMT-A ($t = -3.98, p < 0.05$) and in their corresponding part B ($t = -4.74, p < 0.05$), specifically in the θ band localized in the frontal lobe and anterior cingulate cortex (ACC), respectively. Significant differences in the α band were observed in the pairwise comparison between TMT-B and cTMT-B ($t = -4.28, p < 0.05$) in the superior frontal lobe. Additionally, significant differences were found in the comparison between cTMT-B and ccTMT-B ($t = 4.87, p < 0.05$) in the medial frontal lobe. However, no significant changes were found in the β band for any pairwise comparison between part A and B of TMT and cTMT, TMT and ccTMT, and cTMT and ccTMT.

3.3 Functional Connectivity

The sLORETA FC analysis yielded statistical brain maps for the δ, θ, α, and β frequency bands, displaying the connections between pair-wise comparisons as listed in Table 2.1. These maps can be seen in Figures 3.11, 3.12, and 3.13. It's important to note that these figures show all connections without applying a statistical threshold, allowing for the visualization of all connections. Additionally, for statistically significant connections, the corresponding threshold was applied, and those connections are displayed in Figure 3.14.

When comparing TMT-B and TMT-A ($t = 4.766, p < 0.05$), a significant decrease in lagged θ connectivity was observed for TMT-B. This difference was found in several cortical regions, including the

left ACC, the right MiFG, the left inferior temporal gyrus, the right posterior cingulate (PCC), the left inferior frontal gyrus, and the left medial frontal gyrus. Additionally, TMT-A showed a significant increase in lagged β connectivity between the left postcentral gyrus and right ACC, the right cuneus and left parahippocampal gyrus, and the right paracentral lobule and left superior temporal gyrus.

In contrast, increased lagged δ and θ connectivity was observed for all versions of the TMT compared to the RS across multiple cortical regions, except for the δ band in cTMT-B. These connections were more prominent in the θ band. Furthermore, significant decreases in lagged α connectivity were found in specific comparisons. TMT-A showed a significant decrease in lagged α connectivity between the right postcentral gyrus and the right precentral gyrus compared to RS. Similarly, cTMT-B exhibited a significant decrease in lagged α connectivity between the right postcentral gyrus and the left precentral gyrus compared to RS. The same pattern was observed for ccTMT-A compared to RS, with significant decreases in lagged α connectivity between the left precentral gyrus, left cuneus, and the right postcentral gyrus. For RS compared to TMT-B and ccTMT-B, significant decreases in lagged α connectivity were more distributed across the entire cortex. Additionally, TMT-A showed a significant increase in lagged β connectivity compared to RS ($t = 4.412, p < 0.05$) between the right MiFG and the left inferior frontal gyrus. Similarly, cTMT-A exhibited increased lagged β connectivity compared to the RS($t = 4.355, p < 0.05$) between the left fusiform gyrus and the left ACC.

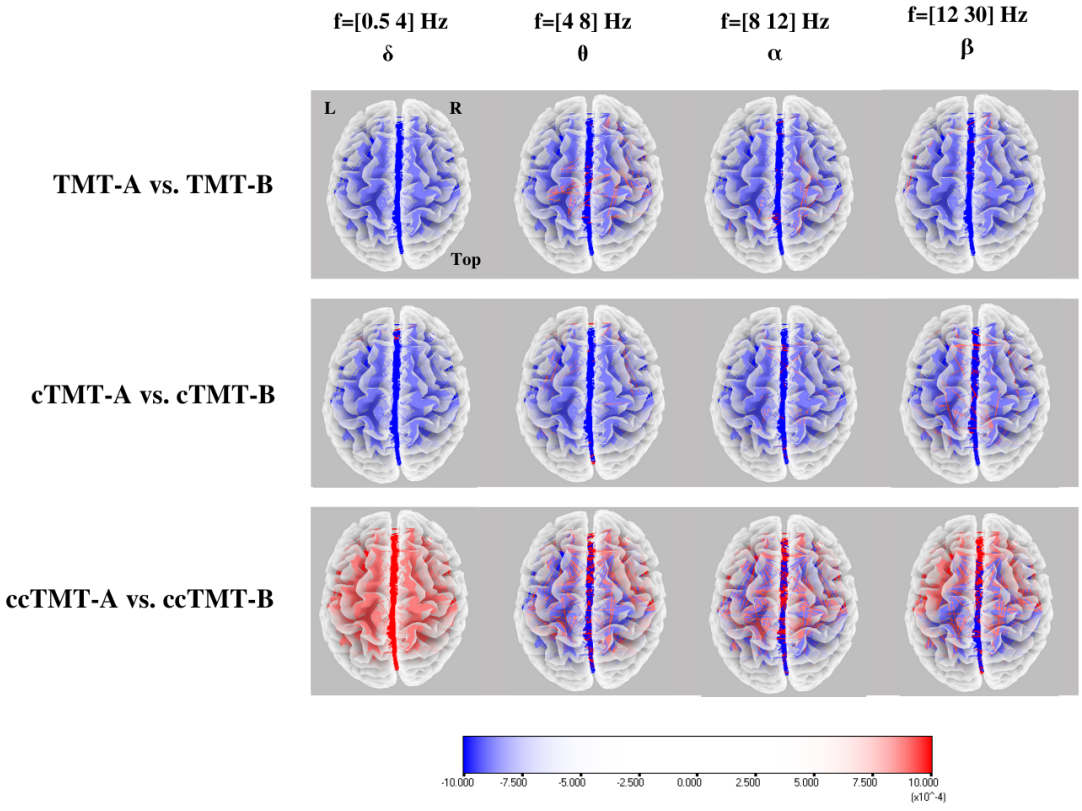

Figure 3.11: sLORETA functional connectivity brain maps showing all connections between part A and part B for TMT, cTMT, and ccTMT versions in the δ, θ, α, and β frequency bands. The color red indicates a significantly higher functional connectivity of part B compared to part A, while blue indicates a significantly lower functional connectivity. Please note that the maps are displayed without a statistical threshold applied, allowing for visualization of all connections. TMT = Trail Making Test. cTMT = color Trail Making Test. ccTMT = color classic Trail Making Test. L = left. R = right.

Finally, ccTMT-B demonstrated increased lagged θ connectivity compared to cTMT-B ($t = 4.648, p < 0.05$) involving several brain regions, such as the right uncus, left anterior cingulate, right

MiFG, and left superior temporal gyrus.

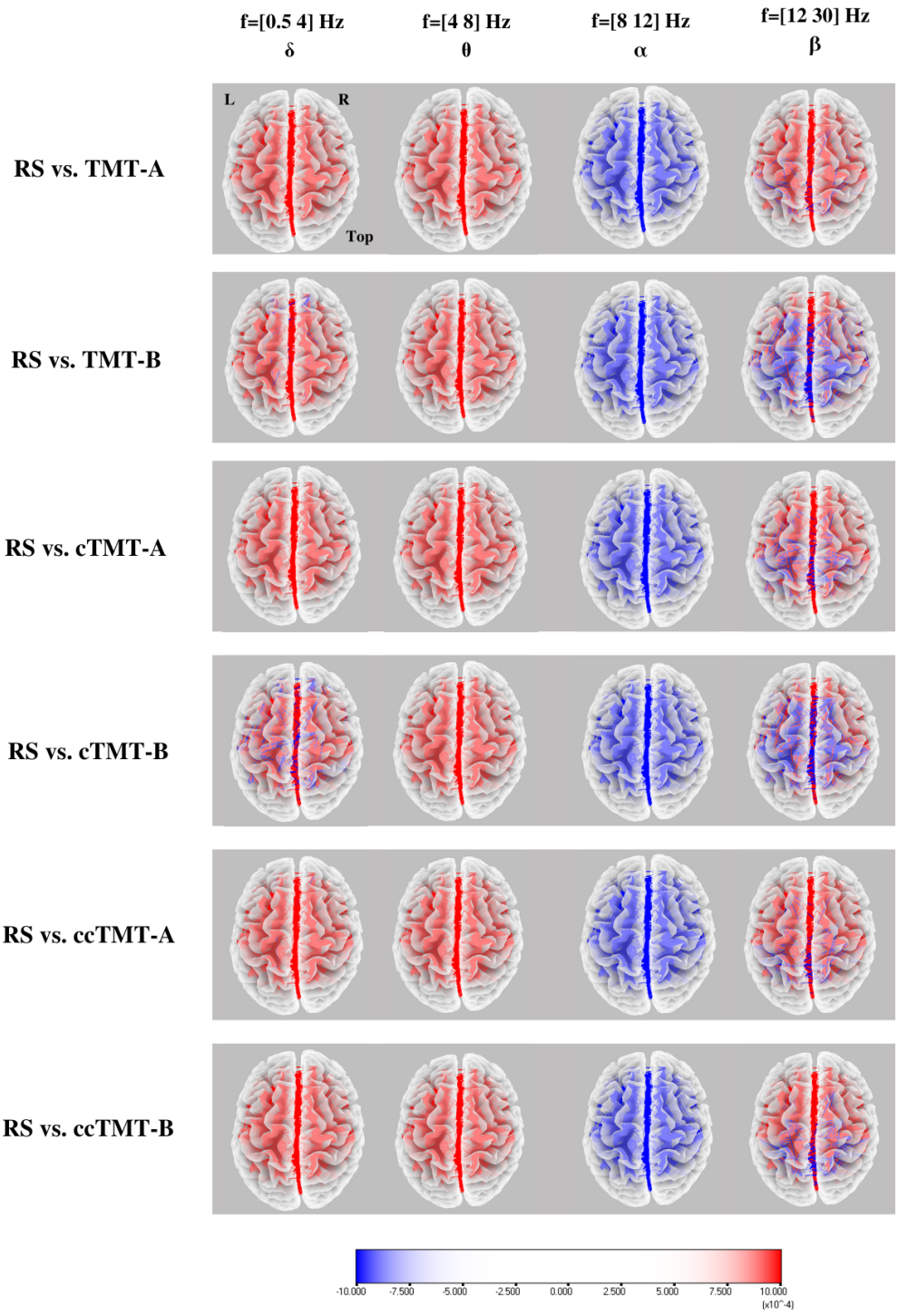

Figure 3.12: sLORETA functional connectivity brain maps showing all connections between RS and part A and B for TMT, cTMT, and ccTMT versions in the δ, θ, α, and β frequency bands. The color red indicates a significantly higher functional connectivity of any TMT version compared to RS, while blue indicates a significantly lower functional connectivity. Please note that the maps are displayed without a statistical threshold applied, allowing for visualization of all connections. TMT = Trail Making Test. cTMT = color Trail Making Test. ccTMT = color classic Trail Making Test. L = left. R = right.

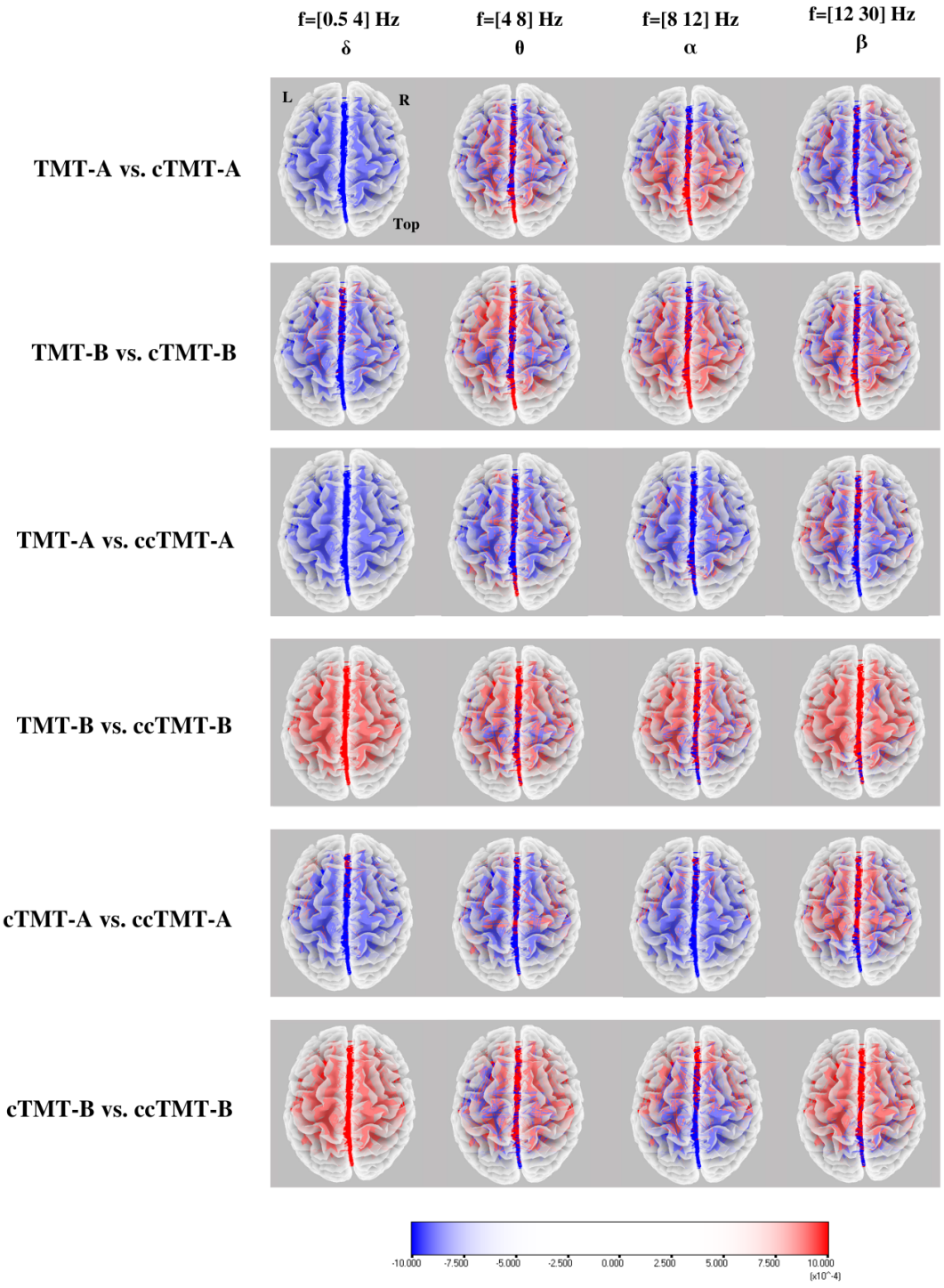

Figure 3.13: sLORETA functional connectivity brain maps showing all connections TMT-A vs. cTMT-A, TMT-B vs. cTMT-B, TMT-A vs. ccTMT-A, TMT-B vs. ccTMT-B, cTMT-A vs. ccTMT-A, and cTMT-B vs. ccTMT-B in the δ, θ, α, and β frequency bands. The color red indicates a significantly higher functional connectivity of condition 2 compared to condition 1, while blue indicates a significantly lower functional connectivity. Please note that the maps are displayed without a statistical threshold applied, allowing for visualization of all connections. RS = Resting State. TMT = Trail Making Test. cTMT = color Trail Making Test. ccTMT = color classic Trail Making Test. L = left. R = right.

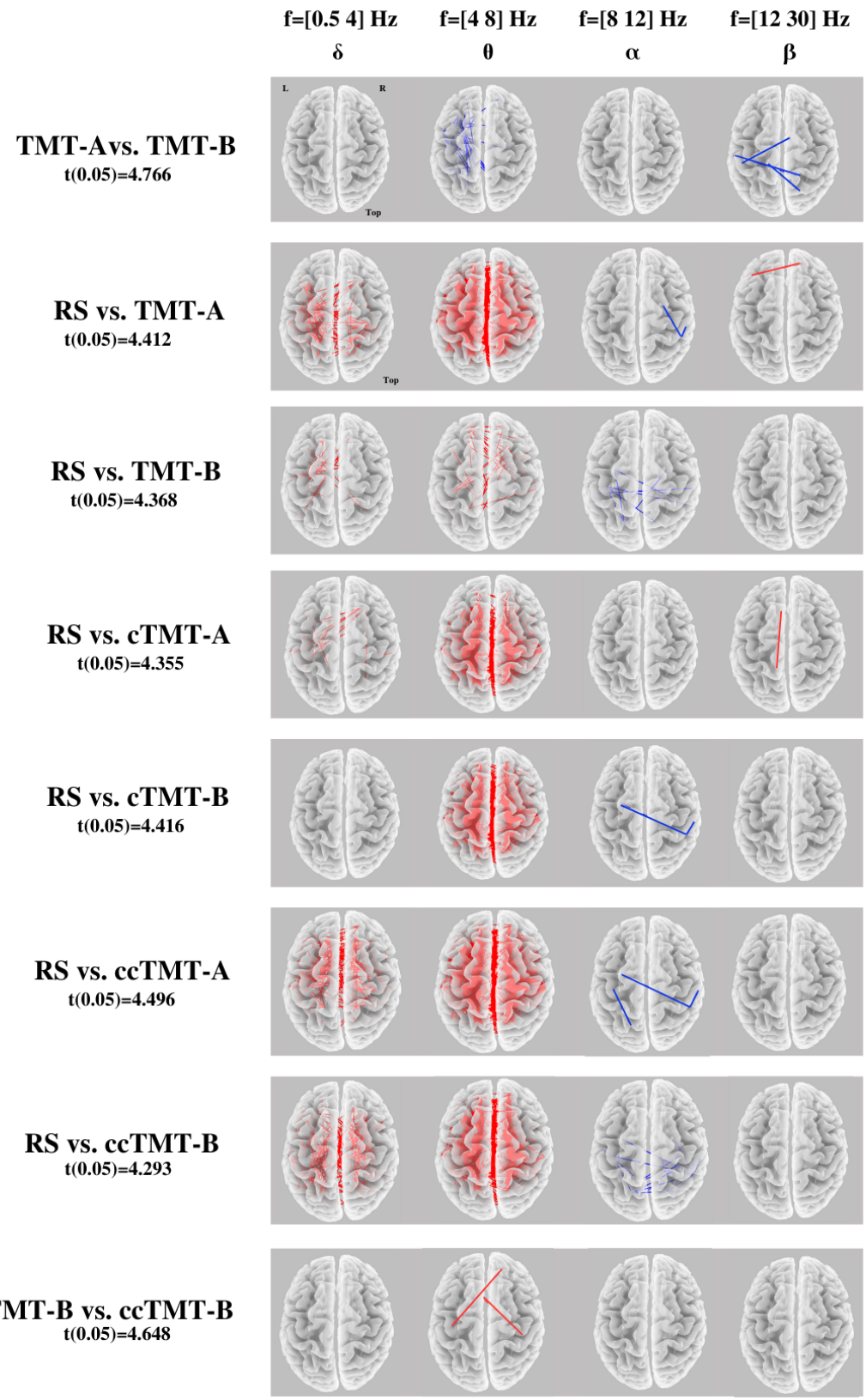

Figure 3.14: sLORETA functional connectivity brain maps showing statistic significant connections TMT-A vs. TMT-B ($threshold; t = 4.766, p < 0.05$), RS vs. TMT-A ($threshold; t = 4.412, p < 0.05$), TMT-B ($threshold; t = 4.368, p < 0.05$), cTMT-A ($threshold; t = 4.355, p < 0.05$), cTMT-B ($threshold; t = 4.416, p < 0.05$), ccTMT-A ($threshold; t = 4.496, p < 0.05$), and ccTMT-B ($threshold; t = 4.293, p < 0.05$), and TMT-B vs. ccTMT-B ($threshold; t = 4.648, p < 0.05$) in the δ, θ, α, and β frequency bands. The color red indicates a significantly higher functional connectivity of condition 2 compared to condition 1, while blue indicates a significantly lower functional connectivity. RS = Resting State. TMT = Trail Making Test. cTMT = color Trail Making Test. ccTMT = color classic Trail Making Test. L = left. R = right.

Chapter 4

Discussion

This study aimed to investigate the executive mechanisms of neuronal activity and their variations during the execution of three different versions of the computerized TMT. The TMT is widely used as a cognitive task for assessing executive functions. To accomplish this, we used a HD-EEG system to analyze the EEG data obtained from a group of 30 healthy participants. Our analysis focused on examining the EEG data in the frequency bands of θ and β, both in the sensor space and source space. By exploring these frequency bands, we aimed to identify the brain regions that exhibited higher levels of activity during the performance of the different TMT versions. Additionally, we investigated the functional connectivity between these regions to gain insights into the network dynamics underlying executive functions, using sLORETA. The TMT versions included a classic version (TMT), as well as two color versions (cTMT and ccTMT). The cTMT version differed from the TMT by introducing encircled colored numbers with a short and identical distance between them. In contrast, the ccTMT maintained the spatial positions of the encircled colored numbers as in the TMT. By comparing these versions, we aimed to determine which one would elicit greater activation in regions associated with executive function. This information could be potentially useful for future clinical applications.

4.1 Activated Structures and Connectivity during TMT Tasks

The involvement of specific brain regions and their interconnections in TMT performance was highlighted by comparing the TMT tasks with the RS condition. During the analysis of our results, we primarily focused on the θ and β frequency bands. The decision not to include the δ and α band in the study's analysis was based on several reasons. The δ band is mainly associated with deep sleep and neural recovery processes (Abhang et al., 2016), which was less relevant to the specific executive functions assessed by the TMT. Similarly, the α band, commonly associated with relaxation and closed-eye states (Berger, 1929), had a lesser role in the executive functions evaluated during the TMT. On the other hand, the θ band was associated with cortical activation during cognitive tasks involving working memory, attention, and executive control (Gevins et al., 1997). The β band, in turn, has been linked to motor coordination and control, which are important aspects during the execution of the TMT. Therefore, our analysis was focused on the θ and β bands as they are more directly related to the cognitive and motor processes relevant to the TMT task.

In our analysis, we observed a significant increase in θ activity in the PFC for all TMT tests compared to the RS, both in the sensor space and source space. θ oscillatory activity in the PFC and hippocampus has been linked to various cognitive processes (Lisman et al., 2008), suggesting its involvement in the execution of the TMT task. The PFC is a crucial structure for higher cognitive functions, including

cognition and executive functions. A previous study (Gevins et al., 1997) reported an increase in frontal θ activity with task difficulty, which aligns with our findings as participants engage in more demanding cognitive processes while connecting the numbers/letters in the TMT tests. The observed changes in the sensor and source spaces were consistent, with significant alterations predominantly found in the frontal lobe. Particularly, the ccTMT-A test showed the highest statistical values in the frontal lobe. The changes in the θ band were localized in the prefrontal areas corresponding to Brodmann Areas 9 and 10, which play a role in executive functions such as planning, initiative, working memory, and attention (Semendeferi et al., 2001). Additionally, there was a significant increase in θ activity in the cingulate cortex, specifically in Brodmann Area 32 (dorsal anterior cingulate cortex or dACC), for TMT-A, TMT-B, and ccTMT-A conditions compared to RS. The dACC is associated with executive control, learning, adjustment, economic choice, and self-control (Heilbronner et al., 2016). Furthermore, we observed significant differences in the β band activity in the PFC for the TMT-A, TMT-B, and cTMT-B conditions compared to the RS. β oscillations in the PFC have been associated with executive control of action (**beta_executive**), working memory (Swann et al., 2009), and prevention of distraction (Hanslmayr et al., 2014).

In a study conducted by Karimpoor et al., 2017, fMRI was used to investigate brain activation during the administration of the TMT. Their findings revealed specific brain regions that exhibited activation during the TMT-A and TMT-B tasks when compared to a baseline condition. When comparing these results to our own study, we observed some similarities in the activation patterns. RS exhibited significantly higher activation compared to TMT-A in regions such as the inferior parietal lobule (IPL), postcentral gyrus, posterior cingulate, and insula. Similarly, RS showed higher activation compared to the TMT-B condition in the insula, anterior cingulate, middle temporal gyrus (MiTG), and postcentral gyri. However, in contrast to the findings reported byKarimpoor et al., 2017, our study did not identify significant activation in the superior parietal lobule (SPL), IPL, and bilateral occipital lobe for TMT-A, nor in SPL, IPL, MiTG, and inferior occipital gyrus (IOG) for TMT-B, compared to the baseline. Nevertheless, both studies did find significant higher activation in specific brain regions during the TMT tasks compared to the RS. Specifically, in our study, we observed significant higher activation in the precentral gyrus for cTMT-A and the MiFG for ccTMT-A when comparing part A to RS. Additionally, significant higher activation in MiFG was observed when comparing part B to RS for TMT-B, cTMT-B, ccTMT-A, and ccTMT-B.

In terms of functional connectivity, our findings revealed increased θ connectivity in multiple cortical regions across both hemispheres for all versions of the TMT compared to the RS. This is consistent with a previous study (Solomon et al., 2017) that investigated θ and γ brain waves during a verbal free-recall memory task, where increased synchronization was observed in θ networks. The regions exhibiting higher θ connectivity in our study, including the frontal, temporal, and medial temporal cortices, are known to play crucial roles in memory encoding and retrieval processes. Furthermore, we observed increased lagged β connectivity for TMT-A between the right MiFG and the left (IFG compared to the RS. The MiFG has been proposed as a convergence zone for the dorsal and ventral attention networks (Corbetta et al., 2008), suggesting its involvement in coordinating attentional processes. Additionally, for cTMT-A, we found increased lagged β connectivity between the left fusiform gyrus (FG) and the left ACC compared to the RS. A study by (Cai et al., 2015) demonstrated a positive linear correlation and increased connectivity between the ACC and the left/right FG, suggesting their involvement in the same network.

4.2 Brain Activity and Theta and Beta Desynchronization in TMT part B vs. part A

In our study, we explored the neural differences between Part A and Part B within each version of the TMT (TMT, cTMT, and ccTMT). Through sensor space analysis, we observed significant changes in the θ band when comparing cTMT-A to cTMT-B. Specifically, cTMT-B showed significantly higher θ band activity in the PFC. Similarly, our source space analysis revealed significant differences in the θ band, with the MiFG exhibiting increased activation during cTMT-B. Thus, the cognitive effort related to set-switching and mental flexibility is greater in part B of the cTMT than in part A. Our results align with a prior study conducted by Talwar et al., 2020, which also reported higher activity in prefrontal regions during more complex tasks involving set-switching and mental flexibility, as seen in TMT Part B. The demand for higher cognitive processing and executive functions is greater in Part B due to the constant switching between numbers and letters. However, our analysis did not reveal any significant differences in the β band when comparing Part A to Part B within each TMT version.

Additionally, we observed a decrease in lagged θ connectivity between TMT-B and TMT-A. This decrease was observed in various cortical regions, including the frontal, temporal, and parietal lobes, with a predominant effect on the left hemisphere. Additionally, we found a decrease in lagged β connectivity between TMT-B and TMT-A in specific regions: the left postcentral gyrus in the parietal lobe, the right ACC in the frontal lobe, the right cuneus in the occipital lobe, the left parahippocampal gyrus in the temporal lobe, and the right paracentral lobule and left superior temporal gyrus in the frontal and temporal lobes, respectively. Higher desynchronization in EEG brain activity has been associated with cognitive processes, sensory processing, and movement (Pfurtscheller et al., 1999). According to this study, their findings showed higher desynchronization during linking periods compared to non-linking periods. Specifically, TMT-B exhibited greater desynchronization during linking periods compared to TMT-A. The increased spectral power in TMT-B suggests higher neural activity and engagement of specific brain regions, indicating increased overall brain activation and enhanced processing of cognitive or sensory processes during TMT-B. The decrease in connectivity strength between TMT-B and TMT-A suggests reduced functional connectivity or synchronization between brain regions. This may reflect a shift in communication patterns within brain networks, indicating a different cognitive or perceptual state during TMT-B. Possible interpretations include the decoupling of brain networks, indicating more segregated processing within different regions, a shift in cognitive processes with enhanced local processing but reduced coordination between regions, and neurophysiological mechanisms such as reduced interregional connectivity due to inhibitory mechanisms, indicating more localized and autonomic neuronal processing.

4.3 Enhanced Theta Band Activation in TMT & ccTMT vs. cTMT

Significant differences were observed in the θ band when comparing different versions of the TMT. Comparing TMT-A and cTMT-A, the ACC exhibited significantly higher activation for TMT-A. Similarly, comparing cTMT-A and ccTMT-A, the ACC showed significantly higher activation for ccTMT-A. When comparing TMT-B and cTMT-B, both the SFG and MiFG displayed higher activation for TMT-B. In the comparison between cTMT-B and ccTMT-B, the SFG and ACC exhibited higher activation for ccTMT-B. However, no significant results were found in the source analysis for the β band. Nevertheless, smaller significant activations were observed in the PFC for ccTMT-A and ccTMT-B, respectively, in the β band. Between the comparisons of TMT-A vs. ccTMT-A and TMT-B vs. ccTMT-B, no sta-

tistically significant differences were found in either the θ or β bands. These findings suggest that the modifications added in the ccTMT, although intended to increase the task complexity, may not have effectively increased the cognitive processing demands beyond what is already present in the TMT.

Overall, these findings indicate that the TMT requires greater attention and cognitive processing compared to the cTMT. One possible explanation for this is that in the cTMT, the distance between each encircled colored number is controlled and smaller compared to the TMT, which has a random and uncontrolled distance between encircled colored numbers. As a result, participants may exert more effort in visually searching for the following number in the TMT. Additionally, our findings suggest that the ccTMT requires greater attention and cognitive processing compared to the cTMT. This can be explained similarly to the previous observation, as ccTMT-A has its encircled colored numbers positioned in the same locations as the TMT. Therefore, the cTMT requires less attentional effort than TMT and ccTMT.

Furthermore, we identified an increased lagged θ connectivity between the right uncus and the left ACC in ccTMT-B compared to TMT-B. This finding aligns with a previous study conducted by Benchenane et al., 2010, which demonstrated that hippocampal-cingulate θ synchrony facilitates information transmission during controlled action selection. Additionally, we observed an increased lagged θ connectivity between the MiFG and the left superior temporal gyrus (STG). The results reported in Shah-Basak et al., 2018 provide compelling evidence for the involvement of the right STG in healthy stimulus-centered spatial processing.

4.4 Study Limitations

One of the main challenges encountered in our study was the trade-off between spatial and temporal resolution inherent in different neuroimaging techniques. While fMRI offers excellent spatial resolution for precise localization of brain activity, its temporal resolution is lower. Conversely, EEG provides high temporal resolution to capture rapid changes in brain activity, but its spatial resolution is relatively lower. To mitigate the limitations of spatial resolution in EEG, we employed LORETA and source localization techniques to estimate the activated brain regions during the TMT. However, it should be noted that even with these techniques, accurately localizing deep brain structures remains challenging. Future investigations could explore advanced approaches, such as combining EEG with fMRI, to overcome spatial resolution limitations and gain a more comprehensive understanding of the neural correlates of TMT performance.

Another limitation of our study was the modest sample size, consisting of only 30 healthy participants. This limited sample size may have restricted the ability to detect statistically significant effects and raised questions about the generalizability of the findings to a larger population. To further investigate and validate the initial findings, conducting an additional study with a larger and more diverse sample would be beneficial. Additionally, exploring the effects of age on the electrophysiological mechanisms during TMT performance by including an elderly population could provide valuable insights into the impact of aging on cognitive processes.

The implementation of computerized versions of the TMT offers several improvements and advantages, such as the automation of data collection, which reduces the manual effort required and allows for efficient data management. However, it is important to acknowledge the potential limitations of a lengthy testing protocol, such as the risk of participant fatigue and the possibility of influencing performance due to prolonged testing sessions. Additionally, future studies should consider incorporating TMT performance measures to enrich result interpretation and provide a more comprehensive understanding of the relationship between brain activity and cognitive performance during the test.

Chapter 5

Conclusion

In conclusion, our study investigated the neural correlates of TMT performance using HR-EEG in a sample of 30 healthy participants. We administered three computerized versions of the TMT, including a classic version and two color-based versions, cTMT and ccTMT. Through spectral analysis, source localization, and connectivity analysis, we observed significant differences in the theta and beta bands between TMT part A and part B, as well as between different test versions and RS. By comparing EEG brain activity during the TMT tests with activity in the RS, we were able to identify the key brain structures involved in task performance, which aligns with previous findings from fMRI studies. Our results revealed that the cognitive demands of the TMT strongly engage regions of the PFC and ACC. Additionally, when comparing cTMT-B to cTMT-A, we found higher θ band activity in the PFC and MiFG, indicating increased cognitive effort related to set-switching and mental flexibility in part B. We also observed decreased connectivity in the θ and β bands between TMT-B and TMT-A in various cortical regions, suggesting reduced interregional connectivity indicating more localized and autonomic neuronal processing. Further, when comparing cTMT with TMT and ccTMT, both the TMT and ccTMT versions showed higher cognitive activation in the ACC, SFG, and MiFG in the θ band. No significant differences were found in the β band. These findings suggest that the TMT and ccTMT require more cognitive attention compared to cTMT, as evidenced by the increased activation patterns in these specific brain regions. The cTMT holds potential as a valuable tool for assessing executive abilities with comparable precision to the classic TMT, particularly in post-stroke patient populations with reduced attentional capacity.

Moving forward, it is crucial to expand our research to include a diverse clinical population, such as individuals with stroke and neurodegenerative diseases, to assess the potential clinical utility of TMT and EEG-HR as a cognitive screening tool. This line of research holds promise for applications in stroke rehabilitation and the assessment of neurodegenerative diseases, ultimately leading to improved patient care and treatment outcomes.

Bibliography

Abhang, P. A. et al. (2016). *Technical Aspects of Brain Rhythms and Speech Parameters*. Ed. by Priyanka A. Abhang, Bharti W. Gawali, and Suresh C. Mehrotra. Academic Press, pp. 51–79. ISBN: 9780128044902. DOI: 10.1016/B978-0-12-804490-2.00003-8.

Barbay, M. et al. (Nov. 2018). "Systematic Review and Meta-Analysis of Prevalence in Post-Stroke Neurocognitive Disorders in Hospital-Based Studies". In: *Dementia and Geriatric Cognitive Disorders* 46, pp. 322–334. DOI: 10.1159/000492920.

Benchenane, K. et al. (June 2010). "Coherent Theta Oscillations and Reorganization of Spike Timing in the Hippocampal- Prefrontal Network upon Learning". In: *Neuron* 66, pp. 921–36. DOI: 10.1016/j.neuron.2010.05.013.

Berger, H. (1929). "Ueber das Elektroenzephalogramm des Menschen". In: *Archiv für Psychiatrie und Nervenkrankheiten* 87, pp. 527–570.

Biasiucci, A. et al. (Feb. 2019). "Electroencephalography". In: *Current Biology* 29. DOI: 10.1016/j.cub.2018.11.052.

Cai, S. et al. (Aug. 2015). "Altered Functional Connectivity of Fusiform Gyrus in Subjects with Amnestic Mild Cognitive Impairment: A Resting-State fMRI Study". In: *Frontiers in Human Neuroscience* 9, p. 471. DOI: 10.3389/fnhum.2015.00471.

Chatrian, G. E. et al. (1985). "Ten Percent Electrode System for Topographic Studies of Spontaneous and Evoked EEG Activities". In: *American Journal of Electroneurodiagnostic Technology* 25, pp. 83–92.

Corbetta, M. et al. (2008). "The reorienting system of the human brain: from environment to theory of mind". In: *Neuron* 58.3, pp. 306–324. DOI: 10.1016/j.neuron.2008.04.017.

Corrigan, J. D. et al. (1987). "Relationships between parts A and B of the Trail Making Test." In: *Journal of clinical psychology* 43 4, pp. 402–9.

Cullen, B. et al. (Sept. 2007). "A review of screening tests for cognitive impairment". In: *Journal of neurology, neurosurgery, and psychiatry* 78, pp. 790–9. DOI: 10.1136/jnnp.2006.095414.

D'Elia, L. F. et al. (1996). *Color Trails Test*. Odessa, FL: PAR.

Dattola, S. et al. (Apr. 2020). "Findings about LORETA Applied to High-Density EEG—A Review". In: *Electronics* 9.4, p. 660. ISSN: 2079-9292. DOI: 10.3390/electronics9040660.

Delis, D. C. et al. (2001). ""Delis-kaplan executive function system (D-KEFS)". In: *San Antonio, TX: The Psychological Corporation*.

Delorme, A. (2019). *Infomax Independent Component Analysis for dummies*. URL: https://arnauddelorme.com/ica_for_dummies/ (visited on 01/30/2023).

Dhakal, A. et al. (Jan. 2023). "Cognitive Deficits". In: *StatPearls [Internet]*. URL: https://www.ncbi.nlm.nih.gov/books/NBK563253/.

Folstein, M. F. et al. (Nov. 1975). "Mini-mental state: A practical method for grading the cognitive state of patients for the clinician". In: *Journal of Psychiatric Research* 12.3, pp. 189–198. DOI: 10.1016/0022-3956(75)90026-6.

Friston, K. J. (1994). "Functional and effective connectivity in neuroimaging: A synthesis". In: *Human Brain Mapping* 2.1-2, pp. 56–78. DOI: 10.1002/hbm.460020107.

Gevins, A. et al. (1997). "High-resolution EEG mapping of cortical activation related to working memory: effects of task difficulty, type of processing, and practice". In: *Cerebral Cortex* 7.4, pp. 374–385. DOI: 10.1093/cercor/7.4.374.

Gollahalli, A. R. (Oct. 2013). "Subconscious Memory using EEG". In.

Grech, R. et al. (Dec. 2008). "Review on solving the inverse problem in EEG source analysis". In: *Journal of neuroengineering and rehabilitation* 5, p. 25. DOI: 10.1186/1743-0003-5-25.

Hanslmayr, S. et al. (2014). "Entrainment of prefrontal beta oscillations induces an endogenous echo and impairs memory formation". In: *Current Biology* 24.8, pp. 904–909. DOI: 10.1016/j.cub.2014.03.007.

Heilbronner, S. R. et al. (2016). "Dorsal Anterior Cingulate Cortex: A Bottom-Up View". In: *Annual Review of Neuroscience* 39, pp. 149–170. DOI: 10.1146/annurev-neuro-070815-013952.

Herrera Pino, J. A. et al. (Apr. 2014). "Ability of the Mini-Mental State Examination to Predict the Neuropsychological Performance of Hispanic Patients with Minor Neurocognitive Disorder". In: *Psychology* 5.5, pp. 533–539. DOI: 10.4236/psych.2014.55063.

Hyvärinen, A. (Feb. 2013). "Independent component analysis: Recent advances". In: *Philosophical transactions. Series A, Mathematical, physical, and engineering sciences* 371, p. 20110534. DOI: 10.1098/rsta.2011.0534.

Kalafat, M. et al. (June 2003). "The Mini Mental State (MMS): French standardization and normative data [Standardisation et étalonnage français du "Mini Mental State" (MMS) version GRÉCO]". In: *Revue de Neuropsychologie* 13, pp. 209–236.

Karimpoor, M. et al. (Oct. 2017). "Tablet-Based Functional MRI of the Trail Making Test: Effect of Tablet Interaction Mode". In: *Frontiers in Human Neuroscience* 11. DOI: 10.3389/fnhum.2017.00496.

Kim, K. et al. (Jan. 2016). "A Comparison of Three types of Trail Making Test in the Korean Elderly: Higher Completion Rate of Trail Making Test-Black and White for Mild Cognitive Impairment". In: *Journal of Alzheimer's Disease Parkinsonism* 6. DOI: 10.4172/2161-0460.1000239.

Klem, G. H. et al. (1999). "The ten-twenty electrode system of the International Federation". In: *Electroencephalography and clinical neurophysiology. Supplement* 52, pp. 3–6.

Klusman, L. E. et al. (1989). "Analysis of errors on the Trail Making Test." In: *Percept. Mot. Skills* 68 (3), pp. 1199–1204.

Kortte, K. B. et al. (2002). "The trail making test, part B: cognitive flexibility or ability to maintain set?" In: *Applied Neuropsychology* 9, pp. 106–109. DOI: 10.1207/S15324826AN0902_5.

Leys, D. et al. (Nov. 2005). "Poststroke dementia". In: *The Lancet Neurology* 4.11, pp. 752–759. DOI: 10.1016/S1474-4422(05)70221-0.

Lin, Z. et al. (2021). "Trail Making Test Performance Using a Touch-Sensitive Tablet: Behavioral Kinematics and Electroencephalography." In: *Front Hum Neurosci.* 15 663463. DOI: 10.3389/fnhum.2021.663463.

Lisman, J. et al. (2008). "A neural coding scheme formed by the combined function of gamma and theta oscillations". In: *Schizophrenia Bulletin* 34, pp. 974–980. DOI: 10.1093/schbul/sbn060.

Lo, J. W. et al. (2019). "Profile of and risk factors for poststroke cognitive impairment in diverse ethnoregional groups". In: *Neurology* 93(24), e2257–e2271. DOI: 10.1212/WNL.0000000000008612.

MacPherson, S. E. et al. (2017). "Processing speed and the relationship between Trail Making Test-B performance, cortical thinning and white matter microstructure in older adults". In: *Cortex* 95, pp. 92–103. DOI: 10.1016/j.cortex.2017.07.021.

Messinis, L. et al. (June 2011). "Color Trails Test: Normative Data and Criterion Validity for the Greek Adult Population". In: *Archives of clinical neuropsychology : the official journal of the National Academy of Neuropsychologists* 26, pp. 322–30. DOI: 10.1093/arclin/acr027.

Moll, J. et al. (2002). "The cerebral correlates of set-shifting: an fMRI study of the trail making test". In: *Arq Neuropsiquiatria* 60(4), pp. 900–905. DOI: 10.1590/s0004-282x2002000600002.

Nunez, P. L. et al. (1981). "Electric fields of the brain: The neurophysics of EEG". In: *Oxford University Press*.

Nuwer, M. R. (1997). "Assessment of digital EEG, quantitative EEG, and EEG brain mapping: report of the American Academy of Neurology and the American Clinical Neurophysiology Society". In: *Neurology* 49, pp. 277–292. DOI: 10.1212/WNL.49.1.277.

Oostenveld, R. et al. (2022). *How does ft prepare neighbours work?* URL: https://www.fieldtriptoolbox.org/faq/how_does_ft_prepare_neighbours_work/ (visited on 05/02/2023).

Oostenveld, R. et al. (2011). "FieldTrip: Open Source Software for Advanced Analysis of MEG, EEG, and Invasive Electrophysiological Data." In: *Computational Intelligence and Neuroscience*. DOI: 10.1155/2011/156869.

Pascual-Marqui, R. D. (2002). "Standardized low-resolution brain electromagnetic tomography (sLORETA): technical details". In: *Methods Find Exp Clin Pharmacol* 24.Suppl D, pp. 5–12.

Pascual-Marqui, R. D. et al. (1994). "Low resolution electromagnetic tomography: a new method for localizing electrical activity in the brain". In: *International Journal of Psychophysiology* 18.1, pp. 49–65.

Pfurtscheller, G. et al. (Nov. 1999). "Event-related EEG/MEG synchronization and desynchronization: basic principles". In: *Clinical neurophysiology : official journal of the International Federation of Clinical Neurophysiology* 110.11, pp. 1842–1857. ISSN: 1388-2457. DOI: 10.1016/s1388-2457(99)00141-8.

Al-Qazzaz, N. K. et al. (2014). "Cognitive impairment and memory dysfunction after a stroke diagnosis: a post-stroke memory assessment." In: *Neuropsychiatr Dis Treat* 10, pp. 1677–1691. DOI: 10.2147/NDT.S67184.

Reimers, K. (2019). "Evaluation of cognitive impairment". In: *The Clinician's Guide to Geriatric Forensic Evaluations*. Chap. Chapter Three, pp. 107–108.

Semendeferi, K. et al. (Mar. 2001). "Prefrontal cortex in humans and apes: a comparative study of area 10". In: *American Journal of Physical Anthropology* 114.3, pp. 224–241.

Shah-Basak, P. P. et al. (May 2018). "The role of the right superior temporal gyrus in stimulus-centered spatial processing". In: *Neuropsychologia* 113, pp. 6–13. DOI: 10.1016/j.neuropsychologia.2018.03.027.

Sharbrough, F. et al. (Jan. 1991). "American Electroencephalographic Society guidelines for standard electrode position nomenclature". In: *Clinical Neurophysiology* 8, pp. 200–202.

Shigemori, K. et al. (2010). "The factorial structure of the Mini-Mental State Examination (MMSE) in Japanese dementia patients". In: *BMC Geriatr* 10, p. 36. DOI: 10.1186/1471-2318-10-36.

Shriram, R. et al. (Aug. 2012). "EEG Based Cognitive Workload Assessment for Maximum Efficiency". In: *IOSR Journal of Electronics and Communication Engineering (IOSR-JECE)*.

Sira, C. S. et al. (2014). "Executive Function". In: pp. 239–242. DOI: 10.1016/B978-0-12-385157-4.01147-7.

Solomon, E. A. et al. (2017). "Widespread theta synchrony and high-frequency desynchronization underlies enhanced cognition". In: *Nature Communications* 8.1, p. 1704. DOI: 10.1038/s41467-017-01763-2.

Stuss, D. T. et al. (2001). "The Trail Making Test: a study in focal lesion patients." In: *Psychological assessment* 13 2, pp. 230–9.

Swann, N. et al. (2009). "Intracranial EEG reveals a time- and frequency-specific role for the right inferior frontal gyrus and primary motor cortex in stopping initiated responses". In: *Journal of Neuroscience* 29.40, pp. 12675–12685. DOI: 10.1523/JNEUROSCI.3359-09.2009.

Talairach, J. (1988). "Co-planar stereotaxic atlas of the human brain". In: *3-D proportional system: An approach to cerebral imaging*.

Talwar, N. et al. (2020). "Functional magnetic resonance imaging of the trail-making test in older adults". In: *PLoS ONE* 15.

Tatum, W. et al. (2008). "Handbook of EEG Interpretation". In: *Demos Medical Publishing*, p. 4.

Towle, V. L. et al. (1993). "The spatial location of EEG electrodes: locating the best-fitting sphere relative to cortical anatomy". In: *Electroencephalography and clinical neurophysiology* 86(1), pp. 1–6. DOI: 10.1016/0013-4694(93)90061-y.

Varjacic, A. et al. (Mar. 2018). "Neural signatures of Trail Making Test performance: Evidence from lesion-mapping and neuroimaging studies". In: *Neuropsychologia* 115. DOI: 10.1016/j.neuropsychologia.2018.03.031.

Wechsler, D. (1997). *Wechsler Adult Intelligence Scale. 3rd Edition*. San Antonio: The Psychological Corporation.

Yap, K. H. et al. (2021). "Challenges for Diagnostic Clarity for Post-stroke Cognitive Impairment and Behavioural Issues in Middle-Income Countries: Case Studies From Malaysia". In: *Frontiers in Neurology* 12, p. 628876. DOI: 10.3389/fneur.2021.628876.

Chapter 6

Appendix

Table 6.1: Inclusion and non-inclusion criteria for participation in this study. If the answer to one of the previous criteria is "No" then the control cannot be included in the study.

Inclusion criteria	
Age between 18-30	Yes ___ No ___
Francophone	Yes ___ No ___
Notice of no objection	Yes ___ No ___
Non-inclusion criteria	
Visual/hearing/motor impairment interfering with taking the tests	Yes ___ No ___
Insufficient knowledge of counting (up to 25) / alphabet / French reading / writing	Yes ___ No ___
Behavioral disorders requiring a stay of more than 2 days in a specialized environment or requiring current treatment other than a single anxiolytic	Yes ___ No ___
Current antidepressant treatment	Yes ___ No ___
Antipsychotic treatment or with multiple anxiolytics	Yes ___ No ___
Single anxiolytic treatment initiated or increased for less than 1 month	Yes ___ No ___
No Current antiepileptic treatment	Yes ___ No ___
No Neurological condition likely to interfere with cognitive assessment, in particular: - Head trauma with loss of consciousness >15 min - Stroke / Hemiplegia / Aphasia - Neurological monitoring for cognitive disorders (memory, language, etc.) - Neurological monitoring for Parkinson's disease, Multiple Sclerosis, etc. - Epilepsy requiring current treatment - Cerebral radiotherapy - Surgical intervention or endovascular cerebral	Yes ___ No ___
Excessive alcohol consumption (>3 drinks per day in men and 2 drinks per day in women) or having presented an alcohol withdrawal syndrome	Yes ___ No ___
Drug use for less than 3 months or history of drug withdrawal syndrome	Yes ___ No ___
General anesthesia for less than 3 months	Yes ___ No ___
History of heart surgery with cardiopulmonary bypass	Yes ___ No ___
Involuntary hospitalization	Yes ___ No ___
Placement under legal protective measures	Yes ___ No ___
Pregnant or breastfeeding woman	Yes ___ No ___

6. APPENDIX

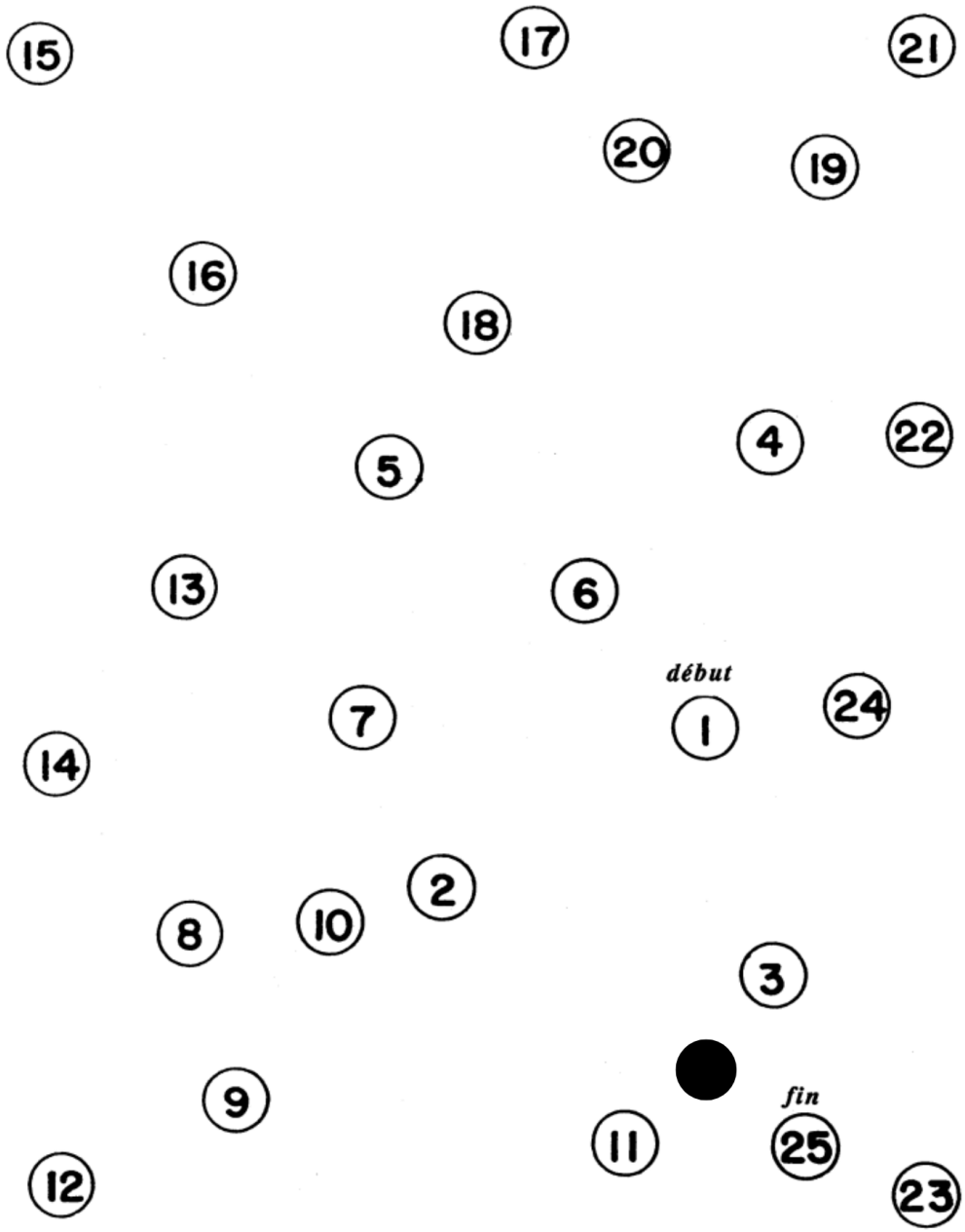

Figure 6.1: Computerized TMT-A. Involves linking encircled numbers from 1 to 25: "1 - 2 - 3 - ... - 25 - ("●")". "début" = beginning. "fin" = end.

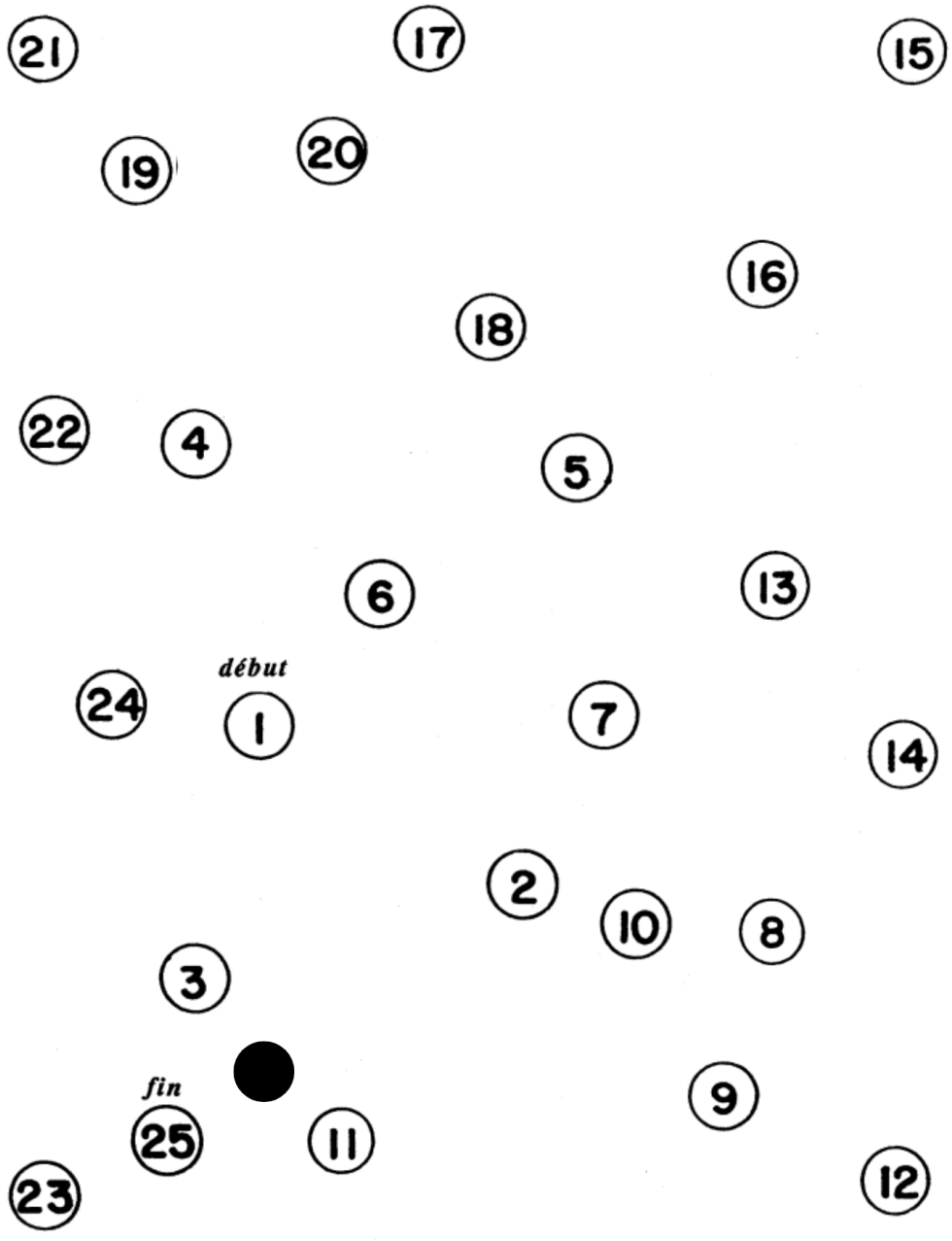

Figure 6.2: Computerized TMT-A inverse. Involves linking encircled numbers from 1 to 25: "1 - 2 - 3 - ... - 25 - ("●")". "début" = beginning. "fin" = end.

6. APPENDIX

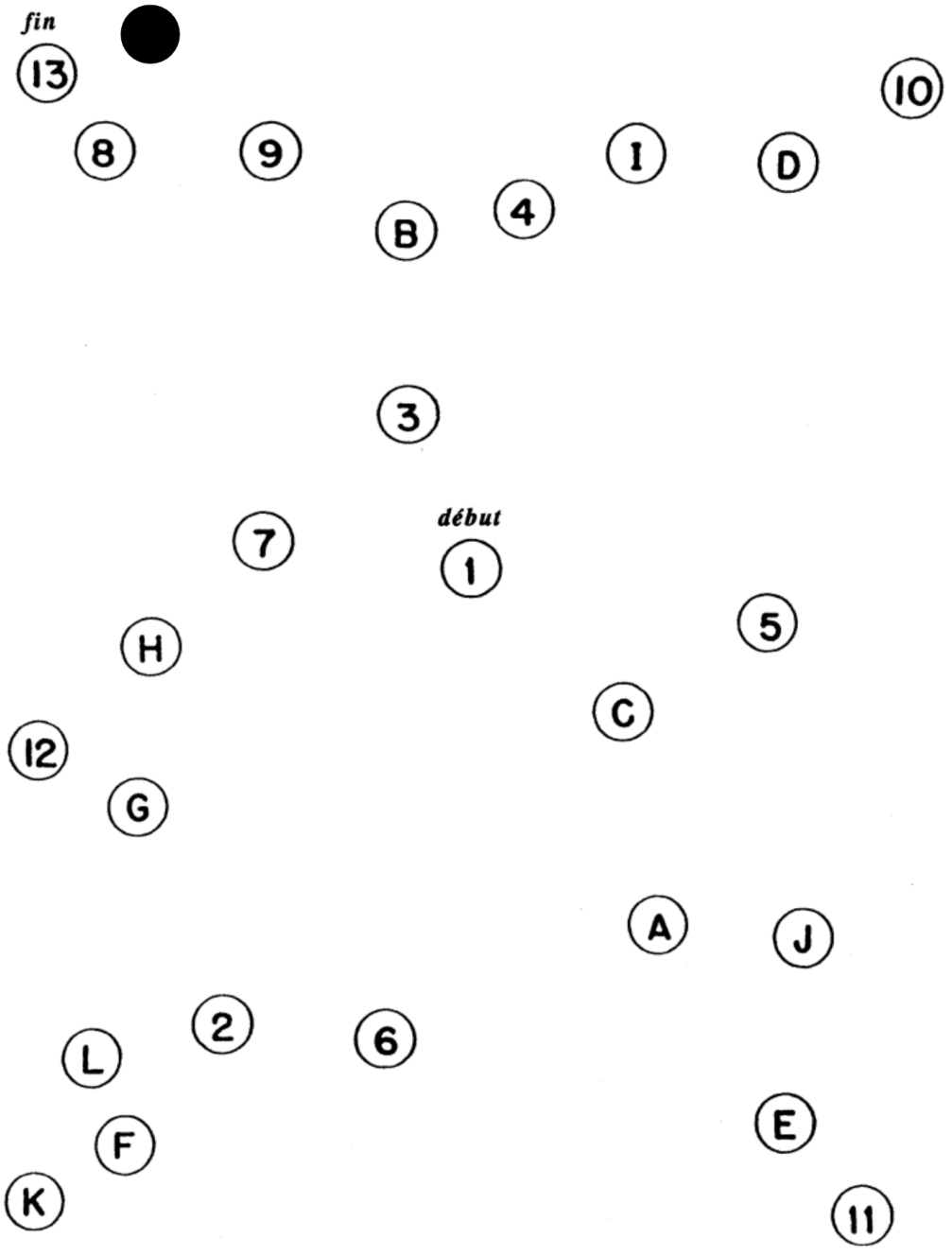

Figure 6.3: Computerized TMT-B. Involves linking numbers (1-13) alternating with letter (A-L) in another random spatial distribution: "1 - A - 2 - B - ... - 13 - ("●")". "début" = beginning. "fin" = end.

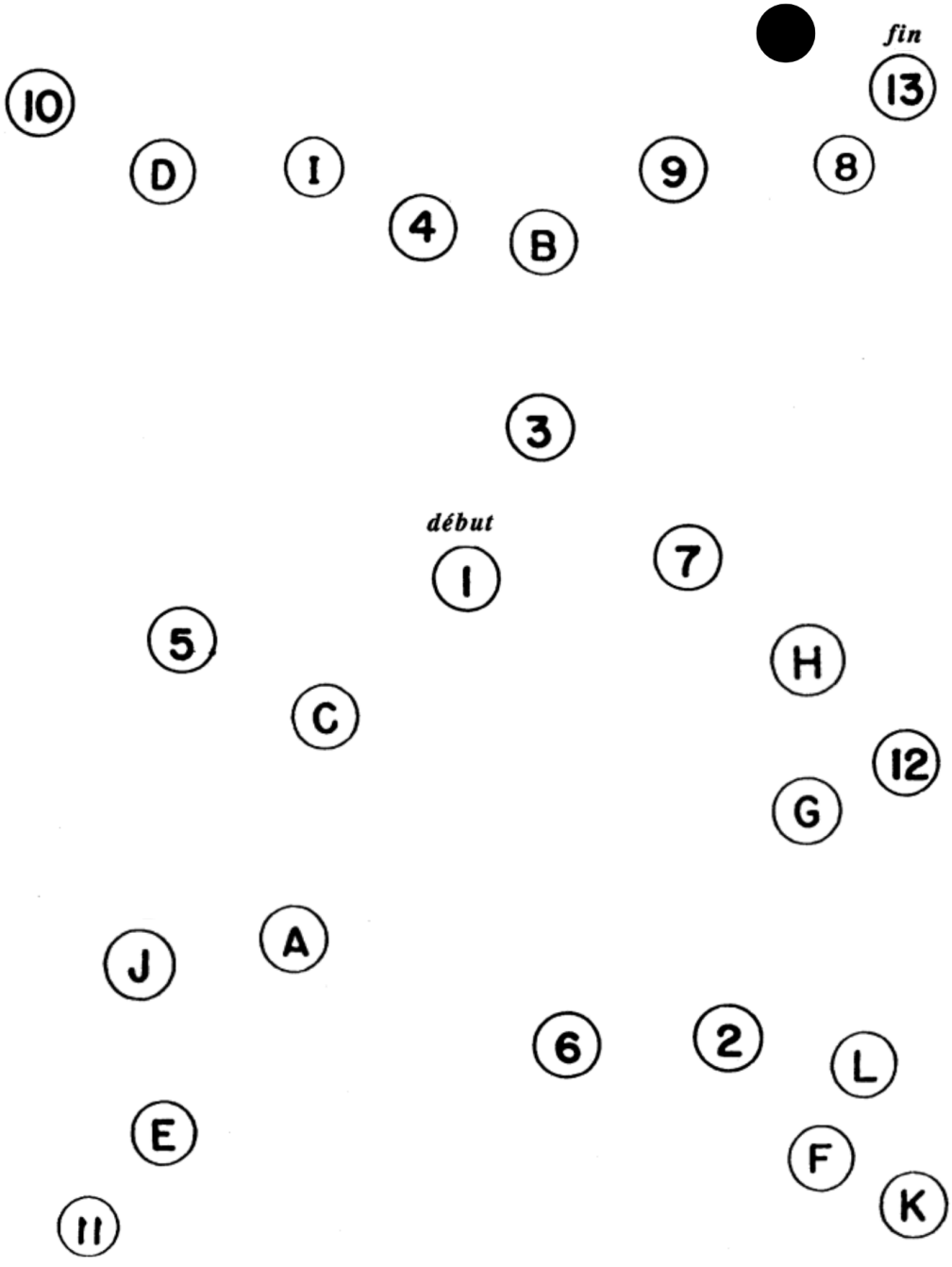

Figure 6.4: Computerized TMT-B inverse. Involves linking numbers (1-13) alternating with letter (A-L) in another random spatial distribution: "1 - A - 2 - B - ... - 13 - ("●")". "début" = beginning. "fin" = end.

6. APPENDIX

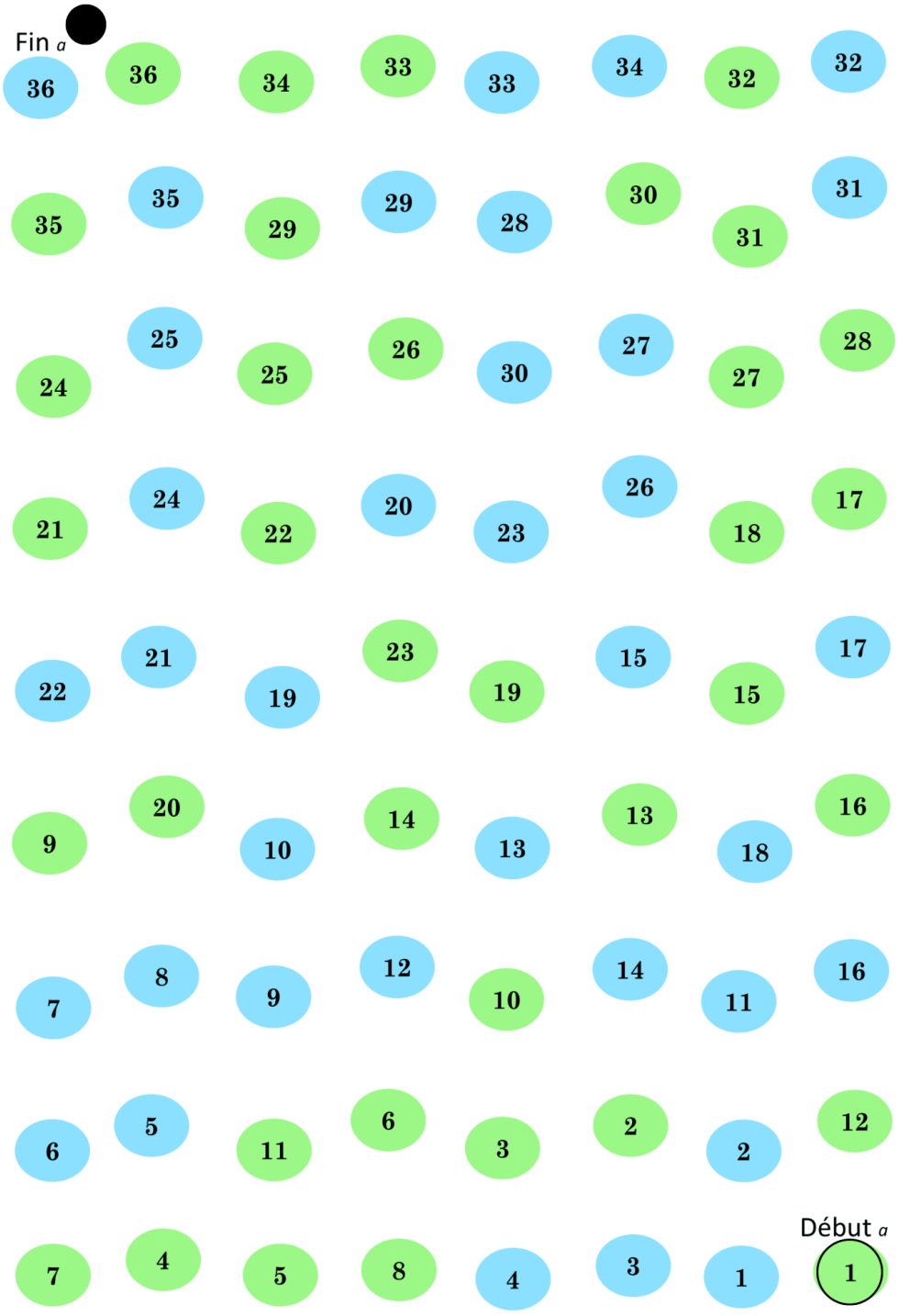

Figure 6.5: Computerized cTMT-A. Involves connecting firstly green encircled numbers colored from 1 to 36 and then blue encircled numbers colored from 1 to 36: "1 - 2 - ... - 36 - ... -1 - 2 - ... - 36 - ("●")". "début" = beginning. "fin" = end.

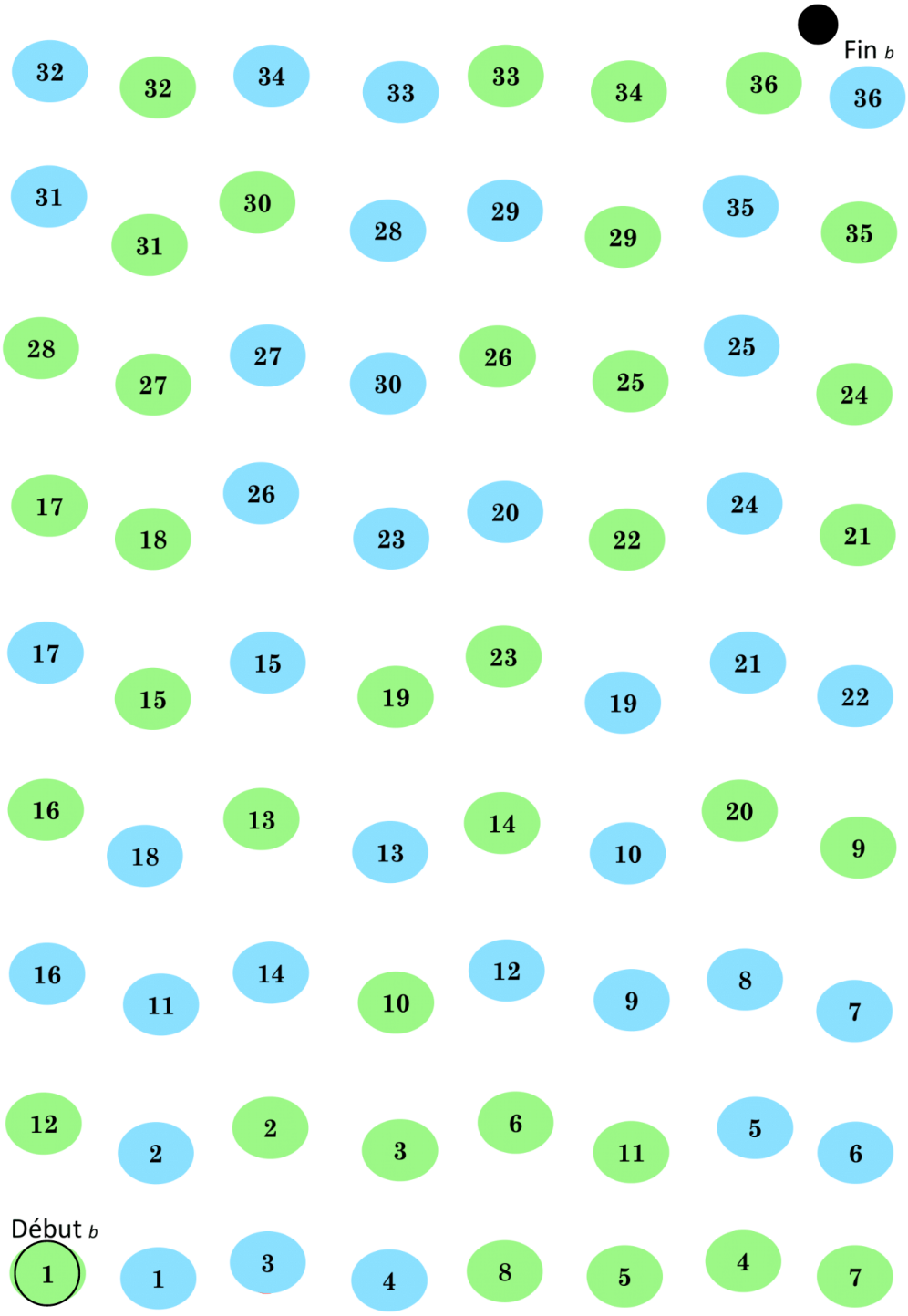

Figure 6.6: Computerized cTMT-A. Involves connecting green encircled numbers alternating with blue encircled numbers, by order: "1 - 2 - 3 - 4 - ... - 36 - ("●")". "début" = beginning. "fin" = end.

6. APPENDIX

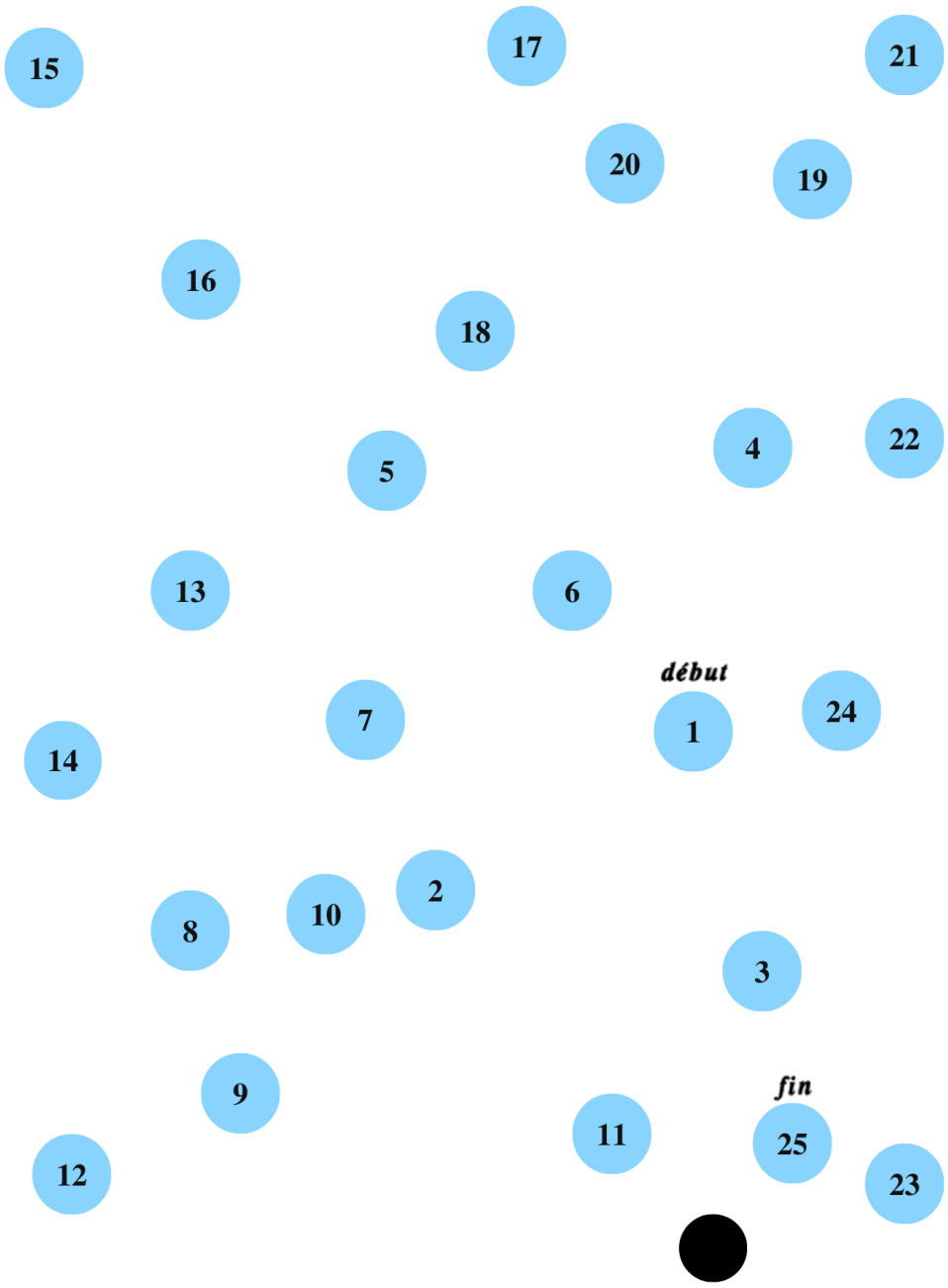

Figure 6.7: Computerized ccTMT-A. Involves connecting encircled numbers colored with blue from 1 to 25: "1 - 2 - ... - 25 - ("●")". "début" = beginning. "fin" = end.

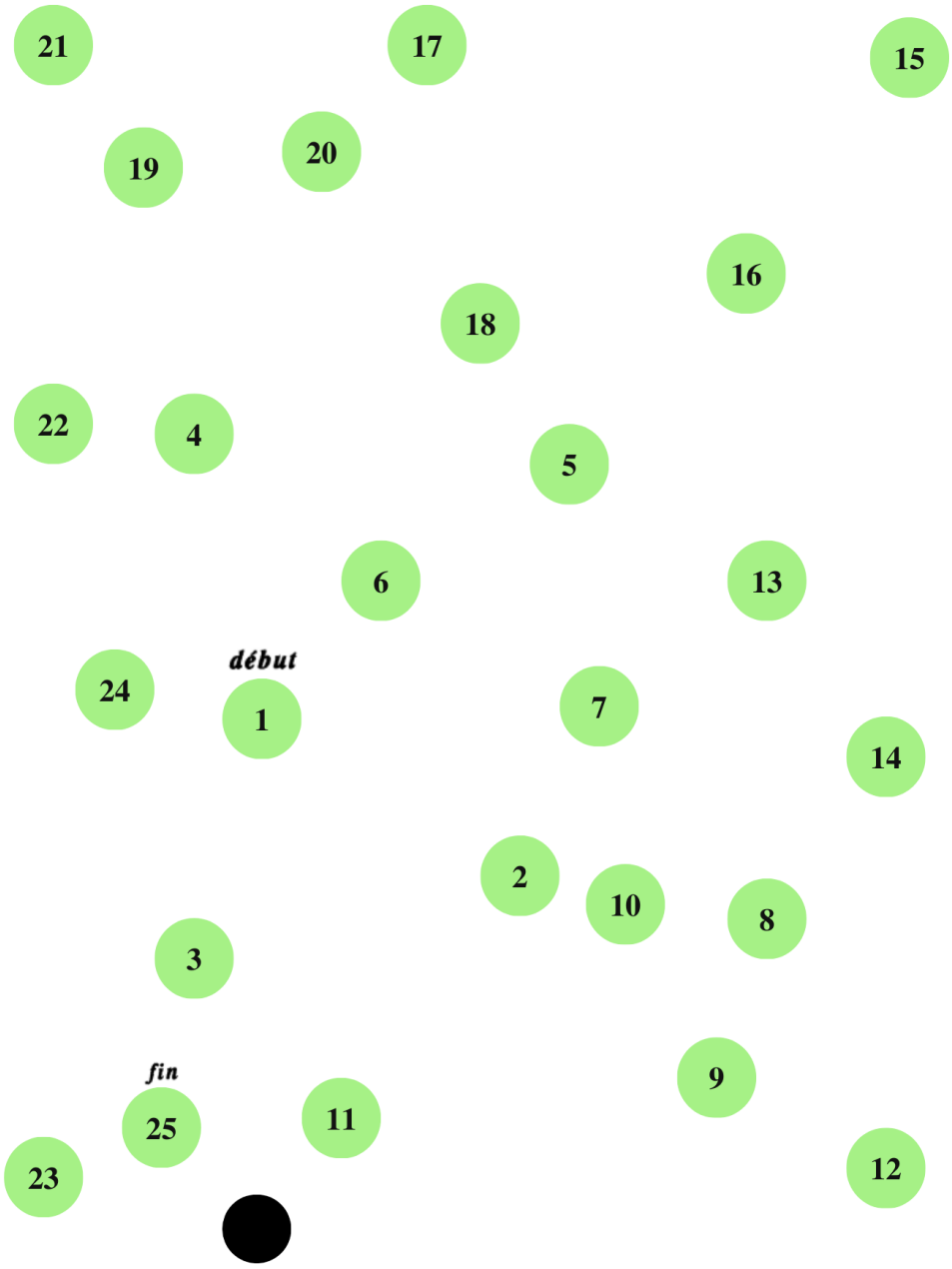

Figure 6.8: Computerized ccTMT-A inverse. Involves connecting encircled numbers colored with green from 1 to 25: "1 - 2 - ... - 25 - ("●")". "début" = beginning. "fin" = end.

6. APPENDIX

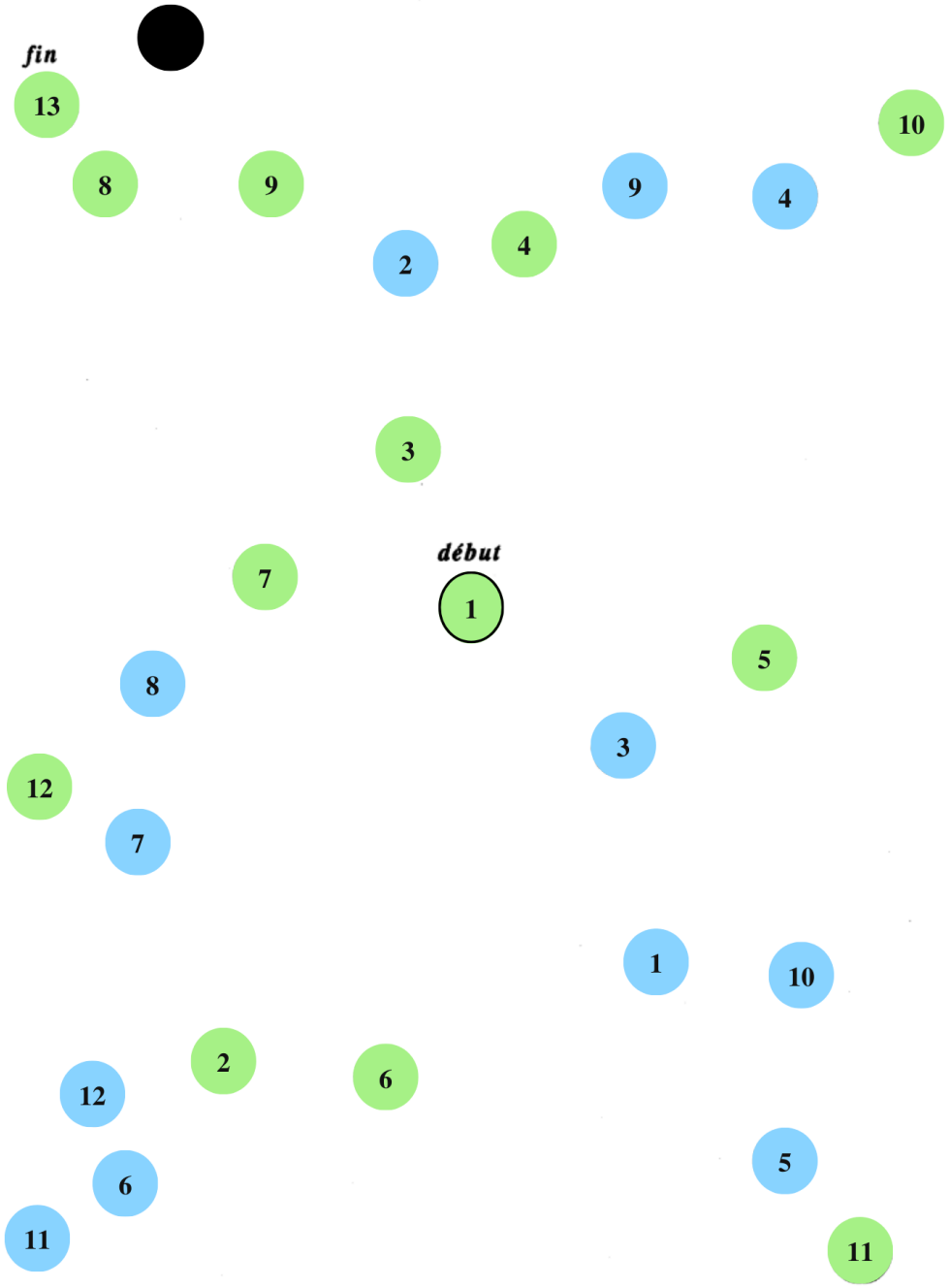

Figure 6.9: Computerized ccTMT-B. Involves connecting alternating green encircled numbers with blue encircled numbers by order: "1 - 2 - 3 – ... - 13 - ("●")". "début" = beginning. "fin" = end.

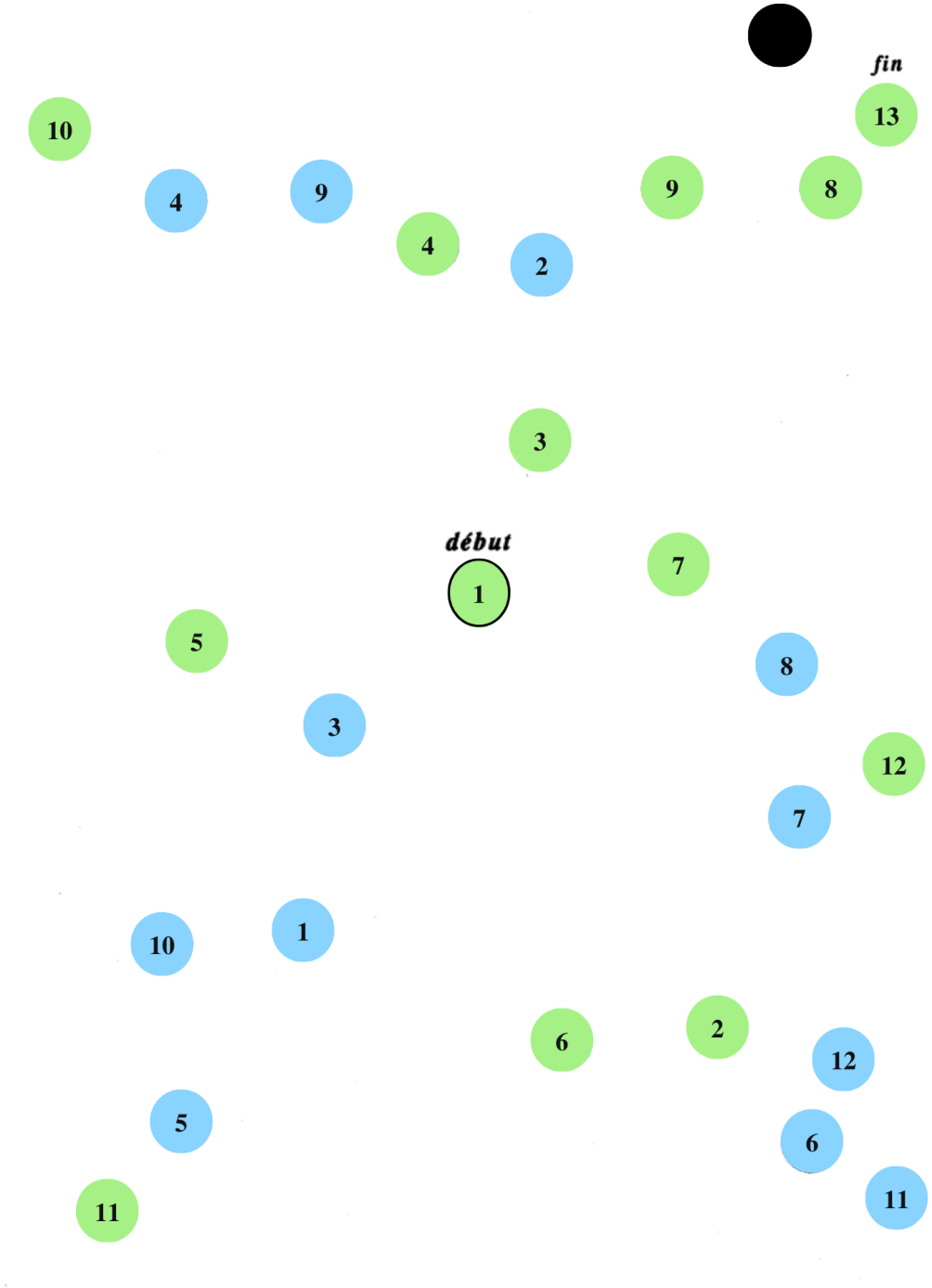

Figure 6.10: Computerized ccTMT-B inverse. Involves connecting alternating green encircled numbers with blue encircled numbers by order: "1 - 2 - 3 – ... - 13 - ("●")". "début" = beginning. "fin" = end.

6. APPENDIX

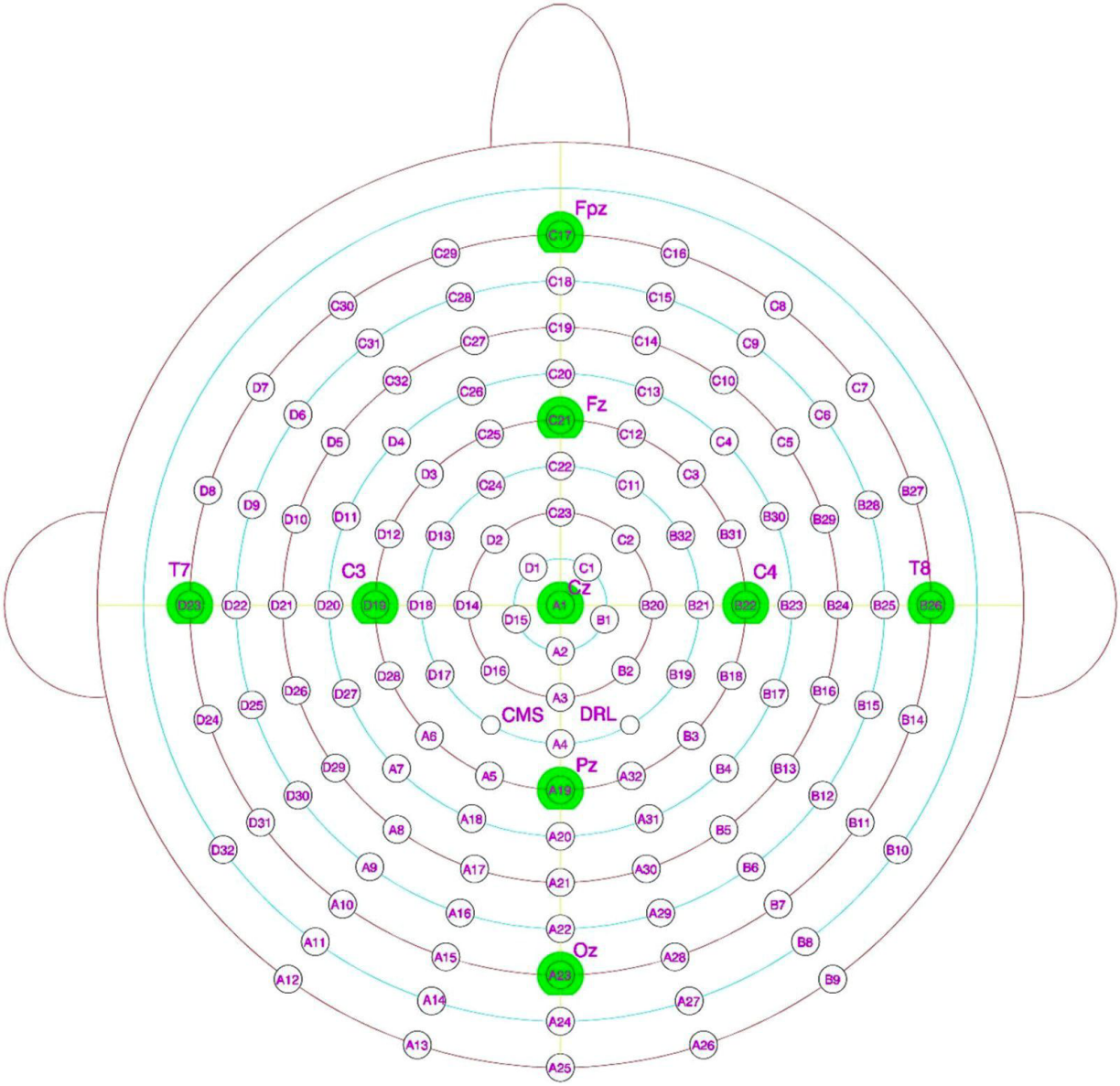

Figure 6.11: EEG electrodes location, including 128 active BioSemi electrodes (32 A, 32 B, 32 C, and 32 D), CMS (Common Mode Sense) and DRL (Driven Right Leg) electrodes. The CMS electrode is used to measure the common reference signal and eliminate common noise interference in EEG recordings. The RDL electrode provides a grounding reference for the EEG system, minimizing common mode noise introduced through the participant's body.

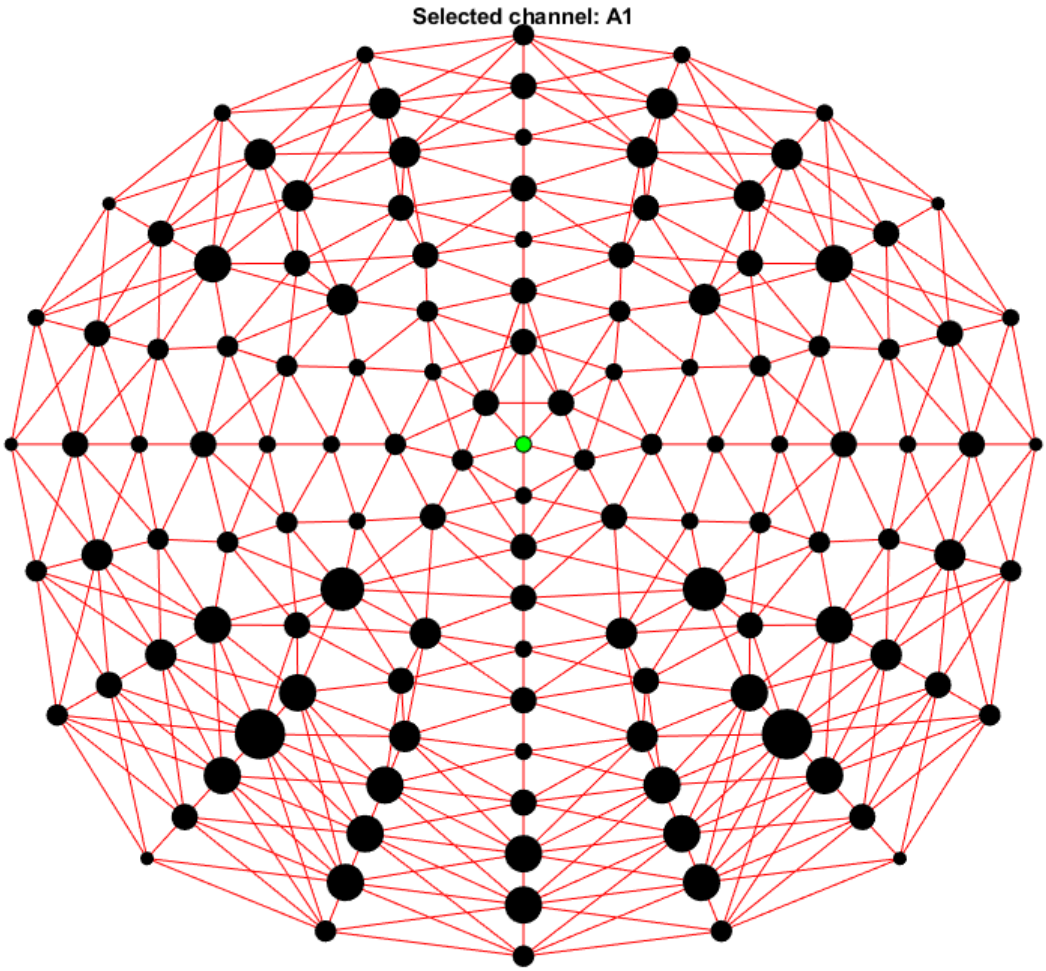

Figure 6.12: Triangulation algorithm graphical representation according to our electrodes positions. This algorithm is used in EEG data analysis to determine the spatial relationships between electrodes based on their physical coordinates. It starts by connecting neighboring electrodes to form small triangles and gradually expands to construct larger triangles, creating a network of interconnected triangles that covers the entire electrode area. This information is valuable for replacing removed channels by estimating missing data through interpolation using the average values of neighboring channels. The algorithm relies solely on the spatial coordinates of the electrodes, independent of their actual distances.